

---

Electronic Thesis and Dissertation Repository

---

1-30-2020 3:00 PM

## System Reliability Analysis of Defected Pile group Foundations

Abdalla E. Adlan Alhashmi, *The University of Western Ontario*

Supervisor: Dr. M. Hesham El Naggar, *The University of Western Ontario*

A thesis submitted in partial fulfillment of the requirements for the Master of Engineering  
Science degree in Civil and Environmental Engineering

© Abdalla E. Adlan Alhashmi 2020

Follow this and additional works at: <https://ir.lib.uwo.ca/etd>



Part of the [Civil Engineering Commons](#), [Geotechnical Engineering Commons](#), and the [Structural Engineering Commons](#)

---

### Recommended Citation

Adlan Alhashmi, Abdalla E., "System Reliability Analysis of Defected Pile group Foundations" (2020).  
*Electronic Thesis and Dissertation Repository*. 6812.  
<https://ir.lib.uwo.ca/etd/6812>

This Dissertation/Thesis is brought to you for free and open access by Scholarship@Western. It has been accepted for inclusion in Electronic Thesis and Dissertation Repository by an authorized administrator of Scholarship@Western. For more information, please contact [wlsadmin@uwo.ca](mailto:wlsadmin@uwo.ca).

## Abstract

Deep foundations design suffers some degrees of uncertainties. This thesis studies the behavior of a geotechnically defected axially loaded pile group foundations installed in sand and calibrates the resistance factor of redundant pile group foundation, utilizing a rational based system reliability analysis. This was achieved by conducting a comprehensive numerical parametric investigation using the computer program ABAQUS/Standard. The result of the parametric study showed that the presence of a defected pile in a pile group foundation causes lateral deflection of the pile cap and hence induces bending moment at the adjacent piles which affects the load distribution mechanism of the system. It was also found that the proposed resistance factor values varied from 0.31 to 0.61, 0.52 to 0.86, 0.34 to 0.63, and 0.45 to 0.96 for different design methods: Nordlund, Bluebook,  $\beta$ -Method, and SPT Meyerhof, respectively. The resistance factors are affected primarily by the ability of the pile cap to redistribute the forces upon failure of one pile or more within the group.

**Keywords:** Piles; Pile groups; defective piles; system-reliability; Target reliability index; Resistance factor; Finite Element analysis; Load-settlement curve.

## Summary for Lay Audience

Pile foundations are structural members that are usually required to support structures when the soil at the ground surface is weak and can't carry the loads imposed by the structure. In common practice, piles are usually made in groups and they are connected together with a thick concrete mat called the pile cap. The function for the pile cap is to connect the group piles together to ensure uniform load distribution among the piles.

Pile group foundation suffers some degrees of uncertainties that can cause some damage to one pile or more. Such damage may occur due to the existence of weakness of the soil itself or from the imperfect execution of the pile. Utilizing advanced numerical simulation and the understanding the uncertainties associated with the behavior of the pile groups foundation, this thesis investigated the effect of one or more damaged piles on the pile group foundation, and to come to conclusion whether such damage will lead to a failure of the system or it has no any significant effect?

It was found that the damage of one or more pile may not affect the pile group. The results of this research will be useful to implement a new parameter during the process of designing the project and provide a new equation to demonstrate how much stronger the system should be for a certain load ( factor of safety), and that will help cut down the expenses of the projects and minimize the usage of any extra unnecessary resources.

## Co-Authorship Statement

This thesis is prepared in accordance with the regulations of an integrated Article based format thesis stipulated by the School of Graduate and Postdoctoral Studies at the University of Western Ontario. The numerical modeling, interpretation of the results and writing of the final version of the thesis were performed by author himself under the supervision of Dr. Hesham El Naggar. Statements of the co-authorship of individual chapters are as follows:

### **Chapter 3: Numerical investigation of defected pile group foundations**

A version from chapter 3 reviewed by Prof. Hesham El Naggar will be submitted for possible publication in Computers and Geotechnics.

### **Chapter 4: Reliability analysis of pile group foundations**

A version of chapter 4 reviewed by Prof. Hesham El Naggar and Dr. Fadi Oudah will be submitted for possible publication in as one journal manuscript in Engineering Structures.

## Acknowledgments

With tremendous respect and appreciation, I would like to express my heartfelt gratitude and acknowledgement to the people and associations who assist me bring this study into reality.

Nobody has been more important to me than my parents, whom I am greatly indebted for helping me survive all the stress during this research and for their understanding, patience, motivation and for pushing me farther than I thought I could go and not letting me give up.

I am grateful to the exceptional Dr. Hesham El Naggar, my supervisor, whom I have had the pleasure to work with during my research. He has provided me with the comprehensive personal and professional guidance in scientific research, he had inspired my interest to show me, by his example, what a good scientist should be. I would also extend my gratitude to Dr. Fadi Oudah for his consistent support and encouragement throughout my research.

last but not least I would like to extend my profound gratitude to the rest of my family, friends and everybody that has supported me physically or emotionally during my journey to achieve a dream.

# Table of Contents

Abstract.....	i
Summary for Lay Audience.....	ii
Co-Authorship Statement.....	iii
Acknowledgments.....	iv
Table of Contents.....	v
List of Tables.....	ix
List of Figures.....	xi
List of Abbreviations, Symbols, and Notations.....	xvi
Chapter 1.....	1
<b>1 INTRODUCTION.....</b>	<b>1</b>
1.1 Overview.....	1
1.2 Research Objectives and Methodology.....	2
1.3 Outline of Thesis.....	3
1.4 References.....	4
Chapter 2.....	6
<b>2 LITERATURE REVIEW.....</b>	<b>6</b>
2.1 Background.....	6
2.2 Static capacity of pile foundations.....	8
2.2.1 Interpretation of static capacity of pile foundations.....	8
2.3 Pile group behavior.....	13
2.4 Defected pile foundations.....	16
2.4.1 Previous Studies on Defected Pile Foundations.....	19
2.5 Reliability analysis in geotechnical engineering.....	20
2.5.1 Limit state design vs Working stress design in geotechnical engineering.....	21

2.5.2	Previous studies related to System-based reliability analysis.....	22
2.6	References.....	26
Chapter 3	.....	29
<b>3</b>	<b>NUMERICAL INVESTIGATION OF DEFECTED PILE GROUP FOUNDATIONS.....</b>	<b>29</b>
3.1	Introduction.....	29
3.2	Objectives and Scope of Work .....	31
3.3	Development of Numerical Models.....	31
3.3.1	Geometry and Boundary Conditions of Finite Element Models .....	32
3.3.2	Sensitivity analysis of effect of boundary conditions.....	34
3.3.3	Sensitivity analysis of mesh density .....	36
3.3.4	Pile-soil interface model .....	37
3.3.5	Constitutive material model and model parameters.....	38
3.3.6	Analysis Steps and Loading Sequence .....	41
3.3.7	Validation of Finite Element Model .....	42
3.3.8	Case study of Pile Group with a Defected Pile.....	45
3.3.9	Parametric Study.....	50
3.4	Results and discussion .....	53
3.4.1	Load-settlement response.....	53
3.4.2	Load re-distribution of defective pile group foundation.....	59
3.4.3	Load-rotation behavior of the pile cap.....	64
3.4.4	Piles Bending Moment Behavior .....	66
3.5	Conclusion .....	70
3.6	References.....	71
Chapter 4	.....	75
<b>4</b>	<b>RELIABILITY ANALYSIS OF PILE GROUP FOUNDATIONS.....</b>	<b>75</b>

4.1	Introduction.....	75
4.2	Recent Development in System-Based Reliability .....	77
4.2.1	Interaction between the sub-structural elements.....	78
4.2.2	Interaction between sub-and super structural elements .....	78
4.3	Objective.....	81
4.4	Methodology for Calibrating the Resistance Factors Based on System-Based Reliability.....	82
4.4.1	Calculations of $\gamma$ factor .....	82
4.4.2	Individual piles reliability index .....	85
4.4.3	Resistance factor calibration method .....	85
4.5	Parametric Study to Calculate $\gamma$ .....	87
4.6	Model Development.....	89
4.6.1	Finite element geometry and boundary conditions.....	89
4.6.2	Constitutive material model and model parameters.....	90
4.6.3	Analysis Result .....	91
4.7	M value based on the failure of one pile or more .....	96
4.8	Resistance factor calibration of redundant group piles.....	98
4.8.1	Survey of statistical data .....	98
4.8.2	Calculations of the number of piles the system can accommodate, M.....	99
4.8.3	Calculation of individual pile reliability index .....	100
4.8.4	Results and discussion .....	101
4.9	Conclusion .....	105
4.10	References.....	106
	Chapter 5.....	109
<b>5</b>	<b>SUMMERY, CONCLUSION AND RECOMMENDATIONS.....</b>	<b>109</b>
5.1	Summery.....	109



5.2	Conclusions.....	109
5.3	Future work and recommendations.....	110
	<b>Curriculum Vitae</b> .....	112

## List of Tables

Table 2-1: Different interpretation methods for ultimate load (AbdelSalam et al., 2012) .....	12
Table 3-1: Comparison in computational time for different geometric order and integration for a hexahedral element .....	33
Table 3-2: Model geometry parameters .....	43
Table 3-3 : pile and pile cap material parameters considered in the FE .....	43
Table 3-4: Properties of sand bed used in the experimental study for FE model validation ..	44
Table 3-5 centrifuge model and numerical model material parameters after Zhang and Wong (2007) .....	46
Table 3-6 Equivalent centrifuge model and prototype dimensions .....	46
Table 3-7: Hoek-Brown's rock mass material parameters .....	49
Table 3-8 Silty sand material parameters considered in the FE.....	49
Table 3-9: Failure scenarios considered in the FE.....	53
Table 3-10: Ultimate capacity of all failure scenarios and pile spacing for 5-pile group.....	56
Table 3-11: Ultimate capacity of all failure scenarios and pile spacing for 7-pile group.....	56
Table 3-12: Ultimate capacity of all failure scenarios and pile spacing for 9-pile group.....	57
Table 4-1: Resistance factor calibration process .....	82
Table 4-2: Material properties for the steel pile considered in the FE model .....	90
Table 4-3: Soil parameters considered in the FE model .....	91
Table 4-4: Parametric study results of 5 piles in a pile group foundation for different design variables and failure scenarios .....	92

Table 4-5 : Parametric study results of 7 piles in a pile group foundation for different design variables and failure scenarios .....	93
Table 4-6:Parametric study results of 9 piles in a pile group foundation for different design variables and failure scenarios .....	94
Table 4-7: Summary of database used in the resistance factor calibration (AbdelSlam, et.al 2012) .....	99
Table 4-8: Comparison in M values using two different methods.....	100
Table 4-9: M-values (Method 2) for different pile group configurations, different design methods and pile spacing .....	100
Table 4-10: The calculated individual piles reliability index for different pile group configurations .....	101

## List of Figures

Figure 2-1: Load transfer mechanism for a single pile foundation.....	6
Figure 2-2 : Graphical representation of Davisson’s failure criteria method .....	9
Figure 2-3 : Graphical representation of Chin-Kondner’s method.....	10
Figure 2-4 : Graphical representation of DeBeer log-log method .....	10
Figure 2-5 : Graphical representation of tangent intersection method .....	11
Figure 2-6: Stress overlap in pile group foundations.....	13
Figure 2-7: Example of Pile group and pile raft systems.....	14
Figure 2-8: Efficiency of the pile groups in sand (after Vesic, 1967) .....	15
Figure 2-9: Illustrations of geological imperfections a) piles founded on boulder; b) Compressible layer bellow founding layer; c) uneven soil layers; d) Clay seams bellow rock socket .....	17
Figure 2-10: Demonstration of imperfections arise from inadequate ground investigation...	18
Figure 2-11: Construction related defects (structural imperfections).....	18
Figure 2-12: Geometrical representation of the reliability index by Cornell (1969).....	21
Figure 3-1: ABAQUS element type characterization .....	32
Figure 3-2: Variation of pile cap settlement with extent of vertical mesh boundaries .....	35
Figure 3-3: Variation of pile cap settlement with extent of vertical mesh boundaries .....	35
Figure 3-4: General configuration of the finite element mesh used in the analysis .....	36
Figure 3-5: Variation of pile cap settlement with number of mesh elements.....	37

Figure 3-6: Relationship between: a) concrete compressive strength and plastic strain, and b) Concrete tensile strength and cracking displacement after Alfarah et al. (2017) .....	39
Figure 3-7 Reinforcement arrangement in the modeled pile cap.....	40
Figure 3-8: Stress-strain relationship for concrete under: a) compression; and b) tension ....	40
Figure 3-9: Redistribution factors for a four-pile group considering elastic and plastic concrete models for the pile cap .....	41
Figure 3-10: Loading protocol and analysis steps for the finite element model.....	42
Figure 3-11: Comparison of numerical and experimental load test results of pile group.....	45
Figure 3-12: Pile group test cases considered in the study .....	47
Figure 3-13: Stress-strain relationship used for the validation case of Zhang and Wong (2007); a) compression; b) Tension .....	47
Figure 3-14: Comparison of the numerical model and the centrifuge experimental load test results of all pile group test cases .....	50
Figure 3-15: Pile group configurations considered in the FE .....	51
Figure 3-16: Different pile group configuration and analysis types considered in the parametric study .....	52
Figure 3-17: Load-settlement curves of 9-pile group for different failure scenarios and pile spacing; a) Effect of pile location ; b) Effect of pile spacing ; .....	55
Figure 3-18: Load-settlement behavior for 5-pile group for different failure scenarios and pile spacing; a) failure of corner pile; b) failure of 2 corner piles .....	57
Figure 3-19: Load-settlement behavior for 7-pile group for different failure scenarios and pile spacing; a) failure of corner pile; b) failure of 2 corner piles; c) failure of 2 corner and 1 edge pile.....	58

Figure 3-20: Example of the impact of a failed pile in a pile group foundation.....	59
Figure 3-21: Schematic view of an intact and defected pile group foundation with strut and tie model.....	61
Figure 3-22: Compression of $\lambda$ between strength-based and settlement-based methods .....	61
Figure 3-23: Redistribution factor for 5-pile group foundation for different failure scenarios; a) corner pile; b) middle pile; c) Two external piles.....	62
Figure 3-24: Redistribution factor for 7-pile group foundation when corner pile fails .....	62
Figure 3-25: Redistribution factor for 9-pile group foundation when corner pile fails .....	63
Figure 3-26: Failure mechanism of the pile group when middle pile fails .....	63
Figure 3-27: Rotational behavior of 7-pile group pile cap when one or more piles fails in the system .....	65
Figure 3-28: Pile cap load-rotation behavior for different pile spacing when two corner piles fails in the 5-pile group .....	65
Figure 3-29: Pile cap load-rotation behavior for a 7-pile group considering two different failure scenarios; a) corner pile b) edge pile .....	66
Figure 3-30: Pile cap load-rotation behavior when one corner piles fails in the 5-pile group	66
Figure 3-31: Bending moment envelop of individual piles in a 7-pile group when a corner pile fail .....	68
Figure 3-32: Effect of center to center pile spacing on the bending behavior of individual piles in a 7-pile group when a corner pile fail .....	68
Figure 3-33: Bending moment behavior of all piles in 7-pile group foundation when an edge .....	69
Figure 4-1: Summary of geotechnical uncertainties based on Phoon and Kulhawy (1999)...	76

Figure 4-2: Typical 3D strut and tie model for four-pile cap .....	83
Figure 4-3: Illustration of failure mechanism of pile group under axial loading when one pile fails.....	84
Figure 4-4: Typical foundation considered in the FE parametric study .....	88
Figure 4-5: Soil type and dimensions considered in the FE parametric study.....	88
Figure 4-6: Pile group configurations considered in the FE parametric study .....	89
Figure 4-7: Different parameter considered in the FE parametric study .....	89
Figure 4-8: Effect of pile spacing on $\gamma$ factor for different pile configurations and failure scenarios a) 5 piles; b) 7 piles; c) 9 piles .....	95
Figure 4-9: Flow chart presenting the framework of calibrating resistance factor for pile group foundations based on M value .....	97
Figure 4-10: Calibrated resistance factor for 5 piles in a pile group foundation for different DL/LL a) 1; b) 2; c) 3; d) 4 .....	102
Figure 4-11: Calibrated resistance factor for 7 piles in a pile group foundation for different DL/LL a) 1; b) 2; c) 3; d) 4 .....	103
Figure 4-12: Calibrated resistance factor for 9 piles in a pile group foundation for different DL/LL a) 1; b) 2; c) 3; d) 4 .....	104





## List of Abbreviations, Symbols, and Notations

SPT	Standard penetration test
CPT	Cone penetration test
Q	Pile axial capacity
$W_p$	Weight of the pile
$Q_s$	Frictional resistance of the pile
$Q_p$	Tip resistance of the pile
STL	Static load test
$\delta$	Pile settlement
P	Applied Load
L	Pile Length
A	Pile cross-sectional area
B	Pile Diameter
$E_p$	Young modulus of the pile
$Q_g$	Ultimate capacity of the group
$Q_u$	Ultimate capacity of individual pile
$\eta$	Group efficiency factor
PIT	Pile integrity test
LSD	Limit state design
WSD	Working stress design
NBCC	National building code of Canada
OHBDC	Ontario highway bridge design

C3D8R	Continuum stress/displacement 8 node linear brick reduced integration element
C3D8	Continuum stress/displacement 8 node linear brick full integration element
C3D20R	Continuum stress/displacement 20 node linear brick reduced integration element
H	pile cap width
$E_s$	Young modulus of the soil
$\nu_s$	Poisson's ratio of the soil
c	Cohesion of the soil
$\Phi$	Internal friction angle of the soil
$\Psi$	Dilation angle of the soil
CPDM	Concrete damage plasticity model
$f_c'$	28-day compressive strength of concrete
$\lambda$	Redistribution factor
$\sigma_3$	Effective normal stresses
$P_a$	Atmospheric pressure
$K_a$	Coefficients of active lateral earth pressure
$K_o$	Coefficients of rest lateral earth pressure
$K_p$	Coefficients of passive lateral earth pressure
$\gamma_s$	Dry unit weight of the soil
$I_p$	Moment of inertia of the Prototype
$I_m$	Moment of inertia of the model
$\sigma_{ci}$	Unconfined compressive strength
mi	Intact rock parameter

GSI	Geotechnical strength index
D	Disturbance factor
mb,a,s	Rock mass parameters
$E_m$	Rock mass modulus of elasticity
$\sigma_{3max}$	Upper limit confining stress
CDG	Completely decomposed granite
UCS	Unconfined compressive strength
FEA	Finite element analysis
$M_p$	Moment at the neutral axis
y	Perpendicular distance to the neutral axis
I	Bending inertia of the pile
AASHTO	American association of state highway and transportation officials
ULS	Ultimate Limit state
SLS	Serviceability Limit State
$P_{f,sysm}$	Probability of failure of the system
M	The number of piles the system can accommodate prior to failure
n	Number of piles
$\gamma$	System-based equivalent pile safety factor
$\beta_i$	Individual pile target reliability index
$\beta_s$	Target reliability index of the system
$\emptyset$	Resistance factor

COV	Coefficient of variation
$\lambda$	Bias ratio
$\gamma_D$	Dead load factor
$\gamma_L$	Live load factor
FS	Equivalent factor of safety

## INTRODUCTION

---

### 1.1 Overview

Failure of structures such as buildings, bridges and tunnels can have catastrophic consequences in terms of human and economic losses. Structures may collapse due to the failure of one or more of its elements, including its foundation. However, foundation failure usually leads to devastating consequences such as complete failure of the system. In practice, many structures are supported by groups of piles, with each group connected by a common pile cap that uniformly distributes the load to the piles within the group.

The reliability of pile group foundations may be significantly different to single pile foundations owing to pile redundancy and pile cap rigidity, where the failure of an individual pile in the group does not necessarily lead to the failure of the system (e.g. Zhang et al., 2001, Paikowsky et al., 2004, Klammler et al., 2013, Oudah et al., 2019). Understanding the pile group behavior and its failure mechanism is crucial to safe yet cost-effective design of pile foundations. Meanwhile, common design practice is to assume that all piles are well constructed as per design and that the soil around and underneath all piles has the idealized strength and stiffness considered in the design. Such assumptions may be valid in the many sites with adequate construction practices and uniform soil conditions across the site. However, site inspections and quality control assurance instructions are not strictly followed in some construction sites (Cunha et al., 2010). A survey conducted by Baker (1994) concerning the U.S. practice in design and construction of drilled pile foundations revealed that 75% of investigated piles were practically defective to some extent.

In general, two approaches are used for the design of structures and foundations: Limit State Design (LSD) and Working Stress Design (WSD). Limit State Design is a rational probabilistic method that accounts for uncertainties associated with design parameters, while the WSD approach relies more on professional judgment and experience. Over the past two decades, there has been a noticeable shift in North American geotechnical design codes towards reliability-based design (e.g. Becker, 1996a, 1996b, Paikowsky et al., 2004, AbdelSalam et al., 2012, Phoon and Retief, 2016,

Oudah et al., 2019). Correspondingly, numerous studies have been conducted involving system reliability analysis in geotechnical engineering (e.g. Zhang et al., 2001, Paikowsky et al., 2004, Kwak et al., 2010, Abdelsalam et al., 2011, Naghibi and Fenton, 2017, Naghibi and Fenton, 2017). However, most studies did not consider unification of reliability index between the super-structure and sub-structure (foundation).

Therefore, the primary focus of this research is on investigating the behavior of defective pile group foundations considering a unified reliability index for both the structure and its foundation. This is achieved by understanding the behavior of defected pile group foundations and calibrating resistance factors for redundant pile group foundations. System-based reliability analysis is then conducted taking into consideration the unification of sub and super-structures

## 1.2 Research Objectives and Methodology

In order to achieve the stated objectives of the study, two main parts are undertaken. In the first part, a comprehensive parametric investigation is conducted utilizing the finite element program ABAQUS/Standard to examine the performance of pile group foundations when one or more piles fails in the group geotechnically. The analyses evaluated the group capacity and load-redistribution, and rotation and bending moment of the piles. In the second part, a new system-based reliability method proposed by Oudah et al. (2019) utilized the findings of the parametric study to determine the number of piles that can fail prior to failure of the group, and to calibrate the resistance factors for redundant group piles. The methodology incorporates a system-based equivalent pile safety factor,  $\gamma$ , with the objective of unifying the target reliability index for sub-structure and super-structure

## 1.3 Outline of Thesis

This thesis is structured following the “Integrated Article “format. In the current chapter, a general overview, objective and methodology of the research are provided. The remainder of the thesis is divided into four chapters as follows.

**Chapter 2:** This chapter provides a general background of the topics covered in this study, and reviews existing literature related to the studies of defected pile group foundations and the reliability analysis in geotechnical engineering.

**Chapter 3:** This chapter investigates the performance of defected pile group foundations in terms of its capacity, load distribution, rotation, and bending moment. A comprehensive three-dimensional non-linear finite element analysis was conducted for different pile group configurations and different failure scenarios in medium dense to dense sandy soil.

**Chapter 4:** In this chapter, the results obtained from the analyses reported in Chapter 3 were utilized in a refined approach to calculate the system-based equivalent pile safety factor,  $\gamma$  for axially loaded pile groups, which is crucial for determination of appropriate resistance factors. The resistance factors for three different pile group configurations (5 piles, 7 piles, 9 piles) installed in sand were presented for different design methods and different structural applications utilizing first-order second-moment reliability method (FOSM). The results of the study showed that the pile spacing is the most influential factor on  $\gamma$ .

**Chapter 5:** This chapter summarizes the research results and findings, as well as recommendations for future work.

## 1.4 References

- AbdelSalam, S.S., Ng, K.W., Sritharan, S., Suleiman, M.T., Roling, M., 2012. Development of LRFD Procedures for Bridge Pile Foundations in Iowa — Volume III: Recommended Resistance Factors with Consideration of Construction Control and Setup, Iowa Department of Transportation. <https://doi.org/10.13140/RG.2.1.2434.6080>
- Abdelsalam, S.S., Sritharan, S., Suleiman, M.T., 2011. LRFD resistance factors for design of driven H-piles in layered soils. *J. Bridg. Eng.* [https://doi.org/10.1061/\(ASCE\)BE.1943-5592.0000253](https://doi.org/10.1061/(ASCE)BE.1943-5592.0000253)
- Baker, C.N., 1994. Current U. S. design and construction practices for drilled piers, in: *Proceeding International Conference on Design and Construction of Deep Foundation*. pp. 305–323.
- Becker, D.E., 1996a. Eighteenth Canadian geotechnical colloquium: Limit states design for foundations. Part II. Development for the national building code of Canada. *Can. Geotech. J.* <https://doi.org/10.1139/t96-125>
- Becker, D.E., 1996b. Eighteenth Canadian geotechnical colloquium: Limit states design for foundations. Part I. An overview of the foundation design process. *Can. Geotech. J.* <https://doi.org/10.1139/t96-124>
- Cunha, R.P. Da, Cordeiro, A.F., Sales, M.M., 2010. Numerical assessment of an imperfect pile group with a defective pile in both initial and reinforced conditions. *Soils and Rocks* 33(2), 81–93.
- Klammler, H., McVay, M., Herrera, R., Lai, P., 2013. Reliability based design of driven pile groups using combination of pile driving equations and high strain dynamic pile monitoring. *Struct. Saf.* 45, 10–17. <https://doi.org/10.1016/j.strusafe.2013.07.009>
- Kwak, K., Kim, K.J., Huh, J., Lee, J.H., Park, J.H., 2010. Reliability-based calibration of resistance factors for static bearing capacity of driven steel pipe piles. *Can. Geotech. J.* 47, 528–538. <https://doi.org/10.1139/T09-119>
- Naghibi, F., Fenton, G.A., 2017. Target geotechnical reliability for redundant foundation systems. *Can. Geotech. J.* 54, 945–952. <https://doi.org/10.1139/cgj-2016-0478>
- Oudah, F., El Naggar, M.H., Norlander, G., 2019. Unified system reliability approach for single and group pile foundations – Theory and resistance factor calibration. *Comput. Geotech.* 108, 173–182. <https://doi.org/10.1016/j.compgeo.2018.12.003>
- Paikowsky, S.G., Bjorn, B., MaVay, M., Nguyen, T., Kuo, C., Baecher, G., Ayyub, B.M., Stenerseen, K., O'Malley, K., Chernauskas, L., O'Neill, M., 2004. *Transportation Research Board (TRB), Washington D.C., USA, NCHRP REPORT 507.*



Phoon, K.K., Retief, J. V., 2016. Reliability of Geotechnical Structures in ISO2394, Reliability of Geotechnical Structures in ISO2394. CRC Press/Balkema, London, UK.  
<https://doi.org/10.1201/9781315364179>

Zhang, L., Tang, W.H., Ng, C.W.W., 2001. Reliability of axially loaded driven pile groups. J. Geotech. Geoenvironmental Eng. 127, 1051–1060. [https://doi.org/10.1061/\(ASCE\)1090-0241\(2001\)127:12\(1051\)](https://doi.org/10.1061/(ASCE)1090-0241(2001)127:12(1051))

## LITERATURE REVIEW

---

### 2.1 Background

Pile foundations are structural members that transfer the loads from superstructure to competent soil layers below ground surface. Pile foundations are typically required as an alternative to shallow foundations when the load demand (axial compression load, axial tension load, lateral load) can't be supported due to unfavorable soil conditions near the ground surface. Pile foundations are classified into three main types based on their load transfer mechanism: frictional piles (aka floating piles), end bearing piles, and combined end bearing and frictional piles. For frictional piles the load is transferred to the piles by the shear resistance developed at the pile-soil interface. For end bearing piles, the total applied load is resisted by soil bearing at the pile base. Figure 2-1 shows the load transfer mechanism for a combined frictional and end bearing pile type.

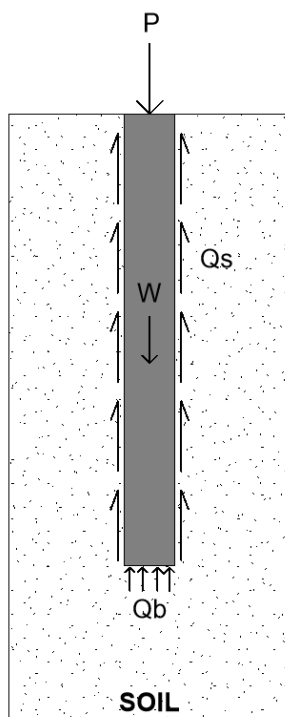


**Figure 2-1: Load transfer mechanism for a single pile foundation**

Canadian Foundation Engineering Manual (2006) categorized pile foundations into six main types based on their installation method: driven piles, bored piles, cast in-situ piles, jetted piles, helical torqued-in piles, and augured piles. Driven piles and cast-in place piles are widely used due to the ease and speed of their installation and long experience with their design and construction methods. In common practice, pile foundations are usually used in groups that consist of piles that are connected at the pile head with a pile cap. The main function of the pile cap is to ensure load distribution among the piles within the group and uniform settlement of the foundation. In the current practice, the determination of the ultimate axial capacity of the pile group foundation relies primarily on the capacity of a single pile foundation.

The prediction of axial capacity of a single pile can be evaluated using two main approaches: static and dynamic. Static methods include empirical methods used for the preliminary design phase or more rigorous methods to determine the pile configuration (length and diameter) and number of piles in the group. The empirical method correlates the side friction and end bearing of the pile with in-situ soil properties utilizing empirical correlations (in-situ tests) such as: standard penetration test (SPT) or cone penetration test (CPT) (Meyerhof, 1976). Alternatively, the pile capacity can be calculated using simple theoretical and semi-empirical equations (Nordlund method,  $\beta$  method, Meyerhof method) by utilizing the strength of the soil, where the pile capacity can be calculated according to Equation (2.1) proposed by (Dennis, 1982):

$$Q + W_p = Q_s + Q_p \quad (2.1)$$

Where  $Q$  is the axial pile capacity,  $W_p$  is the weight of the pile,  $Q_s$  is the frictional resistance of the pile, and  $Q_p$  is the tip resistance of the pile. Generally, the frictional resistance for piles installed in sand is typically fully mobilized at small displacement ranging from 5 to 10 mm (Kulhawy, 1984). In contrast, the pile end bearing resistance is usually fully mobilized at considerably larger displacements. According to Vesic (1977), tip resistance is fully mobilized at almost 8% of the pile diameter. On the other hand, Dynamic methods are based on wave propagation analysis of dynamic excitation due to the impact of hammer during pile driving or high strain testing after pile installation.

## 2.2 Static capacity of pile foundations

### 2.2.1 Interpretation of static capacity of pile foundations

In pile foundation design, the failure of the pile is usually determined using a specific failure criterion interpreted from a static load test (SLT). Several methods have been proposed in the literature to determine the axial capacity of piles from load testing. However, the axial capacity values derived from different methods vary significantly (Fellenius, 1980). For, instance interpretation techniques such as ultimate loading at 10% (Terzaghi, 1942), and 5% the pile diameter or at 25.4 mm don't take into consideration the elastic shortening of piles, which can impact capacity values of long piles but negligible impact for short piles (Fellenius, 2001). This section discusses the most commonly used load testing interpretation methods: Davisson's criterion, Chin-Kondner's, DeBeer log-log method, Tangent intersection method.

#### **Davisson criterion**

The Davison's failure criterion (Davisson, 1972) is widely used to determine the axial capacity of driven piles in North America. The method was proposed especially along with the quick loading test procedure, and gives over conservative estimate of the capacity for slow load test procedures (Fellenius, 2001). One of the main advantages of the method, it is an objective method, where the axial capacity of the pile can be predicted considering the pile elastic shortening and a specified permanent settlement. However, Davison's method underestimates the axial capacity of small diameter piles, less than 610 mm (Hannigan et al. 2016). The Davisson criterion defines the axial capacity of the pile as the load corresponding to a settlement given by:

$$\delta = \frac{PL}{AE} + 4 \text{ mm} + \frac{B}{120} \quad (2.2)$$

Where  $\delta$  is the final settlement, B is the pile diameter, P is the applied load, L is the length of the pile, A is the pile cross-section area, E is the pile Young's modulus. The first parameter (i.e.,  $\frac{PL}{AE}$ ) accounts for the elastic shorting of the pile. The second parameter accounts (i.e., 4 mm) for side friction of the pile, in sand 5 to 10 mm are required to fully mobilize the side friction of the pile.

Finally, the parameter  $\frac{B}{120}$  accounts for the end bearing of the pile. Figure 2-2 illustrates graphical representation of Davisson's failure criteria method.

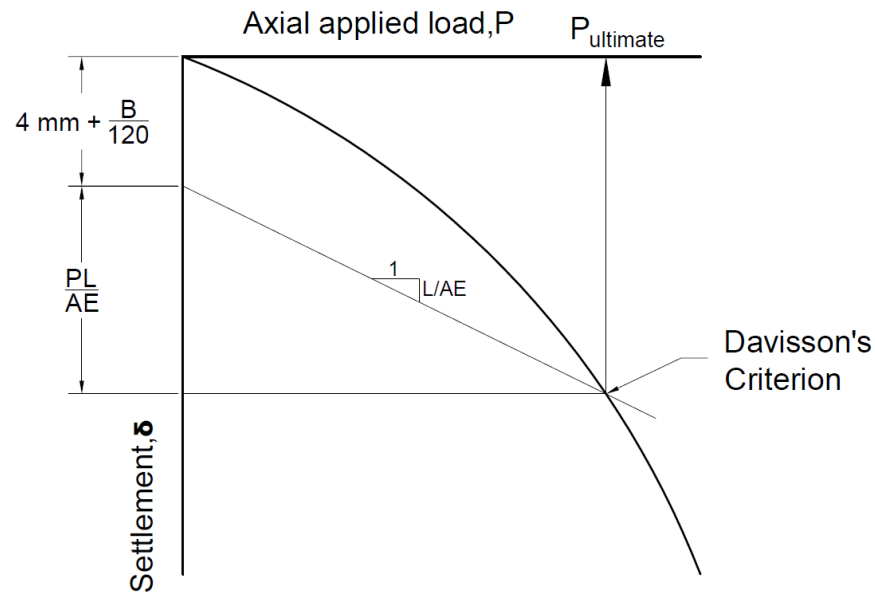


**Figure 2-2 : Graphical representation of Davisson's failure criteria method**

### **Chin-Kondner's Method**

Chin's method (Chin and Vail, 1973) is proposed to work for both slow and quick loading procedures (Fellenius (2001)). However, the load test must be performed at an equal loading increment. The method determines the axial capacity of the pile from a load displacement curve by separating the side friction and end bearing of the pile using "stability plot". Chin and Vail (1973) defined the ultimate capacity,  $P_u$  of the pile as the inverse of the linear trend line slope relating the ratio of pile head settlement to pile head load to the pile head load. Figure 2-3 presents a graphical representation of Chin-Kondner's method.

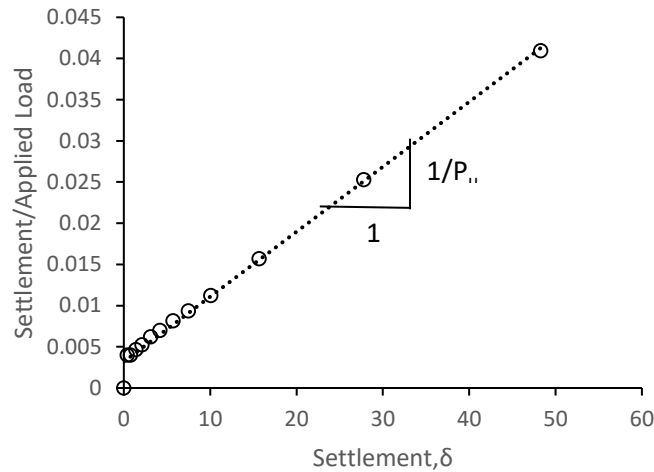


**Figure 2-3 : Graphical representation of Chin-Kondner's method**

### **DeBeer log-log method**

This method is usually implemented when the trend of the load displacement curve is difficult to recognize (Fellenius, 2001). To overcome this problem, the data should be drawn utilizing a logarithmic scale rather than a linear one. The De Beer Yield Load (DeBeer, 1970) is defined as the intersection between two straight portions of the logarithmic scale graph as shown in

Figure 2-4. One of the main draw backs of the method is that the two lines can't be detected clearly in some cases.

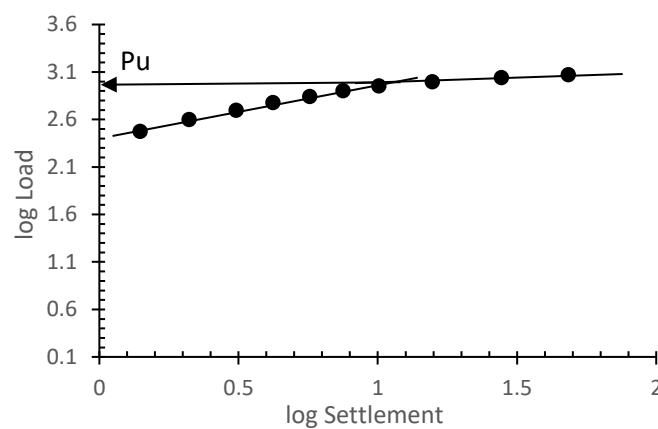


**Figure 2-4 : Graphical representation of DeBeer log-log method**

## Tangent intersection method

Butler and Hoy (1977) defined the pile ultimate capacity as the load corresponding to the intersection of two tangent lines to the load settlement curve obtained from the pile load test; The first line is tangential to elastic compression line portion and the second line is tangential to the plastic region of the load settlement curve. The main disadvantage of the method is that it doesn't account for the elastic shortening of the pile, which makes not suitable for long piles. Figure 2-5 shows an example of tangent intersection method.

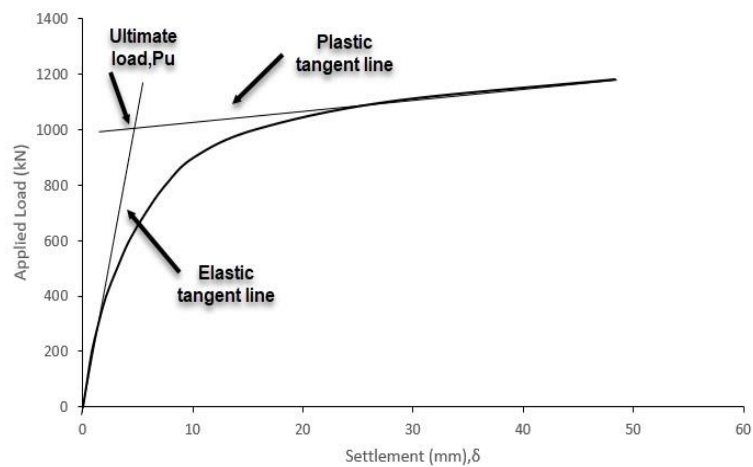


**Figure 2-5 : Graphical representation of tangent intersection method**

Table 2-1 compares the different load interpretation methods discussed.

**Table 2-1: Different interpretation methods for ultimate load (AbdelSalam et al., 2012)**

Method	Recommended pile type	Recommended SLT type	Pros	Cons
Davisson's method	Driven piles and Franki piles	Quick	objective method to determine the failure load	Underestimates the capacity for small diameter piles (< 610 mm).
Chin's method	-	Quick and Slow	-	requires equal load increments. Overestimates pile capacity.
De Beer's method	-	Slow	-	Subjective method. Difficult to detect intersection point between two lines.
Tangent intersection method	Bored, small diameter and belled piles	Quick	interpreted load is close to actual failure load	not suitable for long piles



## 2.3 Pile group behavior

The behavior of closely spaced pile groups differs from the single pile behavior, especially for frictional piles, due to the pile-soil-pile interaction (ie. group effect). Pile groups usually experiences larger settlement compared to singles piles if the soil underneath the pile toe is compressible. This is because, the stresses transferred by piles to the soil will overlap (Braja M. Das, 2011) as shown in Figure 2-6.

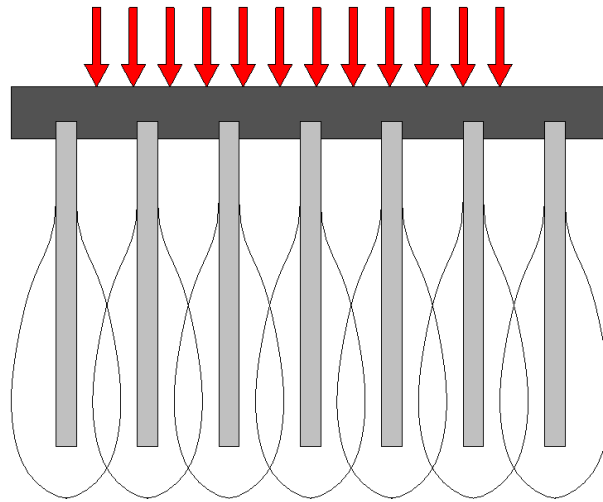


**Figure 2-6: Stress overlap in pile group foundations**

The pile-soil-pile interaction may eventually lead to the reduction of the bearing capacity of the pile group, especially for piles installed in cohesive soils. In this case, the capacity of the pile group is less than the sum of capacities of individual piles within the group:

$$Q_{g(u)} = \eta \sum Q_u \quad (2.3)$$

Where  $Q_{g(u)}$  is the ultimate capacity of the group,  $\eta$  is a group efficiency factor, and  $Q_u$  is the ultimate capacity of individual pile.

However, for groups of piles driven into cohesionless soil, group effect may in fact increase the performance of the system, where the capacity of the group is equal or greater than the summation

of individual pile capacities ( $\eta = 1$  or  $\eta > 1$ ) due to densification of soil around the pile, which eventually leads to the increase of lateral earth pressure around the pile. In this case, the group capacity is given by:

$$Q_{g(u)} = \sum Q_u \quad (2.4)$$

Pile group behavior can be affected by pile-soil-pile interaction and pile cap-soil-piles interaction. This is shown in Figure 2-7: pile-soil-pile interaction (eg. free-standing pile group) and interaction between piles and the pile cap for typical pile group foundations; and cap-soil-pile interaction for piled raft. The main difference between the two interaction methods lies in the relative rigidity of the pile cap and associated load-transfer mechanism. For a free-standing pile group, the pile cap is designed to be relatively rigid and links the piles together, but the group capacity is primarily derived from the individual piles within the group. Whereas for pile raft foundations, the bearing capacity of the group is dominated by the contribution of the pile cap resting on the soil, rather than the individual piles within the group. In this case the pile cap and the piles are designed together to ensure that the allowable settlement is not exceeded.

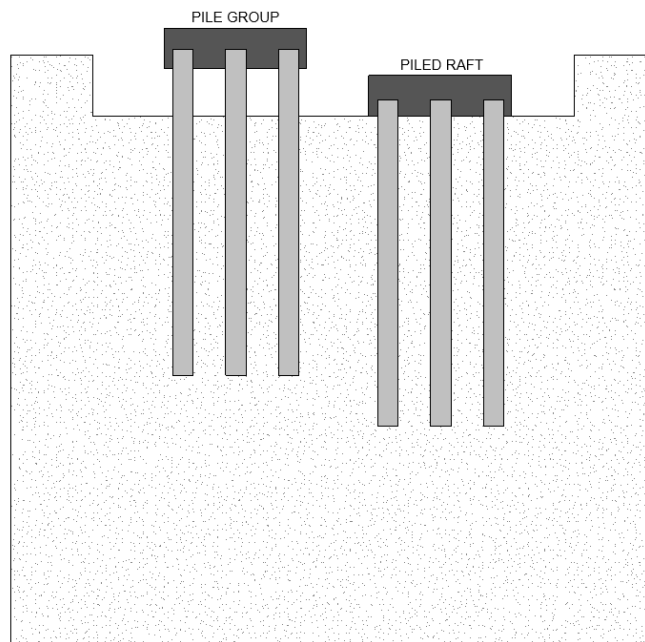


**Figure 2-7: Example of Pile group and pile raft systems**

Vesic (1967) performed static load tests on 4 and 9 pile group foundations driven in sand for different pile spacing 2D, 3D, 4D and 6D. Two different test groups have been carried out. The first group of tests was performed on free-standing pile groups (ie., pile cap is not rested on soil). The second test group was conducted on pile raft foundation (ie., pile cap is rested on soil). The results of Vesic (1967) study are shown in Figure 2-8, which demonstrates that the group efficiency increases with the increase of pile cap bearing capacity. The overall efficiency of the group increases from 1.3 for a free-standing 4-pile group to 1.7 for a 4-pile raft foundation. It is also worth noting that the efficiency of a free-standing pile group increases with the increase of spacing up to 3D but decreases slightly for higher spacing. On the other hand, the efficiency of pile raft foundation increases linearly with the pile spacing.

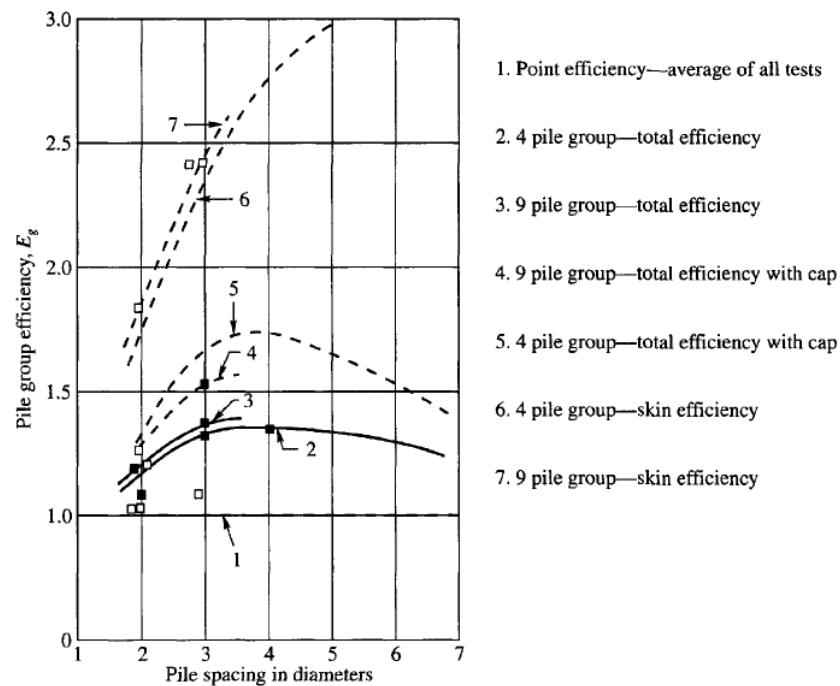


**Figure 2-8: Efficiency of the pile groups in sand (after Vesic, 1967)**

Several studies can be found in the literature related to the effect of pile spacing and group efficiency on the overall performance of pile group foundations. Lee and Chung (2005) studied experimentally the effect of pile group interaction on the overall performance of an axially loaded pile group in sand. They compared the behavior of a single pile and two different 3 x 3 pile groups to investigate the group effect consideration the installation method. They showed that the group interaction has increased the settlement for loosely spaced piles ( $< 3D$ ) but had minor effect on the widely spaced free standing pile groups ( $4D, 5D$ ). On the other hand, for a pile raft foundation, the capacity increased and performance improved as the pile spacing increased.

Mendoza et al. (2015) conducted finite element analyses along with field load testing to investigate the behavior of different pile group configurations in a silty sand soil. The result of the study demonstrated that the group efficiency was equal to unity. Elsamny et al., (2017) studied experimentally the behavior of a closely spaced pile group foundations (i.e.,  $3D$ ) in dense sand to evaluate the distribution of frictional resistance along the pile shaft and the effect of group interaction on the system performance. It was found the group efficiency of the system reached a value of 1.43.

## 2.4 Defected pile foundations

The design of deep foundations usually suffers some degree of uncertainties and imperfections that are not necessarily obvious to the site engineer which may eventually lead to the failure of the foundation. A survey conducted by Baker (1994) about the current U.S practice in design and construction of drilled pile foundations demonstrated that 75% of the investigated piles were defected. Therefore, it essential to assess the severity of the problem by understanding the overall performance of defected single piles and pile groups. Poulos (2005) summarized the main sources of imperfections that may affect the integrity and performance of pile group foundations in the following: natural geological sources, improper site investigation, and construction related aspects. The first type of imperfections usually arises due to the existence of unobserved boulders within a soil layer, sloping bedrock, cavities in limestone rock, the presence of continuous or non-horizontal soil layer or the existence of soft soil layer below a graded soil profile. Figure 2-9 summarizes the geological imperfection after Poulos (2005).

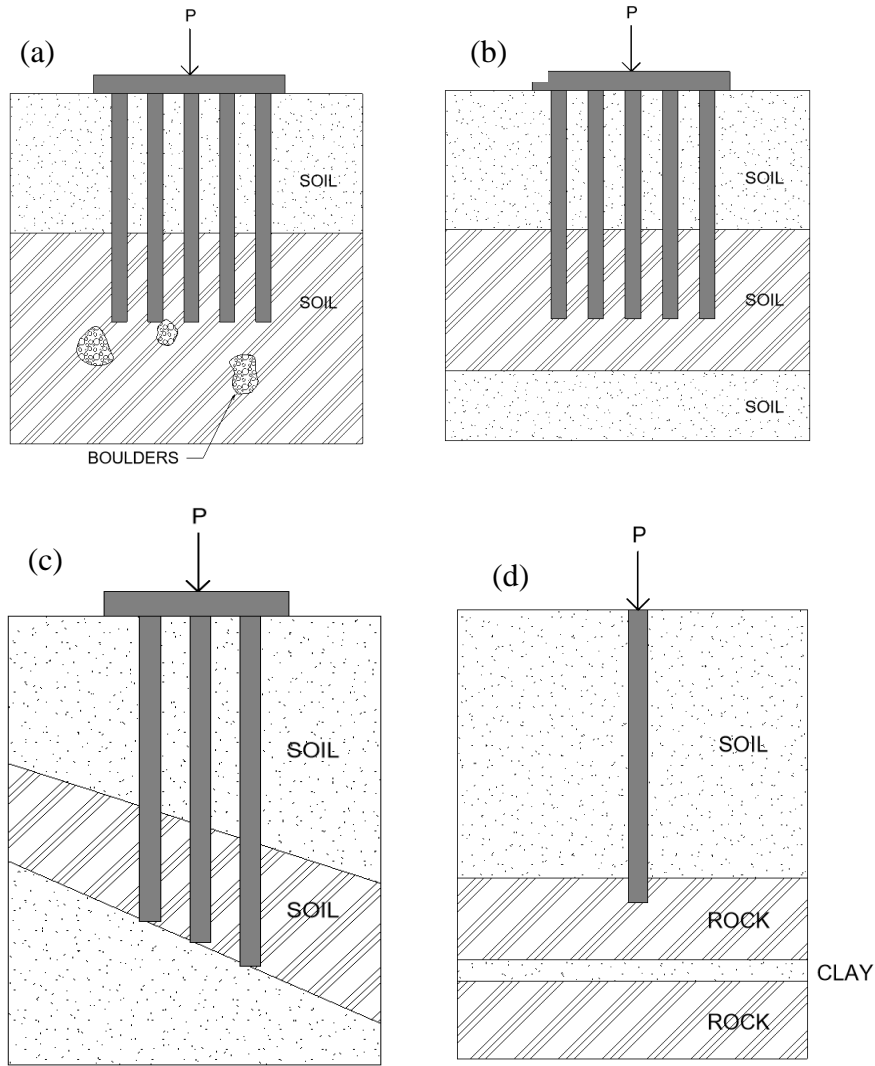


**Figure 2-9: Illustrations of geological imperfections a) piles founded on boulder; b) Compressible layer below founding layer; c) uneven soil layers; d) Clay seams below rock socket**

The second type of imperfections is related to inadequate in-situ soil investigation and testing as presented in Figure 2-10, which usually occurs by taking insufficient number and depth of bore holes or by using inadequate soil parameters which results from improper in-situ soil testing.

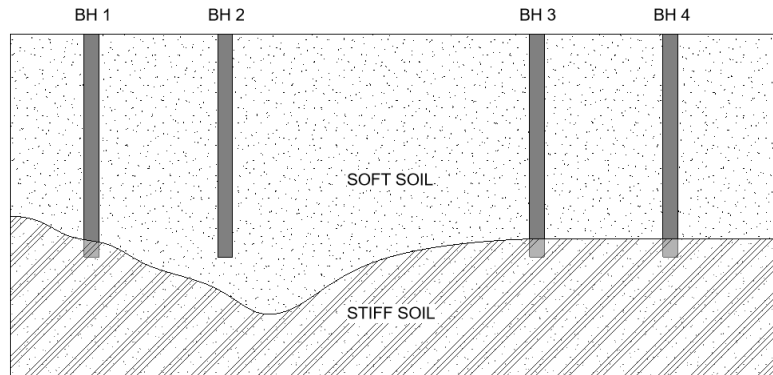


**Figure 2-10: Demonstration of imperfections arise from inadequate ground investigation**

The last type of imperfection is associated mainly with the execution process of the pile and it can be divided into two types: structural and geotechnical imperfections. The former type is related directly to the structural properties of the pile (stiffness, strength and size) which happens primarily due to inadequate site quality control and site inspection such as: necking in steel piles shaft, honeycomb and cracks in concrete piles, short piles, and damage in piles due excessive pile driving. The latter type is linked with misrepresenting in-situ soil conditions during design process or construction related problems which result in reducing the frictional and bearing resistance such as: soft base for bored piles due inadequate soft base inspection or the careless use of bentonite in bored piles. Figure 2-11 presents the construction related defects after Poulos (2005).

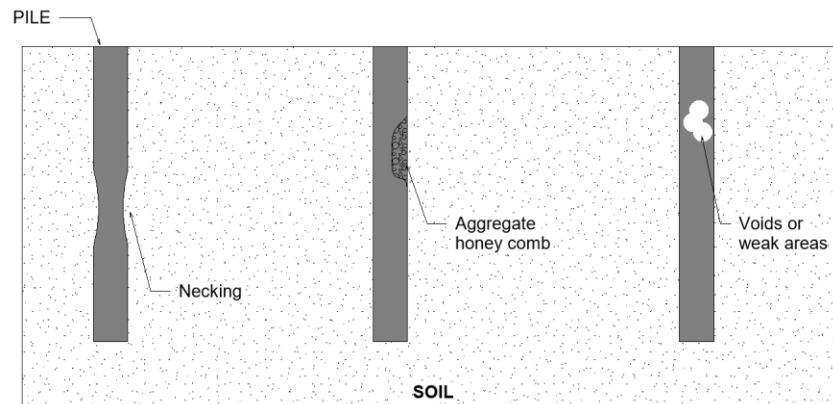


**Figure 2-11: Construction related defects (structural imperfections)**

Most of these defects, especially structural defects as shown in Figure 2-11, can be detected through pile integrity testing. Several methods can be found in the literature to perform a pile integrity testing such as: low strain impact pile integrity test, high strain dynamic testing, thermal integrity testing, cross-hole sonic logging, and parallel seismic testing method. This section will focus on the low strain impact pile integrity test or PIT. PIT is a non-destructive method used primarily for quality assurance for different types of piles to determine the integrity (flaws) and the length of piles. The test involves hammer striking and a receiver to evaluate the dynamic velocity response of the pile head (Liu et al., 2019). The flaws of the pile is detected assuming that the stress wave travels at a wave speed,  $c$  using the stress wave velocity propagation theory (Rausche et al., 1992).

$$C = \frac{\sqrt{E}}{\rho} \quad (2.5)$$

Where,  $E$  is the young modules of the pile, and  $\rho$  is the density mass.

Utilizing this concept, the pile flaw is determined by measuring the pile impedance,  $Z$  as presented in Eq (2.6):

$$Z = \frac{EA}{c} \quad (2.6)$$

Where  $Z$  is the pile impedance,  $E$  is the young modulus of the pile, and  $A$  is the cross-sectional area of the pile.

The change in the impedance of the pile is related directly to the change of the pile cross-sectional area, and the material consistency (Singh et al., 2019). In addition, the pile length is determined by checking velocity signal and measure the time laps between time of impact and the reflection at the top of the pile.

#### 2.4.1 Previous Studies on Defected Pile Foundations

Xu and Poulos (2000) reported the effect of discontinuities on the stiffens and load settlement response of cast-in-situ piles. Theses discontinuities are usually due to the presence of necking on the pile diameter. They concluded that the shapes of the load-settlement curve for the defected and

non-defected piles are similar. However, the necking caused a significant reduction of the pile capacity and stiffness.

Abdrabbo and Abouseeda (2002) studied the impact of construction procedures on the performance of bored piles. They observed that improper sub-surface soil investigation resulted in installing shorter pile which caused a noticeable differential settlement of the building.

Kong and Zhang (2004) and Poulos (2005) investigated the effects of structural and geotechnical deficiencies on the performance of single piles and pile groups. They concluded that the presence of a defected pile in a pile group foundation has much less critical consequence than single pile because the stiffer un-defected piles will carry the additional load, which reduces the significance of the imperfections. It is also worth noting that the existence of a failed pile in the pile group would lead to induced lateral deflection and cap rotation and associated bending moment at the adjacent un-defected piles.

Zhang and Wong (2007) conducted centrifuge testing to investigate the performance of defected single piles and bored pile group under vertical loading. Two types of defects were considered: group containing one pile with a soft toe and one group containing two short piles. The results showed that the existence of soft toe or short pile would lead to significant reduction in the stiffness and capacity of the pile group.

## 2.5 Reliability analysis in geotechnical engineering

Reliability analysis is a methodology of assessing failure events using probability analysis that are related to random variables (uncertainties). Failure is defined as an event that we have an interest of assessing its probability of occurrence (Becker, 1996b). The main parameter to evaluate the probability of failure of a system is the reliability index. Cornell (1969) pioneered the definition of reliability index as an indicator for safety measurement. Mathematically, reliability index,  $\beta_g$ , is defined as the number of standard deviations,  $\sigma_g$ , from the mean value,  $\mu_g$ , until the safety margin becomes zero as shown in Figure 2-12.



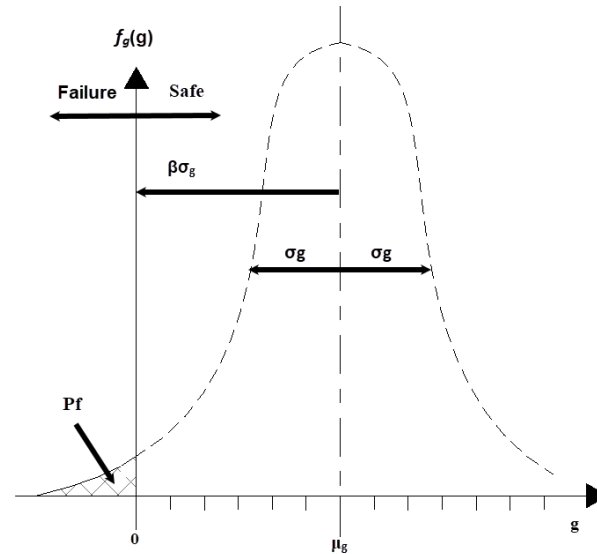


**Figure 2-12: Geometrical representation of the reliability index by Cornell (1969)**

Many studies have been devoted to prescribing target reliability indices and calibrating resistance factors for single piles and pile group foundations. Recent reliability studies in the literature of geotechnical engineering can be divided into two main streams; component-based reliability studies and system-based reliability studies. The component-based reliability studies evaluate the safety of each component or the failure mode solely in the system. For example, dealing with the individual pile frictional resistance or bearing resistance separately. On the other hand, the system-based reliability evaluates the safety of the whole system. For instance, determining the safety for multiple failure modes of sub-structural systems such as: the coupled behavior between the pile surface and the spatial variability of the soil medium (Phoon and Retief, 2016).

### 2.5.1 Limit state design vs Working stress design in geotechnical engineering

There are two methods to design super and sub-structural applications: Working Stress Design (WSD) and Limit State Design (LSD). The former method uses single global factor of safety that depends mainly on the engineering subjective judgment and does not account for uncertainties correlated with the applied load, material, and resistance performance which may lead to an un-

economical design (Becker, 1996a). On the other hand, the LSD approach has a more rational design philosophy that takes into consideration these aspects:

- uncertainties in resistance and loading. Probability-based design analysis is conducted to assure a fixed range of safety (Paikowsky et al., 2004)
- different design aspects. Partial factors of safety are applied to different load and resistance components.

LSD has been used in Canada by structural engineers since the 1970's as the main design approach in order to meet the requirements of the Canadian structural design codes such as NBCC and CSA. The LSD approach was first introduced to the geotechnical field in Europe in the 1950s. Canada followed suit shortly after by incorporating the LSD approach in the second edition of the 1983 Ontario highway bridge design (OHBDC). Most geotechnical engineering design codes and guidelines promote the use of LSD as a more rational design philosophy to guarantee the serviceability and safety of structures (Allen, 1975); however, most geotechnical engineers still apply the conventional WSD approach. A statistical survey done by Paikowsky et al. (2004) in the United States shows that 90% of geotechnical designers were still practicing WSD for designing foundations, whereas only 28% were using LSD approach. Perhaps, this is due to the lack of experience and confusion regarding the concepts of LSD. The inconsistency in using two different design approaches between the superstructure and substructure would lead to confusion and discontinuity in the factor of safety of the whole system. Therefore, many researchers have started to implement more reliability analysis theory to appeal to the geotechnical design committee.

### **2.5.2 Previous studies related to System-based reliability analysis.**

Although, most geotechnical problems are indeed system-based problems, the vast majority of reliability studies analyzed geotechnical problems utilizing component-based reliability. Perhaps, this is due to the complexity of the problem which is manifested in the interaction between superstructure and substructure, or the interaction between various elements in the system. Generally, geotechnical systems can be divided into two types: parallel systems and series systems. In parallel systems, the failure of one component will not lead to the system failure. In contrast, the failure of one component in a series system will lead to the failure of the whole system.

Tang and Gilbert (1993) described the pile group system performance by proposing system and redundancy factors using simple mathematical and numerical models. These factors were used to compare the performance of the pile group with the critical pile used in the design. Equation (2.7) shows the complexity factor (CF) and redundancy factor (RF) respectively:

$$CF = \frac{P(Y)}{P(Y_{crit})} \quad (2.7)$$

Where  $P(Y)$  is the probability a pile yielding and  $P(Y_{crit})$  is the probability of plastic hinge formation for the critical pile.

$$RF = \frac{P(Y)}{P(S)}, \quad 1 \leq RF < \infty \quad (2.8)$$

Where  $P(S)$  is the probability of system collapse.

A complexity factor (CF) equal to  $n$ , where  $n$  is the number of piles, indicates that each pile in the system will be treated equally which means that the failure of one pile will lead to the failure of the system. On the other hand, if CF is equal to 1 this indicates that failure of one pile will not necessarily lead to the failure of the system. The latter equation discusses mainly occurrence of redundancy in the system if RF is equal 1 that means that the system has no redundancy (non-redundant pile group) as RF increases this indicates that the system redundancy increases. Tang and Gilbert (1993) found that CF in most cases is equal to unity and RF ranges from 5 to 42. However, Tang and Gilbert (1993) overlooked an important factor in system reliability: which is the interaction between superstructure and sub structure. Becker (1996a, 1996b) and Paikowsky et al. (2004) considered the interaction between the superstructure and substructure by suggesting a target reliability index of substructure lower than the super structure as the failure of substructure will lead to the failure of super structure not the other way around. They also considered the interaction between the individual elements of the group system by proposing a prescribed target reliability index. Becker (1996b) suggested  $\beta = 2-2.5$  for single piles and pile groups. On the other hand, Paikowsky et al. (2004) suggested  $\beta = 2.33$  for non redundant pile groups (1 to 4 piles) and  $\beta = 3$  for redundant pile groups (5 and more piles). However, the suggested reliability indices are based on inconsistent probability of failures among different pile systems.

Zhang et al. (2001) calculated the reliability index of axially loaded driven pile group foundation accounting for the group and system effects (interaction between the super structure and substructure). Their method was based on a collected data base for static load tests on pile foundations utilizing a first-order reliability method (FORM) and the LSD to determine the reliability of driven pile group. They concluded that the interaction between the pile groups with superstructure would result in increasing the reliability of the system. For example, the reliability index of a pile group system without the system effects ranges from 2 to 4.1, whereas for a pile group system with a system factor equal to 1.25 the group index increases by 13% to reach 2.3 to 4.2. However, the system factor suggested by (Zhang, Tang, & Ng, 2001) accounts for the system as a whole and does not account for individual elements in the pile group system.

Kwak, Kim, Huh, Lee, & Park (2010) conducted reliability analysis for different static load tests of driven steel pipe piles by devolving a statistical data base for capacity of driven piles by comparing their measured (field) and predicted values using empirical formula (e.g. Meyerhof, 1976). The reliability index used in calculating the resistance factor of the driven pile foundation was based on the Monte Carlo Simulation (MCS) and the First-Order reliability method (FORM). The target reliability indices used for calibrating the resistance factors were 2 for single piles, 2.5 for non-redundant pile group (4 or less piles in pile group), and 2.33 for redundant pile groups (5 or more piles in pile group system). The author concluded that the reliability indices from both methods gave a statistically identical result. Although there was no good argument between the predicted and measured capacities. Kwak, Kim, Huh, Lee, & Park, 2010 have found that Davisson criteria performed the best.

Klammler et al. (2013) determined the resistance factor of driven pile groups utilizing dynamic equations and dynamic measurements by achieving a target reliability index to account for superstructure and substructure interaction and pile group redundancy. Klammler et al. (2013) used reliability index of single pile lower than the pile group system. However, decreasing the reliability index of single piles in a pile group system will not take into consideration all the uncertainties associated pile group foundation which may require a sophisticated Finite element modeling of the problem or an actual load testing.

Fenton et al. (2016) described a unified method for shallow and deep foundations to evaluate the probability of failure and resistance and consequence factors by considering the spatial variability of the soil, failure consequence and ground understanding. The resistance factor calibration depended mainly on the soil behavior. Nevertheless, the suggested methodology didn't account for foundation redundancy.

Naghibi & Fenton (2017) examined the occurrence of redundancy in individual foundations and system reliability for a redundant pile group foundation. They determined the individual target reliability index of the component of a pile group by utilizing a predefined target reliability index for system equal to 3. Nevertheless, they didn't consider the unification of the reliability induces for redundant and nonredundant pile group foundations.

In summary, it is worth noting that most of the previous studies have overlooked in their studies four main aspects:

- They used inconsistent probability of failure among different pile systems (single piles, redundant and non-redundant pile group foundation).
- No consideration was given to the interaction between the super structure and substructure
- The probability of failure used didn't take into the account the gross human error, which is a vital element in calculating the probability of failure. According to (Ellirtgwood, 1987) gross human error are responsible of 85% structural failures.
- There was no consideration for the unification of target reliability index of the super-structure and sub-structure.

## 2.6 References

- AbdelSalam, S.S., Ng, K.W., Sritharan, S., Suleiman, M.T., Roling, M., 2012. Development of LRFD Procedures for Bridge Pile Foundations in Iowa — Volume III: Recommended Resistance Factors with Consideration of Construction Control and Setup, Iowa Department of Transportation. <https://doi.org/10.13140/RG.2.1.2434.6080>
- Abdrabbo, F., Abouseeda, H., 2002. Effect of construction procedures on the performance of bored piles. *Geotech. Spec. Publ.* 1438–1454. [https://doi.org/10.1061/40601\(256\)103](https://doi.org/10.1061/40601(256)103)
- Allen, D.E., 1975. Limit States Design - a Probabilistic Study. *Can. J. Civ. Eng.* 2, 36–49. <https://doi.org/10.1139/175-004>
- Baker, C.N., 1994. Current U. S. design and construction practices for drilled piers, in: *Proceeding International Conference on Design and Construction of Deep Foundation*. pp. 305–323.
- Becker, D.E., 1996a. Eighteenth Canadian geotechnical colloquium: Limit states design for foundations. Part II. Development for the national building code of Canada. *Can. Geotech. J.* <https://doi.org/10.1139/t96-125>
- Becker, D.E., 1996b. Eighteenth Canadian geotechnical colloquium: Limit states design for foundations. Part I. An overview of the foundation design process. *Can. Geotech. J.* <https://doi.org/10.1139/t96-124>
- Braja M. Das, 2011. *Principles of Foundation Engineering*, Seventh. ed. Cengage Learning, Stamford, USA.
- Butler, H.D., Hoy, H.E., 1977. *Users Manual for The Texas Quick-Load Method for Foundation Testing*. Federal Highway Administration, Office of Development, Report No. FHWA-Tp-77-0, Washington, D.C.
- Canadian Geotechnical Society, 2006. *Canadian foundation engineering manual*. Richmond, B.C.
- Chin, F., Vail, A.J., 1973. Behavior of piles in alluvium, in: *Proceedings from the 6th International Conference on Soil Mechanics and Foundation Engineering*. pp. 47–52.
- Coduto, D.P., 2001. *Foundation design: principles and practices*. Prentice Hall.
- Cornell, C.A., 1969. A probability-based structural code, in: *Journal Proceedings*. pp. 974–985.
- Davisson, M., 1972. High Capacity Piles. *Proceedings, Soil Mech. Lect. Ser. Innov. Found. Constr.* ASCE 81–112.
- DeBeer, E., 1970. Proefondervindelijke bijdrage tot de studie van het grandsdraagvermogen van zand onder funderinger op staal. English version. *Geotechnique Vol. 20*, 387–411.
- Dennis, N.D., 1982. Development of correlations to improve the prediction of axial pile capacity.

University of Texas at Austin.

- Ellirtgwood, B., 1987. Design and construction error effects on structural reliability. *J. Struct. Eng. (United States)* 113, 409–422. [https://doi.org/10.1061/\(ASCE\)0733-9445\(1987\)113:2\(409\)](https://doi.org/10.1061/(ASCE)0733-9445(1987)113:2(409))
- Elsamny, M., Ibrahim, M.A., S.A., G., Abd-Mageed, M.F., 2017. Experimental Study on Pile Groups Settlement and Efficiency in Cohesionless Soil 6, 967–976.
- Fellenius, B.H., 2001. What Capacity Value to Choose from the Results a Static Loading Test. *Deep Found. Inst.*
- Fellenius, B.H., 1980. The analysis of results from routine pile load tests 13, 19–31.
- Fenton, G.A., Naghibi, F., Griffiths, D. V., 2016. On a unified theory for reliability-based geotechnical design. *Comput. Geotech.* 78, 110–122. <https://doi.org/10.1016/j.compgeo.2016.04.013>
- Hannigan, P.J., Rausche, F., Likins, G.E., Robinson, B.R., Becker, M.L., 2016. Design and Construction of Driven Pile Foundations. Federal Highway Administration Report No. FHWA-HI-05, Washington, D.C.
- K.J.Xu, H.G.Poulos, 2000. Measured and predicted axial response of piles with diameter discontinuities. *Geotech. Eng. J.* 31.
- Klammler, H., McVay, M., Herrera, R., Lai, P., 2013. Reliability based design of driven pile groups using combination of pile driving equations and high strain dynamic pile monitoring. *Struct. Saf.* 45, 10–17. <https://doi.org/10.1016/j.strusafe.2013.07.009>
- Kong, L., Zhang, L., 2004. Lateral or torsional failure modes in vertically loaded defective pile groups. *Geotech. Spec. Publ.* 625–636.
- Kulhawy, F.H., 1984. Limiting tip and side resistance: Fact or fallacy. *ASCE Spec. Conf. Anal. Des. Pile Found.* 80–98.
- Kwak, K., Kim, K.J., Huh, J., Lee, J.H., Park, J.H., 2010. Reliability-based calibration of resistance factors for static bearing capacity of driven steel pipe piles. *Can. Geotech. J.* 47, 528–538. <https://doi.org/10.1139/T09-119>
- Lee, S.H., Chung, C.K., 2005. An experimental study of the interaction of vertically loaded pile groups in sand. *Can. Geotech. J.* 42, 1485–1493. <https://doi.org/10.1139/t05-068>
- Liu, H., Wu, W., Jiang, G., El Naggar, M.H., Mei, G., Liang, R., 2019. Benefits from using two receivers for interpretation of low-strain integrity tests on pipe piles. *Can. Geotech. J.* 56, 1433–1447. <https://doi.org/10.1139/cgj-2018-0406>
- Mendoza, C.C., Cunha, R., Lizcano, A., 2015. Mechanical and numerical behavior of groups of screw (type) piles founded in a tropical soil of the Midwestern Brazil. *Comput. Geotech.* 67,

187–203. <https://doi.org/10.1016/j.compgeo.2014.09.010>

- Meyerhof, G.G., 1976. Bearing capacity and settlement of pile foundations. *J. Geotech. Eng. Div. ASCE* 102, 195–228.
- Naghibi, F., Fenton, G.A., 2017. Target geotechnical reliability for redundant foundation systems. *Can. Geotech. J.* 54, 945–952. <https://doi.org/10.1139/cgj-2016-0478>
- Paikowsky, S.G., Bjorn, B., MaVay, M., Nguyen, T., Kuo, C., Baecher, G., Ayyub, B.M., Stenerseen, K., O'Malley, K., Chernauskas, L., O'Neill, M., 2004. Transportation Research Board (TRB), Washington D.C., USA, NCHRP REPORT 507.
- Phoon, K.K., Retief, J. V., 2016. Reliability of Geotechnical Structures in ISO2394, Reliability of Geotechnical Structures in ISO2394. CRC Press/Balkema, London, UK. <https://doi.org/10.1201/9781315364179>
- Poulos, H.G., 2005. Pile behavior - Consequences of geological and construction imperfections. *J. Geotech. Geoenvironmental Eng.* 131, 538–563. [https://doi.org/10.1061/\(ASCE\)1090-0241\(2005\)131:5\(538\)](https://doi.org/10.1061/(ASCE)1090-0241(2005)131:5(538))
- Rausche, F., Likins, G., Shen, R.-K., 1992. Pile Integrity Testing and Analysis, in: Proceedings, 4th International Conference on the Application of Stress-Wave Theory to Piles. The Netherlands.
- Singh, B., Arora, V. V., Patel, V., Chowdhary, N., 2019. Non-destructive testing of bored piles using the low strain pile integrity method. *Indian Concr. J.* 98, 41–48.
- Tang, W.H., Gilbert, R.B., 1993. Case study of offshore pile system reliability. the 25th Annual OTC, Houston, Texas, U.S.A, 677–686.
- Terzaghi, K., 1942. Discussion of the Progress Report of the Committee on the Bearing Value of Pile Foundations. Proceedings, ASCE Vol. 68, 311–323.
- Vesic, A.S., 1977. Design of pile foundations. In National Cooperative Highway Research Program, Synthesis Highway Practice Report No. 42, Transportation Research Board, Washington, D.C.
- Vesic, A.S., 1967. Study of Bearing Capacity of Deep Foundations"Final Report. School of Civil Engg., Georgia Inst. Tech., Atlanta, U.S.A.
- Zhang, L., Tang, W.H., Ng, C.W.W., 2001. Reliability of axially loaded driven pile groups. *J. Geotech. Geoenvironmental Eng.* 127, 1051–1060. [https://doi.org/10.1061/\(ASCE\)1090-0241\(2001\)127:12\(1051\)](https://doi.org/10.1061/(ASCE)1090-0241(2001)127:12(1051))
- Zhang, L.M., Wong, E.Y.W., 2007. Centrifuge modeling of large-diameter bored pile groups with defects. *J. Geotech. Geoenvironmental Eng.* 133, 1091–1101. [https://doi.org/10.1061/\(ASCE\)1090-0241\(2007\)133:9\(1091\)](https://doi.org/10.1061/(ASCE)1090-0241(2007)133:9(1091))



## Chapter 3

## NUMERICAL INVESTIGATION OF DEFECTED PILE GROUP FOUNDATIONS

---

### 3.1 Introduction

Concrete cast-in-place and driven pile foundations are widely used to support a variety of structures, such as bridges, buildings and transmission towers, due to their cost efficiency and speed of their installation. Several pile design methods have been proposed in the literature to evaluate the axial capacity of driven piles and drilled shafts (e.g., Terzaghi, 1943, Meyerhof, 1976, Vesic, 1963). However, predicting the axial capacity of piles in sand is affected by significant uncertainties and design guidelines are not entirely consistent with the physical processes involved (Randolph et al., 1994). In addition, it is common for designers to assume ideal soil and pile conditions at the construction site. For example, it is often assumed that piles are installed in uniform homogeneous soil, while the soil is actually non-uniform plastic inhomogeneous material. Additionally, the construction procedure of cast-in-place concrete piles can affect the piles performance (Abdrabbo and Abouseeda, 2002). The construction procedure of cast-in-place piles involves drilling a large diameter borehole, then installing the reinforcement casing, and finally filling the borehole with concrete. To support the borehole from collapsing it is usually filled with “drilling mud” or bentonite. The excessive use of bentonite causes a very common phenomenon known as “mud cake”, where the mud (bentonite and soil) accumulates at the borehole wall and deposits at the bottom of the borehole. Depending on the thickness of the accumulated mud layer it may cause a huge reduction in the frictional resistance of the pile which can seriously compromise the integrity of the foundation (Zhang et al., 2009). Hence, it is necessary to investigate the behavior of defected pile foundations and evaluate its impact on the overall pile foundation capacity. Poulos (2005) categorized sources of pile imperfections into two main categories: natural imperfections (geotechnical defects) and construction imperfection (structural defects). The geotechnical defects are mainly due to inadequate soil characterization (e.g. wrong assumptions about soil profile) or due to natural geological sources (e.g. the existence of soft layers below the graded soil profile). Structural defects (e.g. necking in steel piles and cracks or honeycomb in concrete piles) are caused primarily by inadequate field quality control or by human

error. Another type of structural imperfection happens particularly in driven steel piles, when the pile experiences an excessive driving which causes a top pile head deformation known as “pile head mushrooms”. In this case the steel pile yields and eventually leads to total loss of stiffness.

The behavior of a pile group foundation differs from that of a single pile due to the pile-soil-pile interactions (i.e. group effect) which makes the problem even more complex. For pile group foundations, interference between zones of influence among piles lead to increased settlement and deflections for piles within the pile group foundation (Lv and Zhang, 2018). This complex behavior requires investigation of the problem using experimental testing and advanced numerical modeling, especially in the case of a defected pile or more within the group. However, very limited number of studies reported the performance of imperfect single pile foundations (e.g., Hobbs, 1957, K.J.Xu and H.G.Poulos, 2000, Tabsh and O’Neill, 2001, Petek et al., 2002, Albuquerque et al., 2017) and pile group foundations experimentally. Zhang and Wong (2007) evaluated the performance of a geotechnically defected 2x2 bored pile group foundation under vertical loading utilizing centrifuge testing. Two types of defects have been investigated: a group containing one pile with a soft toe and another group containing a short pile. The results of the study demonstrated that the existence of soft toe or short pile will lead to a substantial reduction of the stiffness and capacity of the pile group foundation.

Numerical analysis is increasingly used to investigate the behavior of single piles and pile groups instead of full-scale testing since physical tests are costly and time consuming. Numerous studies have been conducted for assessing the performance of pile group foundations using various numerical approaches (e.g., Yang and Jeremić, 2003, Moayed et al., 2013, Alnuaim et al., 2016, Lv and Zhang, 2018, El Sharnouby and El Naggar, 2018). These studies have demonstrated that numerical analysis can be a powerful tool for simulating complex geotechnical problems, including pile group foundations. Yet, very few studies can be found in the literature for problems related to numerical analysis of defected pile group foundations. Kong and Zhang (2004), Xu and POUIOS (2001), Poulos (1997, 2005), Cunha et al. (2007,2010) and Garcia et al. (2017) investigated the possible effects of structural and geotechnical deficiencies on performance of pile group foundations using numerical approaches. These studies concluded that the existence of a defected pile within a pile group foundation might lead to induced lateral deflection and cap

rotation, which could eventually cause an extra bending moment at the adjacent un-defected piles. It is worth noting that results of the preceding studies did not consider different failure scenarios.

This review clearly demonstrates that there is a need to investigate systematically the behavior and failure mechanisms of imperfect pile group foundations in case one or more piles in the system fail. In addition, there is a need to evaluate the impact of individual pile defects on different relevant factors of the group behavior including: bending moment at the pile heads, load redistribution, rotation of the pile cap and overall capacity of the group.

## 3.2 Objectives and Scope of Work

This study investigates the performance of defected pile group foundations numerically by evaluating the impact of failure of one or more piles on the performance of axially loaded redundant and non-redundant pile group foundations considering different failure scenarios. Failure considered in the analysis can be either strength-related or settlement-related failure. Strength-related failure is induced at the target pile by reducing its frictional and bearing capacity to zero. The settlement related failure is induced at the soil surroundings (sides and tip) of the target pile, which simulates a soil failure and increased settlement. These objectives will be achieved through a comprehensive parametric study using three-dimensional nonlinear finite element analysis of different pile configurations commonly used in building foundations.

## 3.3 Development of Numerical Models

The response of defected pile group foundations to vertical loading is analyzed employing the finite element method. The analyzed pile group problem is three-dimensional (3D) in nature. Thus, the soil and the pile group were simulated in 3D space utilizing the finite element program ABAQUS. In order to establish the load-displacement curves and the failure mechanisms of the examined pile groups, finite element models were developed and validated using two case histories. The verified modeling techniques are then used to establish suitable finite element models to analyze the response of pile groups with one or more defected piles.

### 3.3.1 Geometry and Boundary Conditions of Finite Element Models

The investigated problem involves typical pile group foundations supporting structural loads from building columns. ABAQUS library contains several types of elements in 3D, each type of element in the library can be characterized as shown in Figure 3-1 (SIMULIA, 2013b).

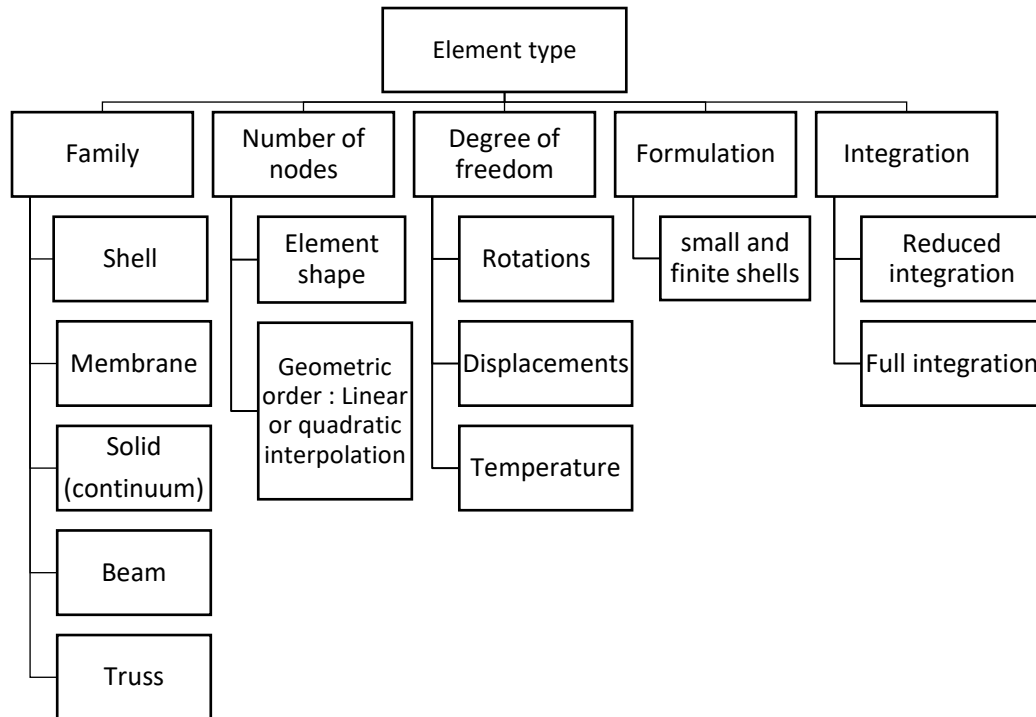


**Figure 3-1: ABAQUS element type characterization**

The selection criteria of the element type depend primarily on the nature and geometry of the problem. In addition, it should provide a balance between the computational time, accuracy and the meshing characteristics of the problem. In this study, solid elements were selected to model all the geometric components of the problem. The 3D solid elements library contains four main types: hexahedral, tetrahedral, wedge and pyramid elements. Each type of element can be either (reduced integration or full integration) linear First-order element or quadratic second-order elements. In linear elements, nodes are placed at the corner of element and don't contain intermediate nodes.

Linear elements are usually suggested when the problem contains high degree of mesh distortion or it includes a contact between two deformable bodies. In contrast, second order elements contain high order elements and are suitable for problems associated with complex geometry such as: curvatures or bending dominated problems. Although, second order elements may provide a more accurate results, they can be more computationally demanding.

Moreover, two main concerns should be considered in selecting an appropriate type of element: shear locking and hourglass. Shear locking is always a concern for fully integrated first-order tetrahedral, wedge and pyramid elements, especially for thin elements like beams subjected to pure bending. Shear locking occur when the element deforms under pure bending forces, where the edge elements must remain straight following Bernoulli role (plane section must remain plane) (SIMULIA, 2013b). In this case, the angle between the integration points is less than 90 degrees and the element detects shear strains instead of bending forces. This type of problem is solved by using a reduced integration method, where there is only one integration point in the element ideally at the center. On the other hand, hourglass problem is a concern for first-order reduced integration hexahedral elements. In hourglass, the element suffers mesh instability (ie., rigid body motion) and it does not cause any strain. To solve this problem, an artificial “hourglass control” stiffness can be added (SIMULIA, 2013b). Table 3-1 compares the different elements types in terms of their computational time.

**Table 3-1: Comparison in computational time for different geometric order and integration for a hexahedral element**

Element type	Relative CPU time
C3D8R	1
C3D8	1.25
C3D20R	31.22

Based on the discussion above the structural column, pile cap, soil, and piles were modelled using 8 nodes hexahedral, first order, reduced integration solid element (C3D8R).

The design of pile groups commonly assumes the pile cap does not transfer vertical load to the soil underneath it. Therefore, a 100 mm gap was set underneath the pile cap to prevent bearing of pile cap on soil beneath it. The connection between the pile cap and the piles was assumed to be fixed (i.e. pile cap can transfer moment to the piles). The structural concrete column was modeled as a rigid element since the response of the column does not impact the results. The column area was only used to transfer the load from the superstructure (building) to the substructure (pile cap and piles). The soil at the base of the model is restrained in all directions, while the sides are allowed to move in the vertical direction only.

### 3.3.2 Sensitivity analysis of effect of boundary conditions

A sensitivity analysis was conducted to determine the extent of the FE model boundaries. The depth and width of the soil layer will be represented in terms of multiples ( $X$ ) of the pile cap width ( $H$ ) as shown in Figure 3-2. The value of  $X$  ranged from 1 to 3 in the sensitivity analysis. The sensitivity analysis was conducted for only one FE model, and the findings were implemented in all models included in Figure 3-16 and Table 3-9. Tannant and Regensburg (2001) investigated the extent of the tire pressure and its influence zone within the soil and indicated that the boundaries of the FE model should extend to 1.0 times the width of the tire. This information can be used as a benchmark to gauge the results obtained from the FE sensitivity analysis since it is related to the context of the modeled piles. However, the results obtained from the sensitivity analysis indicated that boundary effects were eliminated only when  $X$  value reached 2 as shown in Figure 3-3.

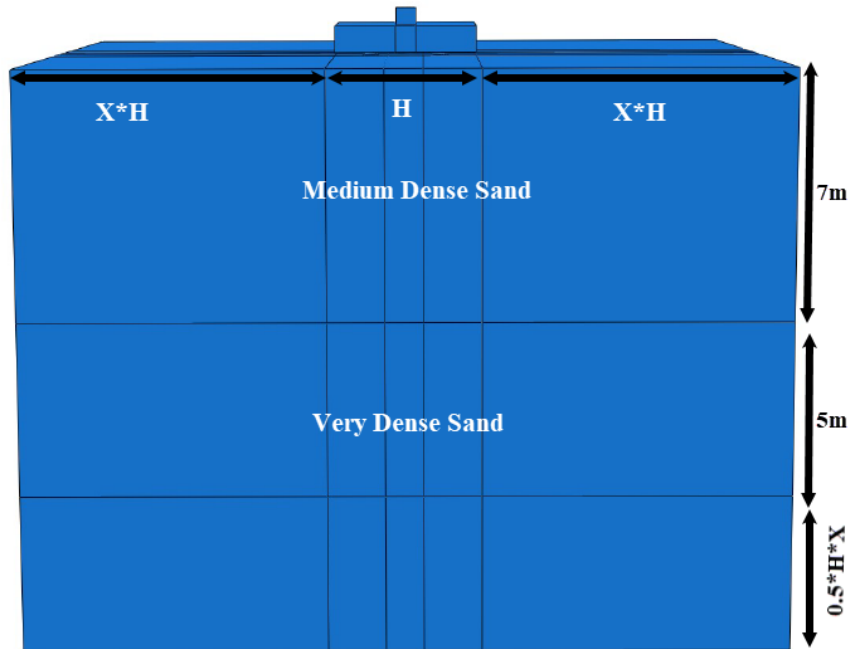


Figure 3-2: Variation of pile cap settlement with extent of vertical mesh boundaries

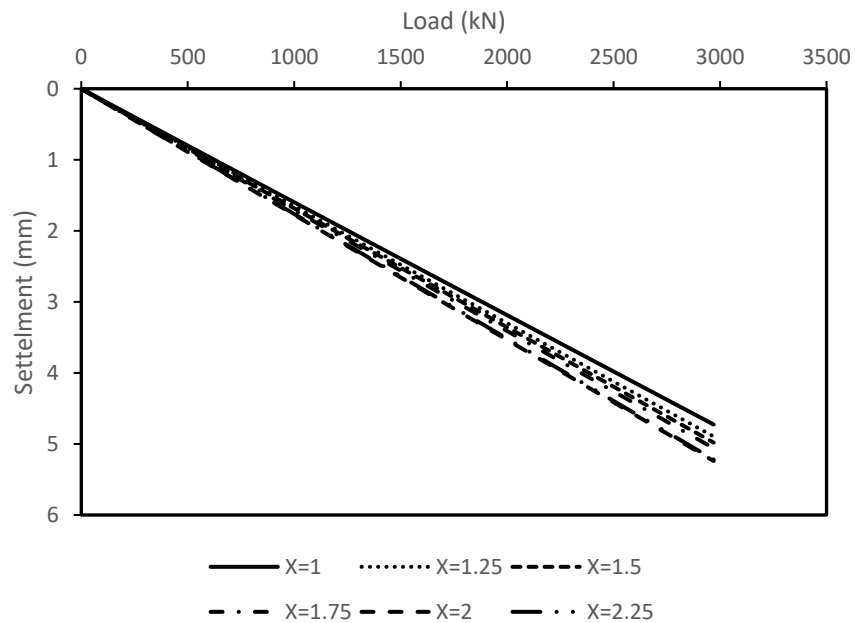
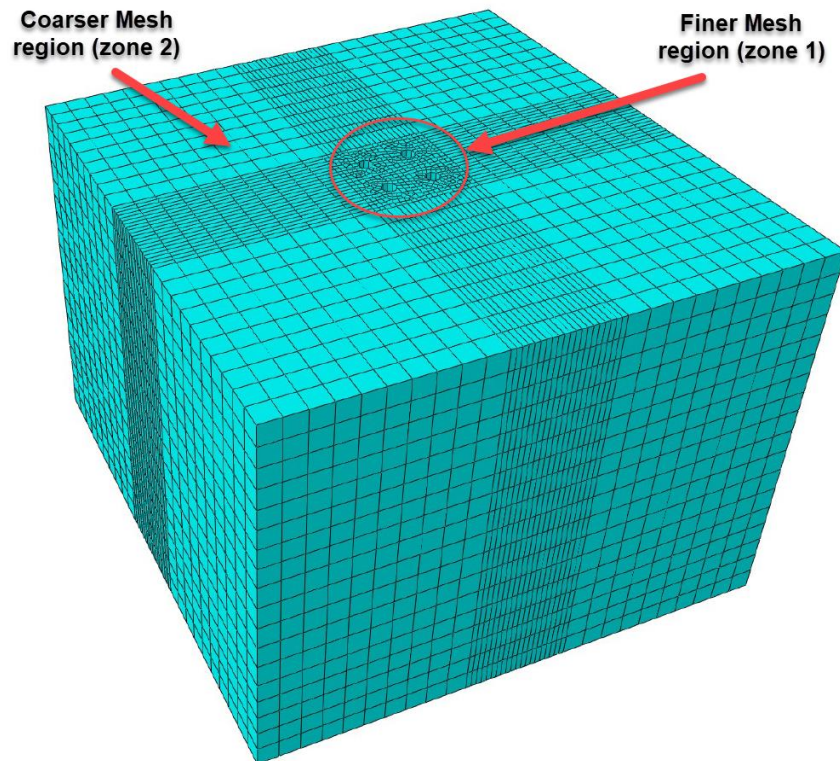


Figure 3-3: Variation of pile cap settlement with extent of vertical mesh boundaries

### 3.3.3 Sensitivity analysis of mesh density

The mesh density was optimized to yield accurate results while reducing the computational effort. The sensitivity analysis was conducted on one model as a benchmark, the density of the soil was selected and used to run the simulation. The soil block was discretized into two zones as shown in Figure 3-4 a fine mesh at zone 1 (pile-soil interface) and a coarse mesh at zone 2 (away from the piles). The mesh density was increased gradually at zone 1, and in each time the results were compared with the denser mesh until the change in pile cap settlement between two consecutive models is less than 1%. Figure 3-5 presents the mesh sensitivity study results. The optimum mesh density was selected based on the sensitivity analysis results to be 98,000 elements in total. A maximum aspect ratio of 10.5 for the element sides was set in all models to ensure a consistent FE results.



**Figure 3-4: General configuration of the finite element mesh used in the analysis**



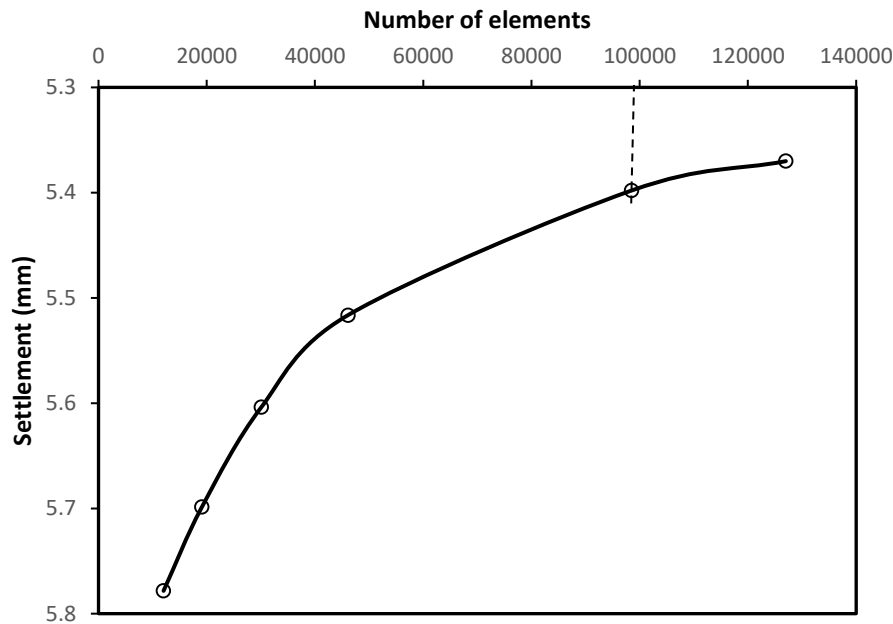


**Figure 3-5: Variation of pile cap settlement with number of mesh elements**

### 3.3.4 Pile-soil interface model

The pile-soil interface was simulated using the surface to surface contact pair method incorporated in ABAQUS, which is based on a penalty contact constraint. In this method, the tangential behavior between the pile element and adjacent soil element is defined by coulomb's frictional model. Two types of surfaces are defined in the model: master and slave surfaces; the former was defined for the more rigid material surface (i.e. piles). The latter was defined for the less rigid material (i.e. soil). No relative tangential behavior would occur at the pile soil-interface, unless the contact shear stresses have exceeded the critical shear stresses. The critical shear stress was defined as a function of the coefficient of friction ( $\tan \delta$ ). The friction coefficient was assigned a value of 0.57 or 0.7 for all models to represent the interface conditions between the soil and the steel piles. These values were assigned according to the suggested values by Canadian Geotechnical Society (2006). The normal behavior was also defined using the penalty method and was assumed to be "hard" contact with separation allowed.

### 3.3.5 Constitutive material model and model parameters

#### 3.3.5.1 Soil parameters and material model

The soil conditions considered in all numerical models were chosen to represent general cohesionless soil conditions, and the soil properties were obtained from the handbook of geotechnical investigation Look (2007) using the suggested range of values for medium dense sand and very dense sand. In order to simulate the sand densification during the installation processes for axially loaded driven piles, the coefficient of lateral earth pressure  $K_s$  was chosen based on the proposed values by for driven steel piles by Kulhawy (1984) and Mansur and Hunter (1970)

The behavior of sand was modeled as linearly elastic perfectly plastic material and its shear strength was simulated using Moher-coulomb failure criterion. The elastic behavior was defined by Young's modulus (E) and Poisson's ratio ( $\nu$ ). The plastic behavior of the model was controlled by the cohesion (c), internal friction angle ( $\Phi$ ) and dilation angle ( $\Psi$ ).

#### Pile Cap Material Model

The pile group foundations were designed for axial compression force only for the purpose of this study. The design of the pile cap was conducted in accordance with (CSA A23-14/A23.2-14, 2014). The concrete compressive strength was taken as 30 MPa. The yield strength of the reinforcing bars was considered 400 MPa. The pile cap reinforcements were modeled using elastic perfectly plastic material model. The reinforcement bars were treated as a uniaxial one-dimensional strain element embedded in concrete using beam elements as shown in Figure 3-6 and assuming perfect bond between the steel and concrete.

To accurately examine the redistribution of the forces for a code-compliant pile cap, the reinforced concrete pile cap was modeled using a concrete damage plasticity constitutive model (CPDM). The main advantage of utilizing such a model that it combines the behavior of concrete through damage factors (tensile cracking and compression crushing) and the behavior of steel using plasticity factors. Alfarah et al. (2017) developed a method to determine the damage variables of the CPDM model without the need for an experimental calibration. The model is mainly defined by the uniaxial compressive stress variation with the plastic strain, and the variation of uniaxial tension stress with cracking displacement as shown in Figure 3-6. Figure 3-7 displays the stress-strain relationship for tension and compression used in the model.

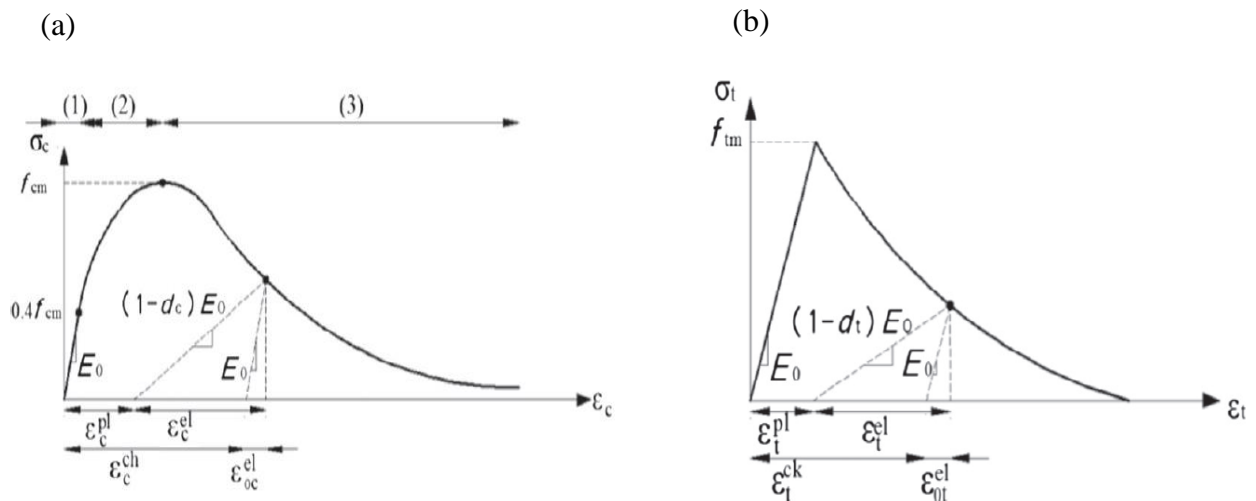


**Figure 3-6: Relationship between: a) concrete compressive strength and plastic strain, and b) Concrete tensile strength and cracking displacement after Alfarah et al. (2017)**

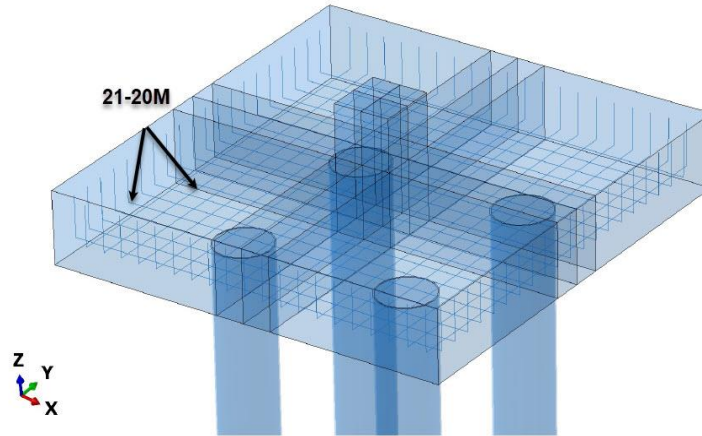


**Figure 3-7 Reinforcement arrangement in the modeled pile cap**

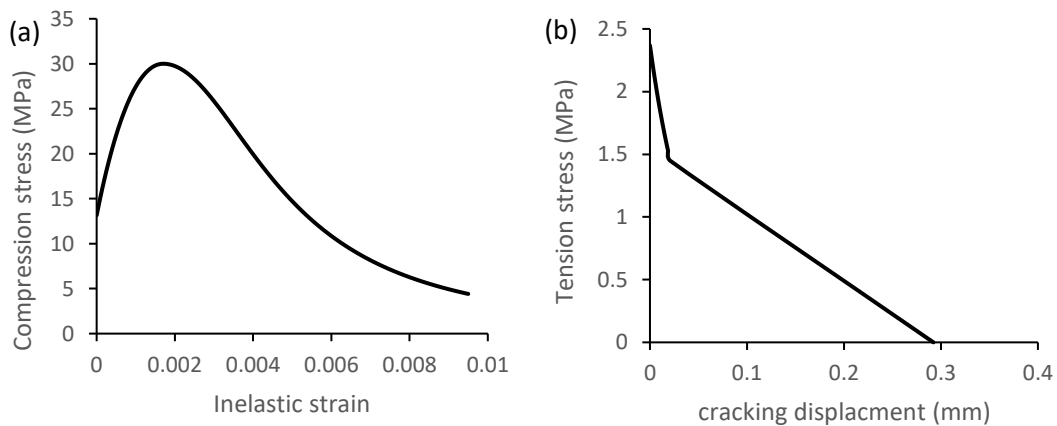


**Figure 3-8: Stress-strain relationship for concrete under: a) compression; and b) tension**

In order to reduce the computational time and effort, a linear-elastic model was also considered for simulating the pile cap behavior. In this case, the concrete elastic modulus was taken equal to  $4500\sqrt{f_c'}$  where  $f_c'$  is the 28-day compressive strength of concrete. The results obtained from the linear elastic model of the pile cap were compared with those obtained considering the CPDM for one pile group configuration to investigate the effect of the pile cap material model on the redistribution of the forces when one pile fails in a pile group system. Figure 3-8 compares the results in terms of the redistribution factor,  $\lambda$ , which is defined as (Ratio of the axial load

redistributed from the failed pile to the adjacent piles). It is noted from Figure 3-9 that the difference between the redistribution factor  $\lambda$ , value obtained from both models is insignificant. This is because the governing failure mechanisms for the pile cap when one pile fails is the rotation behavior towards the failing pile and pile lateral deflection, and hence an induced bending moment at the adjacent intact piles (Poulos,1997). In another words, the concrete pile cap will not reach its yielding point where cracks can occur within its cross-section due to absence of bending forces.

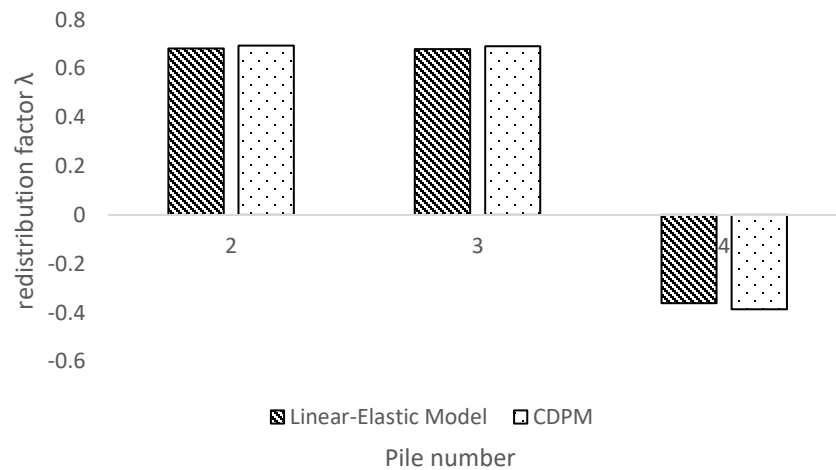


**Figure 3-9: Redistribution factors for a four-pile group considering elastic and plastic concrete models for the pile cap**

### 3.3.6 Analysis Steps and Loading Sequence

Figure 3-10 summarizes the loading protocol and analysis steps for the FE model. The foundation will be loaded in a load-controlled manner up to the maximum applied load.

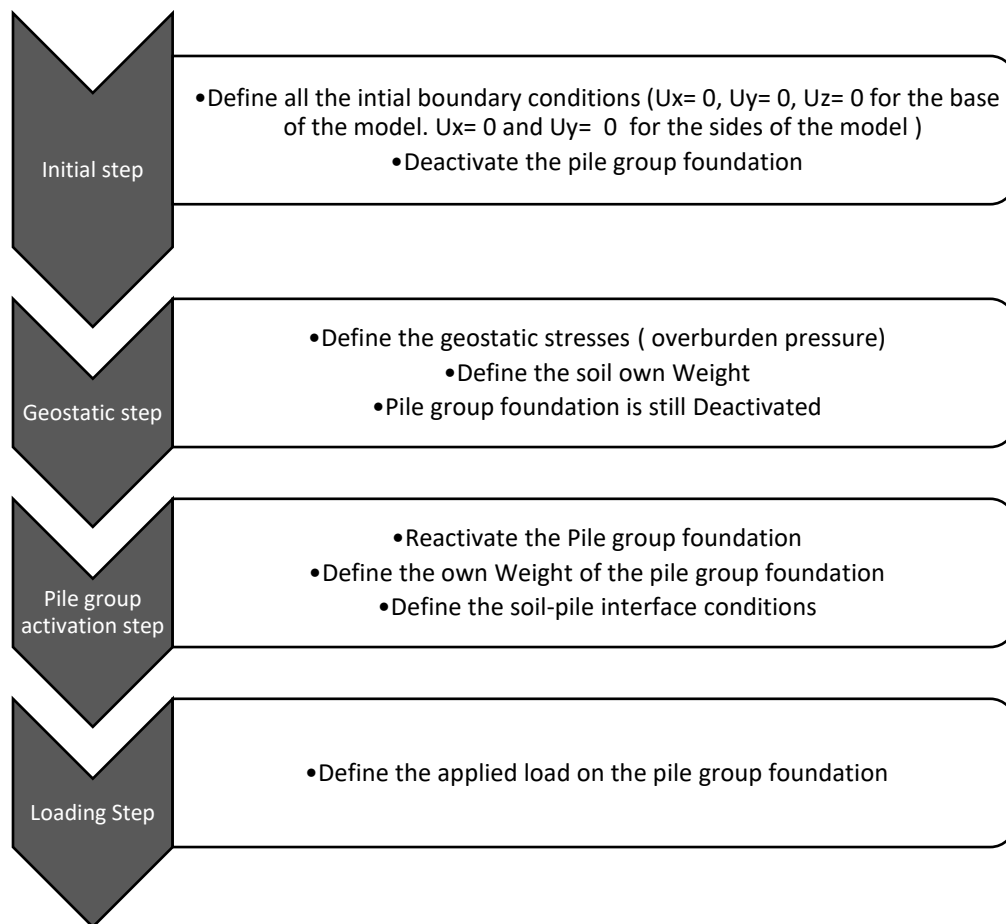


**Figure 3-10: Loading protocol and analysis steps for the finite element model**

### 3.3.7 Validation of Finite Element Model

The material, mesh, and boundary condition assumptions discussed in the preceding sections were validated by comparing the FE response results against those obtained from experimental testing. The numerical results were compared with the results reported by Choi et al. (2017) for laboratory load tests of a pile group under compressive loading. Choi et al. (2017) have load tested a pile group foundation that comprised of 4 driven piles in sand arranged in a (2x2) square configuration under lateral and vertical loading for 3 different values of sand relative density 40 (loose sand), 60 (medium dense sand) and 90% (dense sand). The test was performed in a large-scale soil chamber with a 1600 mm height and 2000 mm in diameter. Table 3-2 and Table 3-3 summarizes the pile group configuration and material used in test and the numerical modeling.

**Table 3-2: Model geometry parameters**

Description	Model	Unit
Pile diameter	30	mm
Pile Length	1200	mm
Spacing	3D	-
Pile cap width and length	210	mm

**Table 3-3 : pile and pile cap material parameters considered in the FE**

Description	Material	Youngs' modulus (Gpa)	Unit Wight (kN/m3)
closed-ended pipe piles	stainless	180	78.5
Pile cap	steel		

To accurately simulate the actual behavior of the pile group under axial loading the boundary, configuration, and interface conditions were compatible of that used for the load testing reported by Choi et al. (2017) as shown in Figure 3-11. Furthermore, the calibration processes of the numerical models were accomplished by adjusting some of the soil properties that were not measured until the response between the experimental results and the response of the numerical model is attained. Table 3-4 summarizes the initial material properties used in the numerical model. All soil parameters in Table 3-4 were selected based on the soil properties used in the load test experiment except for Young modulus  $E_s$  and the coefficient of lateral earth pressure  $K_s$ , that were calculated using empirical correlations available in the literature due to the lack of these information in Choi et al. (2017). The former parameter was determined as a function of the effective normal stresses  $\sigma_3$  based on the power function proposed by Janbu (1963):

$$E = Pa * k * \left(\frac{\sigma_3}{Pa}\right)^n \quad (3.1)$$

Where E is the Young modulus of the soil,  $\sigma_3$  is effective normal stresses,  $P_a$  is the atmospheric pressure, k and n are material constants chosen to be 215 and 0.6 for the medium dense sand, 425 and 0.6 for the dense sand respectively. The material constants K and n where chosen based on the suggested values by Kulhawy et al. (1969) , where the value of K is mainly dependent on the

relative density of sand  $D_r\%$  and varies between 200 to 1200. The value of  $n$  varies between 0.45 to 0.6 for a sandy soil.

The latter parameter was determined as an average of 3 values  $K_a$ ,  $K_o$ ,  $K_p$  based on the function proposed by Bowles (1996) for short piles:

$$K_s = \frac{K_a + K_o + K_p}{3} \quad (3.2)$$

Where  $K_a$ ,  $K_o$ ,  $K_p$  are the coefficients of active, rest and passive lateral earth pressure respectively. The value of  $K_s$  shown in Table 3-4 was calculated by multiplying Eq. (3.2) with a correction factor to account for the installation method and boundary conditions of the soil chamber, which causes a significant increase in the horizontal confinement pressure of the soil along the pile shaft.

**Table 3-4: Properties of sand bed used in the experimental study for FE model validation**

Soil Type	Young modules $E_s$ (MPa)	Poisson's ratio, $\nu_s$	Friction angle $\phi$ (degrees)	Dilation angle $\psi$ (degrees)	Dry unit Wight $\gamma_s$ (kN/m <sup>3</sup> )	Earth pressure coefficient $K_s$
Medium dense sand	8	0.3	32.8	2.8	16.3	3.5
Dense sand	17	0.3	34	4	18	3.5



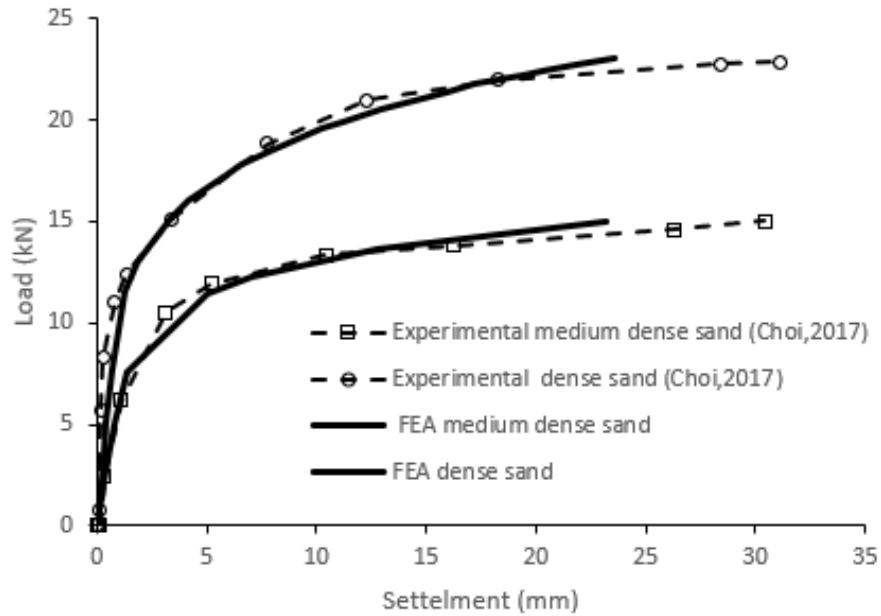


**Figure 3-11: Comparison of numerical and experimental load test results of pile group**

### 3.3.8 Case study of Pile Group with a Defected Pile

This section presents a validation case study for the work of Zhang and Wong (2007) on the performance of defected pile group foundations. The purpose of this study is to verify the ability of the numerical model to simulate the behavior of different types of soils, and failure conditions.

Zhang and Wong (2007) investigated the behavior of axially loaded defected group of concrete bored piles using centrifuge testing. The prototype pile group comprised 4 piles, each was 15 m long and 2 m in diameter arranged in a square configuration (2x2) at a spacing of 6 m center to center. Two types of defects were considered in the experimental study. The first type involved two shorter piles (10 m long) in the group; and the second defect was simulated by making the tip of two piles weaker than the other piles, which was accomplished by filling a 300 mm thick concrete ring with a 70 % of the pile diameter by a weak material (polystyrene). The pile dimensions, configuration, material and spacing of the prototype was taken as indicated in Zhang and Wong (2007) as shown in Table 3-5 & Table 3-6.

**Table 3-5 centrifuge model and numerical model material parameters after Zhang and Wong (2007)**

Element	Material	Young's modulus, E (Mpa)	Unit Wight, $\gamma$ (kN/m <sup>3</sup> )	Compressive strength (kN/m <sup>2</sup> )
Pile	Grout	25,000	23.5	50-58
Pile cap	Aluminum	70,000	26.6	290
Soft toe fill	polystyrene	0.3	0.16	-

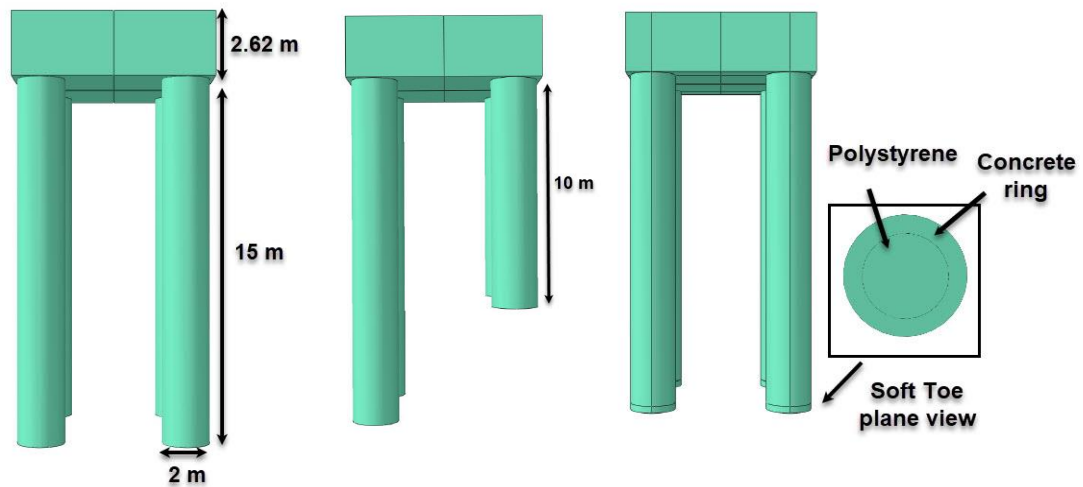
**Table 3-6 Equivalent centrifuge model and prototype dimensions**

Description	Model	Prototype	Unit
n	75 g	1g	m/s <sup>2</sup>
Pile diameter	26.7	2000	mm
Spacing	76.2	6000	mm
Pile length	175	15,000	mm
Pile cap width and length	110	8250	mm
Pile cap thickness	35	2620	mm

Due to absence of the pile cap thickness in Zhang and Wong (2007), it was calculated using centrifuge scaling laws (Garnier et al., 2007), i.e.

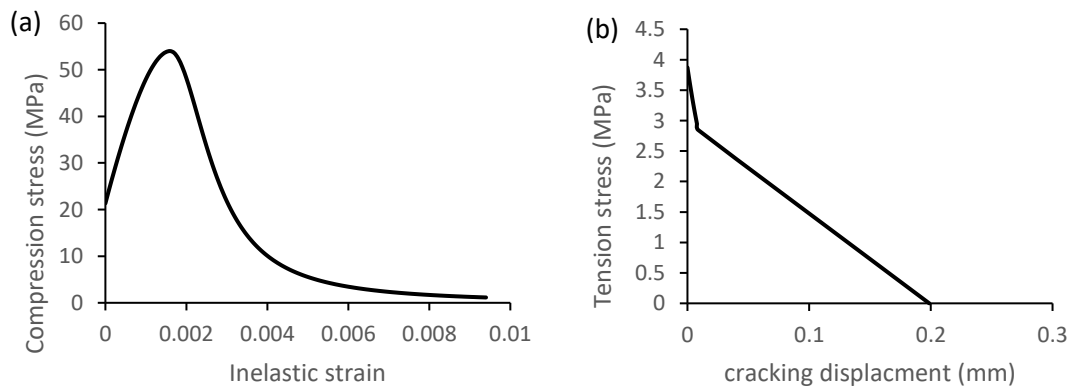
$$\frac{E_p I_p}{E_m I_m} = n^4 \quad (3.3)$$

Figure 3-12 shows the three different test cases considered in the study and numerical model used for the validation of modeling technique.



**Figure 3-12: Pile group test cases considered in the study**

Due to the existence of the stiff bedrock, the grouted piles might exceed the yielding point at the contact area between the pile and bedrock. For the purpose of capturing the non-linearity between the piles and the bedrock, CPDM was used to simulate the concrete behavior with a value of 54 MPa for the compressive strength as reported in Zhang and Wong (2007). Figure 3-13 illustrates the stress-strain relationship for concrete in compression and tension used in the model.



**Figure 3-13: Stress-strain relationship used for the validation case of Zhang and Wong (2007); a) compression; b) Tension**

The soil profile consisted of two layers. The first layer was a completely decomposed granite (CDG) which could be classified as a silty sand. The second layer was a grade III bedrock with an equivalent point load index,  $PLI_{50}$  less than 1 MPa (Buildings Department, 2009) which was simulated in the centrifuge using grout mix of 0.7:1.0:3.0 (water-sand-cement ratio) to achieve a 26 MPa unconfined compressive strength (UCS).

To accurately simulate the bedrock in the numerical model, the Hoek-Brown constitutive model was used for the bedrock material. ABAQUS' material model library doesn't contain this constitutive model. Thus, the parameters of Hoek-Brown material model was converted to Mohr-Coulomb material model soil parameters. The equivalent soil parameters were calculated as shown follows:

$$\phi' = \sin^{-1} \frac{(6am_b(s+m_b\sigma'_{3n}))^{a-1}}{2(1+a)(2+a)+6amb(s+b_b\sigma'_{3n})^{a-1}} \quad (3.4)$$

$$c' = \frac{\sigma_{ci}[(1+2a)s+(1-a)m_b\sigma'_{3n}](s+m_b\sigma'_{3n})^{a-1}}{(1+a)(2+a) \sqrt{\frac{1+6am_b(s+m_b\sigma'_{3n})^{a-1}}{(1+a)(s+a)}}} \quad (3.5)$$

$$E_m(MPa) = 100000 \left( \frac{1-\frac{D}{2}}{75+25D-GSI} \right) \frac{1}{1+e^{\frac{11}{11}}} \quad (3.6)$$

Where  $m_b, a, s$ , is the rock mass parameters,  $m_i$  is the intact rock parameter,  $\sigma'_{3n}$  is the ratio of the upper limit confining stress  $\sigma'_{3max}$  stress to its unconfined compressive strength  $\sigma_{ci}$ ,  $E_m$  is the rock mass modulus of elasticity,  $D$  is disturbance factor and  $GSI$  is the geotechnical strength index. Table 3-7 summarizes all the soil parameters of the bedrock used in the FE models. All parameters and equations used in modeling the bedrock were obtained from Balmer et al. (2006).

**Table 3-7: Hoek-Brown's rock mass material parameters**

Parameter	Symbol	Bedrock	Unit
Unconfined compressive strength	$\sigma_{ci}$	26	MPa
Intact rock parameter	$m_i$	7	-
Geotechnical strength index	GSI	33	-
Disturbance factor	D	0	-
	$m_b$	0.64	-
Rock mass parameters	s	0.0006	-
	a	0.518	-
Upper limit confining stress	$\sigma_{3max}'$	6.5	MPa
Rock mass modulus of elasticity	$E_m$	2149.55	MPa
Friction angle	$\phi'$	22.68	degrees
Cohesion	$c'$	0.855	MPa

Furthermore, CDG soil parameters including friction angle and unit weight were taken exactly as reported by Zhang and Wong (2007) apart from cohesion and young modulus, which was not reported by the authors. The cohesion of the CDG soil was taken in accordance to Zhou and Xu (2015) correlations between friction angle, suction strength and cohesion. The elastic modulus of the silty sand were taken as depicted by Elkasabgy and El Nagggar (2019). Table 3-8 summarizes the silty sand soil parameters used in the model.

**Table 3-8 Silty sand material parameters considered in the FE**

Soil Type	Young modulus $E_s$ (MPa)	Friction angle $\phi$ (degrees)	Poisson's ratio, $\nu_s$	Dilation angle $\Psi$ (degrees)	Dry unit Weight $\gamma_s$ (kN/m <sup>3</sup> )	Cohesion $c'$ (Kpa)
Silty sand (CDG)	88	38.7	0.25	1	17	40

The analysis of the three test cases were conducted using the finite element model as per the established parameters of the sensitivity studies and the soil, rock and concrete properties as discussed above. The results are compared in Figure 3-14 with the experimental results. As shown in Figure 3-14, a reasonable match between the FEA and experimental results has been achieved, which confirms the suitability of the developed numerical models to predict the behavior of defected pile groups.

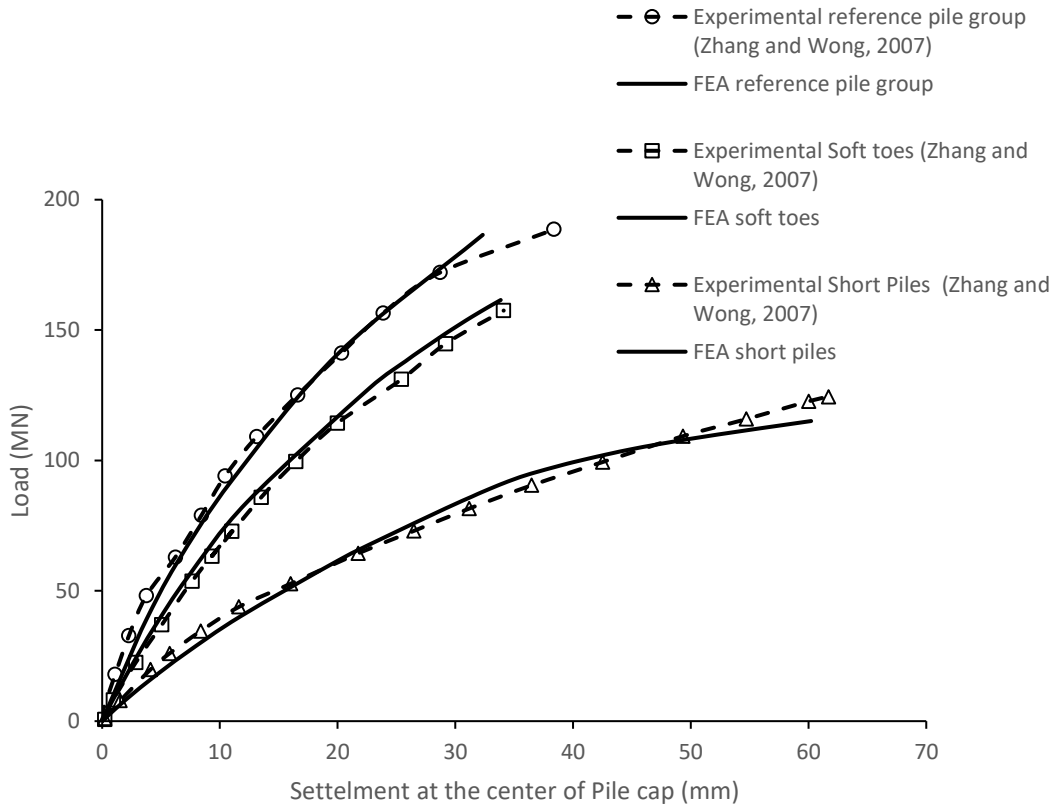


**Figure 3-14: Comparison of the numerical model and the centrifuge experimental load test results of all pile group test cases**

### 3.3.9 Parametric Study

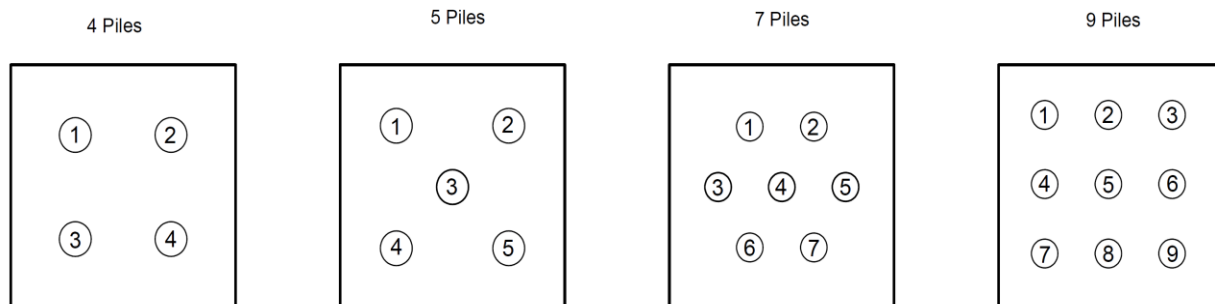
The main objective of the parametric study is to examine the ability of a code-compliant pile cap to redistribute the forces upon failure of individual piles within a pile group foundation. As mentioned previously, failure considered in the analysis is either strength-related (reduced frictional and bearing capacity) or settlement-related failure (reduced stiffness of soil surrounding sides and tip of the target pile).

The piles are considered to be installed in either medium dense or dense sand. Table 3-9 summarizes the soil material properties used in the model.

**Table 3-9: Soil parameters considered in the FE model**

Soil Type	Young's modulus $E_s$ (Mpa)	Poisson's ratio $\nu_s$	Friction angle $\phi$ (degrees)	dilation angle $\Psi$ (degrees)	Dry unit weight $\gamma_s$ (kN/m <sup>3</sup> )	Cohesion $c$ (Kpa)	Earth pressure coefficient $K_s$
Medium dense sand	40	0.3	30	0	18	1	1.25
Dense sand	60	0.3	35	5	18	4	1.25

The design variables pertaining to the individual piles are varied for different pile group configurations, while the design of the pile cap is adjusted accordingly for code-compliance. The parametric study covered typical pile configurations used to support building columns. All members within the pile group system are designed for a utilization ratio of unity. Four design variables are considered in the parametric study including: failure limit state, pile spacing, number of piles, and number of failed piles. A total of 63 numerical models were established of different pile group configurations varying from 4-pile group to 9-pile group as shown in Figure 3-15 using the finite element program ABAQUS (SIMULIA.,2013). These numerical models were used to conduct a comprehensive parametric study that comprised 134 different analyses as presented in Figure 3-16 and Table 3-9.

**Figure 3-15: Pile group configurations considered in the FE**

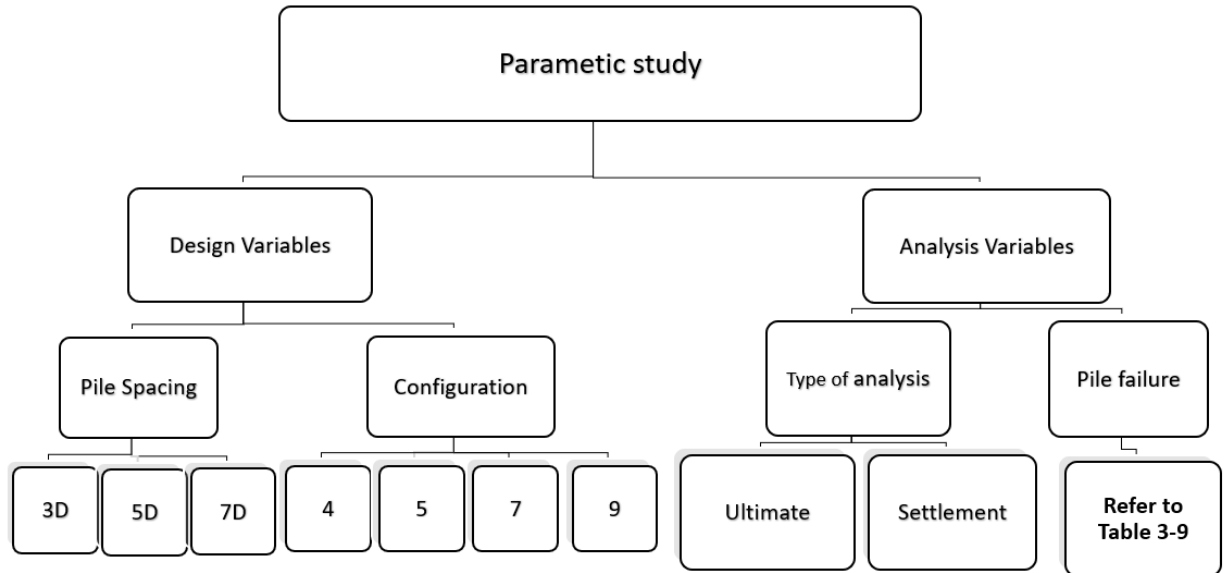


**Figure 3-16: Different pile group configuration and analysis types considered in the parametric study**

<sup>a</sup> refers to Figure 3-15 for pile group configuration

The foundation will be loaded in a load-controlled manner up to the design load that corresponds to a utilization ratio of unity of the pile cap and the individual piles within the pile group system. For strength-based analyses, the failure was induced at the target pile by reducing its frictional and bearing capacity to zero. The design load will be held constant at 3000 kN for all cases to examine the force redistribution and determine the pile distribution factors,  $\lambda$ . Afterwards, the pile group was loaded to failure to determine the maximum capacity of the pile group foundation.



**Table 3-9: Failure scenarios considered in the FE**

Case	Pile failure <sup>b</sup>			
	4 piles	5 piles	7 piles	9 piles
A	1	1	1	1
B	1,2	3	3	2
C		1,2	4	5
D		1,3	1,2	1,3
E		1,5	1,3	1,2
F			1,4	1,5
G			1,6	1,7
H			1,7	-
I			2,5,7	1,4,7
J			1,2,4	1,2,4
K			3,6,7	2,5,8
L			1,4,7	1,2,3,6
M			3,4,5	-

<sup>b</sup> refers to Figure 3-15 for designation of individual piles in a group

## 3.4 Results and discussion

### 3.4.1 Load-settlement response

Resistance of pile group foundations is usually influenced by four main factors: soil type, installation method, pile type and length, and spacing between piles. As an example, for the results obtained from the FEA, Figure 3-17 presents the load-displacement curves for a 9-pile group foundations, with different failure scenarios and pile spacing considered. It can be observed that the load settlement response of defected pile group foundation is very similar to the behavior of intact pile group foundations. However, a notable decrease in the stiffness and capacity between the two behaviors is observed as the location of the failed pile changes where the failure of corner pile causes the most substantial effect. It can be also observed that as the spacing between piles increases the ultimate capacity of the group decreases linearly as shown in Figure 3-17 and Table 3-10 to 3-12, which conforms the studies conducted by Vesic (1967). This behavior can be justified due to the absence of contact between the pile cap and the soil which eventually leads to the reduction in the group efficiency and bearing capacity of the system.

To determine the most critical case in terms of their ultimate capacity, it is essential to choose an adequate failure load interpretation method. There are numerous interpretation methods to determine the axial capacity of pile group foundations, (e.g. DeBeer log-log method (DeBeer, 1970, Davisson's criterion (Davisson, 1972), limiting total settlement at 10% pile diameter (Terzaghi, 1942), limitation of settlement at 25.4 mm). In this study, the ultimate axial capacity of the pile group foundation was evaluated by using the Davisson's failure criteria (Davisson, 1972). In this criterion, the pile axial capacity (failure load) corresponds to a settlement given by:

$$\delta = \frac{PL}{AE} + 4 \text{ mm} + \frac{B}{120} \quad (3.7)$$

Where  $\delta$  is the final settlement, B is the pile diameter, P is the applied load, A is the pile cross-section area, E is the pile Young's modulus.

From Table 3-10 to Table 3-12, it is noted that the most critical failure scenario for all group configurations is the failure of a single corner pile (case A). Moreover, when two piles fail in the system, the failure of two corner piles (case C) for a 5- pile group was the critical scenario, whereas for 7 and 9-pile group the failure of corner and edge pile (case E) was the most critical failure scenario. When three piles fail in the system for a 7 and 9-pile group, the failure sequence of an edge and two corners pile (case I) was the most critical failure scenario.

Figure 3-18 & 3-19 show the effect of failing more than one pile on the overall performance of the pile group system. It is interesting to note that as the number of failed piles increases there is a significant decrease in the capacity and stiffness of the system. For a 5-pile group foundation, a total failure of the system is noticed when two pile failed, whereas for a 7- pile group foundation, the system fails when three piles failed. The definition of failure in this case is related to the context of increased settlement at a very low rate of loading.

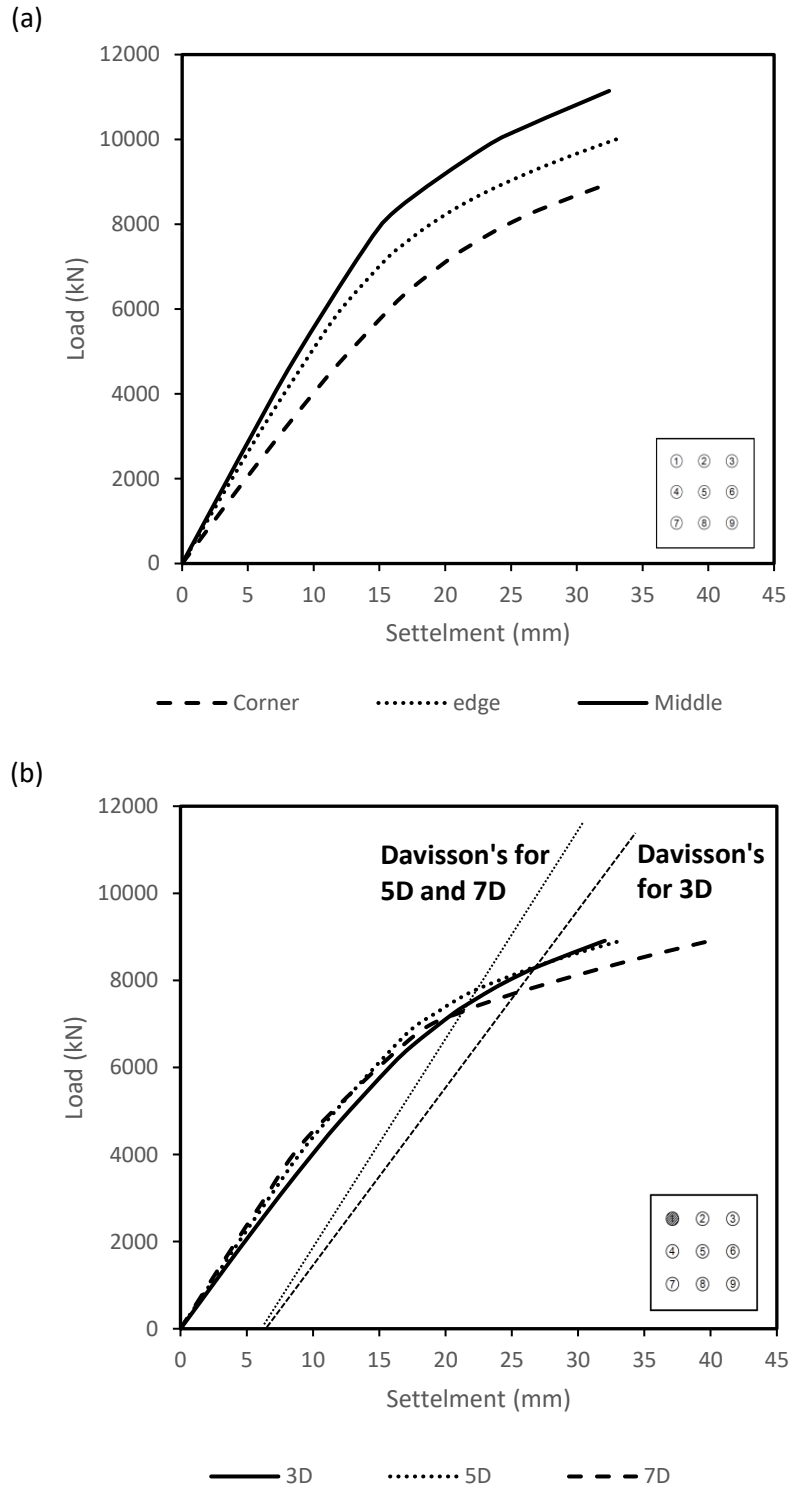


**Figure 3-17: Load-settlement curves of 9-pile group for different failure scenarios and pile spacing; a) Effect of pile location ; b) Effect of pile spacing ;**

**Table 3-10: Ultimate capacity of all failure scenarios and pile spacing for 5-pile group**

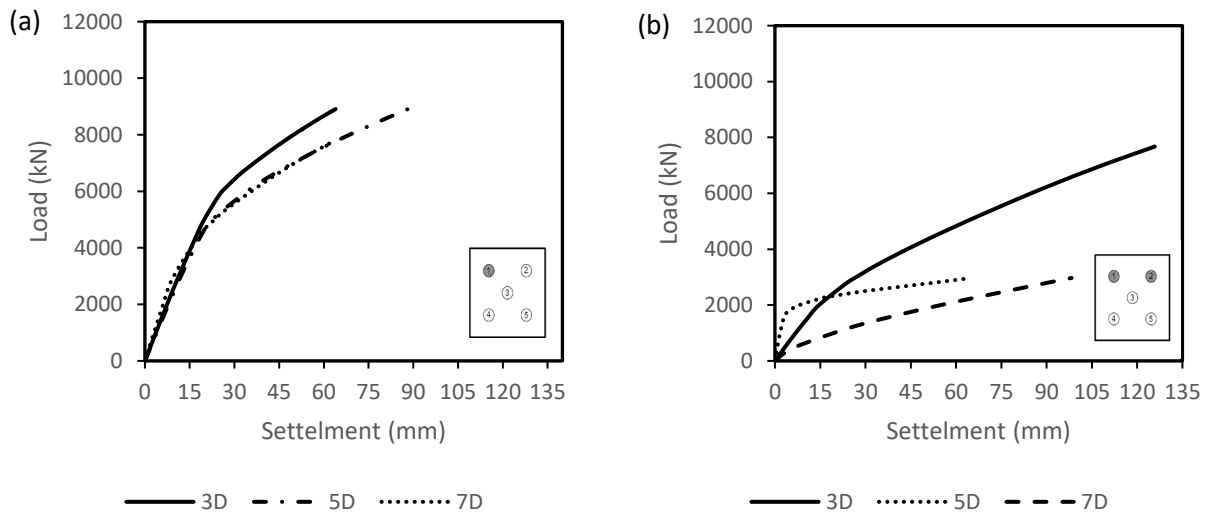
ID	Spacing	Ultimate capacity (kN)	ID	Spacing	Ultimate capacity (kN)	ID	Spacing	Ultimate capacity (kN)
5-A		6800	5-A		5700	5-A		4900
5-B		9150	5-B		8420	5-B		7500
5-C	<b>3D</b>	3200	5-C	<b>5D</b>	2120	5-C	<b>7D</b>	1000
5-D		4500	5-D		3800	5-D		1820
5-E		6500	5-E		5800	5-E		5120

**Table 3-11: Ultimate capacity of all failure scenarios and pile spacing for 7-pile group**

ID	Spacing	Ultimate capacity (kN)	ID	Spacing	Ultimate capacity (kN)	ID	Spacing	Ultimate capacity (kN)
7-A		7950	7-A		7000	7-A		6200
7-B		8100	7-B		7320	7-B		6420
7-C		10700	7-C		10100	7-C		9290
7-D		5450	7-D		4450	7-D		3500
7-E		5100	7-E		4200	7-E		3400
7-F		6250	7-F		4850	7-F		3920
7-G	<b>3D</b>	6620	7-G	<b>5D</b>	6000	7-G	<b>7D</b>	4300
7-H		8350	7-H		7720	7-H		4000
7-I		2910	7-I		2000	7-I		1400
7-J		3000	7-J		3250	7-J		1820
7-K		2920	7-K		2100	7-K		1420
7-L		6730	7-L		6320	7-L		5600
7-M		6700	7-M		6300	7-M		5500

**Table 3-12: Ultimate capacity of all failure scenarios and pile spacing for 9-pile group**

ID	Spacing	Ultimate capacity (kN)	ID	Spacing	Ultimate capacity (kN)	ID	Spacing	Ultimate capacity (kN)
9-A		8300	9-A		7900	9-A		7300
9-B		8800	9-B		8600	9-B		7900
9-C		10100	9-C		10300	9-C		9550
9-D		6130	9-D		5900	9-D		5320
9-E		5800	9-E		5580	9-E		4980
9-F	<b>3D</b>	6900	9-F	<b>5D</b>	6700	9-F	<b>7D</b>	6000
9-G		6220	9-G		6000	9-G		5300
9-I		3900	9-I		3020	9-I		2810
9-J		4250	9-J		3080	9-J		3250
9-K		7550	9-K		7450	9-K		6800
9-L		2680	9-L		2200	9-L		1600

**Figure 3-18: Load-settlement behavior for 5-pile group for different failure scenarios and pile spacing; a) failure of corner pile; b) failure of 2 corner piles**

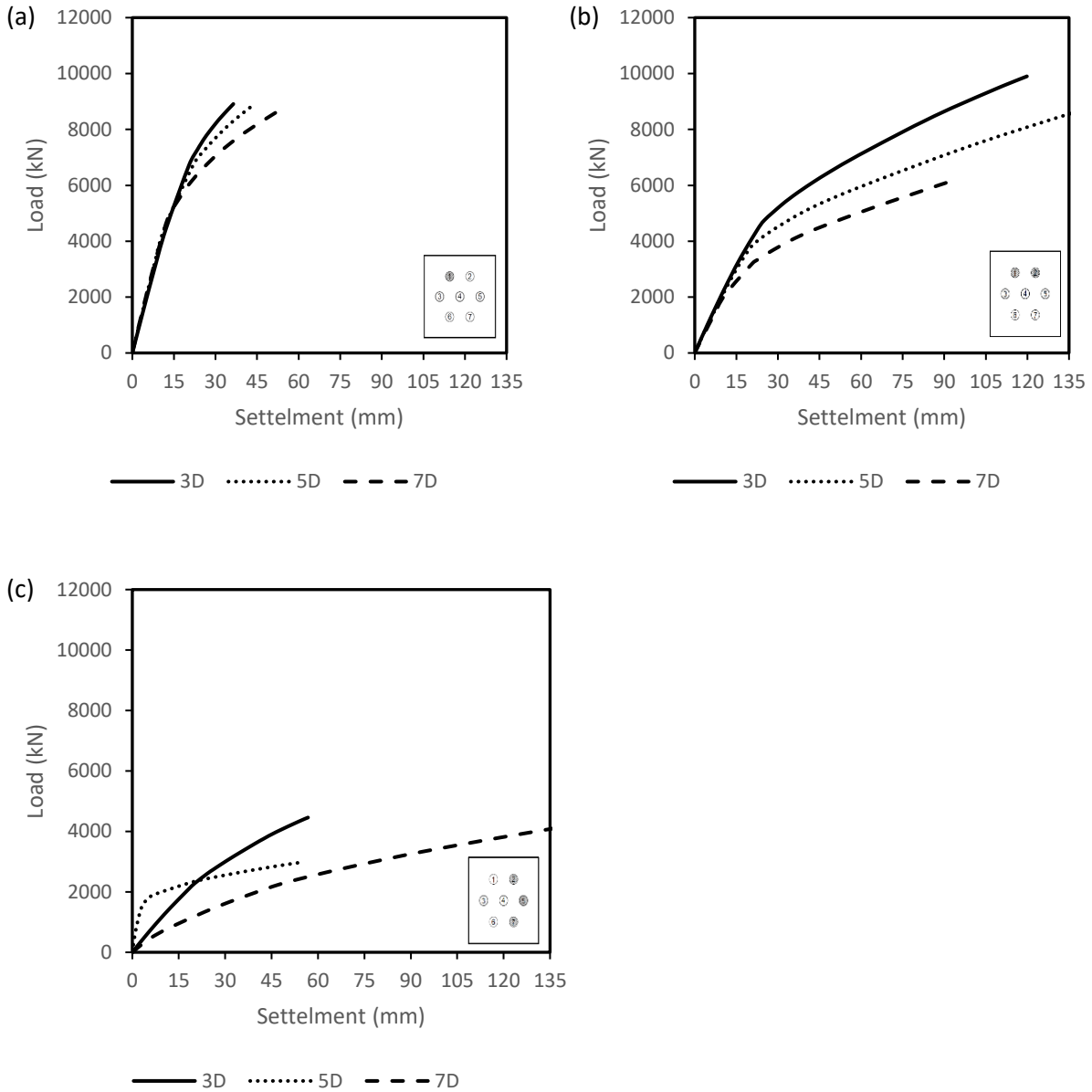


**Figure 3-19: Load-settlement behavior for 7-pile group for different failure scenarios and pile spacing; a) failure of corner pile; b) failure of 2 corner piles; c) failure of 2 corner and 1 edge pile**

### 3.4.2 Load re-distribution of defective pile group foundation

The load sharing mechanism in a pile group foundation is primarily influenced by three main factors: pile spacing, piles arrangement, and the location of the failed pile with respect to the adjacent intact piles. The load sharing mechanism can be quantified using redistribution factors,  $\lambda$  that may be given by:

$$\lambda_i = \frac{(P_{after} - P_{before})_i}{\sum P_{failed\ piles}} \quad (3.8)$$

Where  $\lambda$  is the ratio of the axial load redistributed from the failed pile to the adjacent piles,  $P_{after}$  is the increased axial load in pile  $i$  after the target pile fails,  $P_{before}$  is the axial load of pile  $i$  before the target pile fails, and  $P_{failed\ piles}$  is the axial load resisted by the target pile before failure. Figure 3-20 illustrates the impact of a failed pile on a nine-pile group system and the definition of  $\lambda$ .

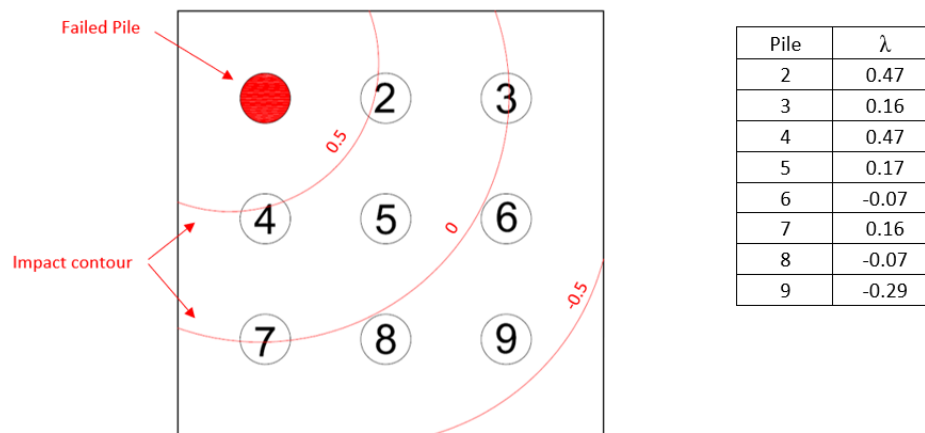


**Figure 3-20: Example of the impact of a failed pile in a pile group foundation**

Figure 3-21 shows comparison between two types of defects with respect to  $\lambda$  for a 5-pile group foundation. It was found that the maximum redistribution difference between the two methods is less than 7%, which indicates that the factor  $\lambda$  is not sensitive to the type of failure; rather it is influenced by the geometric configuration and stiffness of the pile cap. For a rigid pile cap with a symmetric pile configuration and fixed headed piles, it is acceptable to assume that for the same settlement, piles within the group carry an equal fraction of the applied load except for corner and middle piles (Poulos and Davis ,1980) . In case of closely spaced pile group, the highest load is

always distributed to the external piles and the lowest to the middle piles. For widely spaced symmetric pile groups, the highest load will be distributed to the middle piles and the lowest to the external piles (Comodromos et al., 2009). The existence of defected pile in a pile group foundation eliminates the symmetry in the problem, which lead to eccentric loading even if the load was concentric originally.

From a structural point of view, the load transfer within the pile cap can be represented by a strut and tie model for the case of a thick pile cap ( $L/D < 1$ ). The load will be transferred from the pile cap to the piles through diagonal struts (compression) and horizontal ties (tension) as shown in Figure 3-21. The presence of a defected pile within the group will lead to the elimination of the diagonal strut, which eventually causes significant instability in the pile cap as shown in Figure 3-21. In other words, the distribution factor  $\lambda$  mainly depends on the strut and tie angle. As the pile spacing increases, the strut and tie angle decreases, and hence decreases the diagonal compression force.

Due to the negligible difference between the two methods (strength based, and settlement based). The investigation of  $\lambda$  factor was carried out using only the strength-based method. Figure 3-23 & Figure 3-24 presents  $\lambda$  factor for different pile spacing and different failure scenarios for 5, 7 and 9-pile group foundation. From Figure 3-23 to Figure 3-24 four main observations can be made:

- As the spacing between piles increases, the axial loads of the middle piles increase, and axial loads of the external piles decrease.
- For a 5-pile group (case A), the load was distributed to the middle pile with  $\lambda = 56\%$  and  $49\%$  to the external piles. Whereas, for a 7 and 9-pile group (case A),  $\lambda = 50\%$  for the external piles and  $\lambda = 24, 17\%$  for the middle pile in 7-pile group and 9-pile group respectively. This is due to the existence of eccentricity and decreased strut and tie angle in both cases. As the eccentricity increases the value of  $\lambda$  for the middle pile decreases.
- As the spacing between the intact pile and the defected pile increases,  $\lambda$  decreases and, in some cases,  $\lambda$  can be negative. This is because the highest axial load will transfer to the adjacent piles when the failing pile is surrounded with a smaller number of piles due to the increase of settlement, which eventually leads to reduction in the load at the farthest pile.



- Failing the middle pile causes even load re-distribution for all piles in the system. This is attributed to two reasons: rigidity of pile cap and its failure mechanism. The governing failure mechanism of the pile cap when the middle pile fails is bending behavior at the pile cap rather than rotational behavior, which causes an even load re-distribution as shown in Figure 3-26.

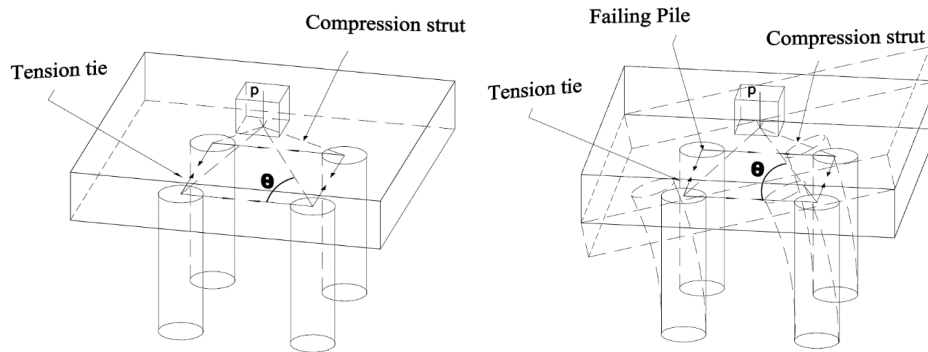


**Figure 3-21: Schematic view of an intact and defected pile group foundation with strut and tie model**

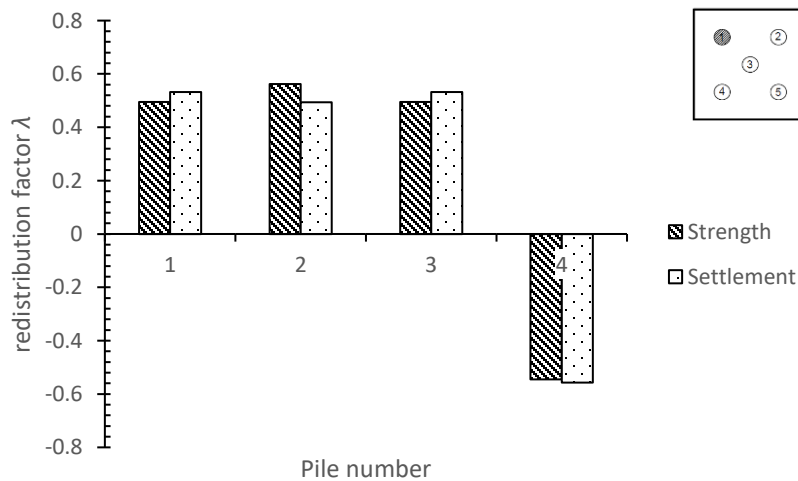


**Figure 3-22: Compression of  $\lambda$  between strength-based and settlement-based methods**

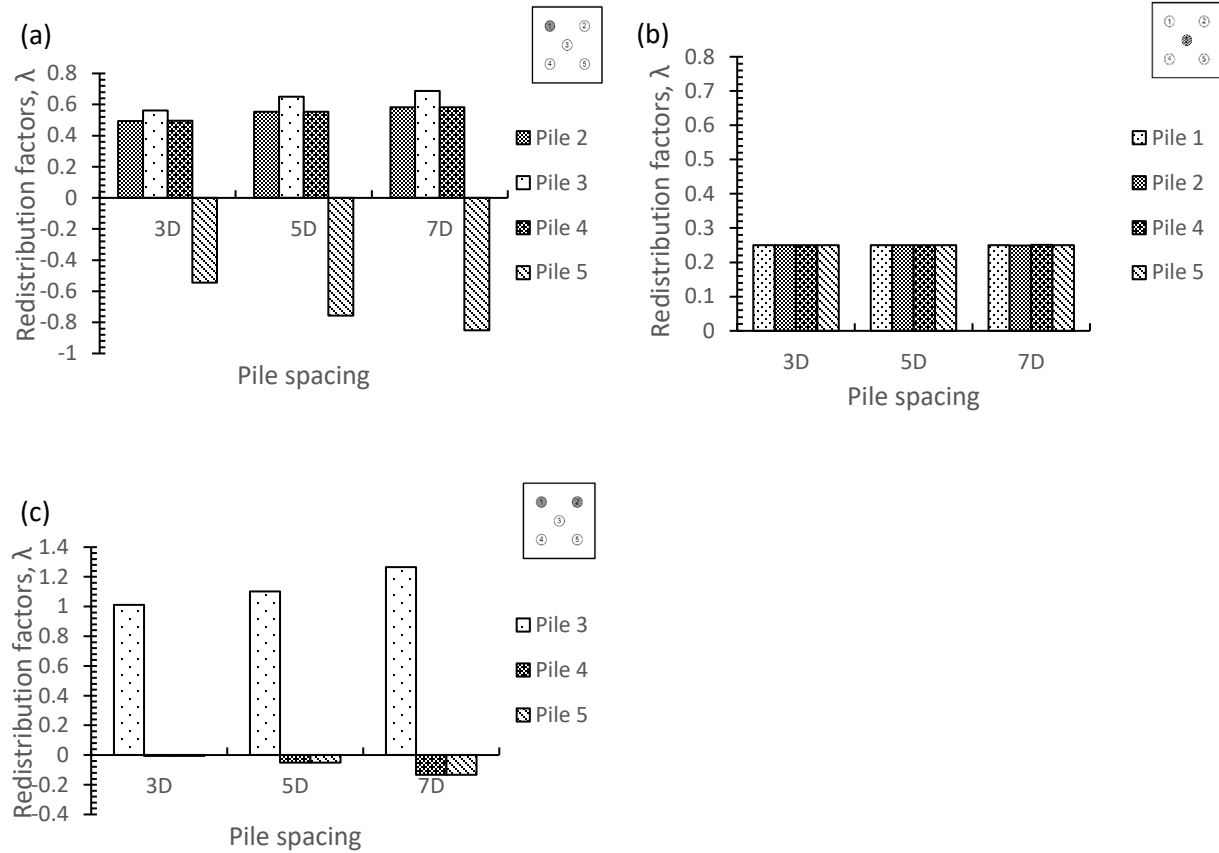


**Figure 3-23: Redistribution factor for 5-pile group foundation for different failure scenarios; a) corner pile; b) middle pile; c) Two external piles**

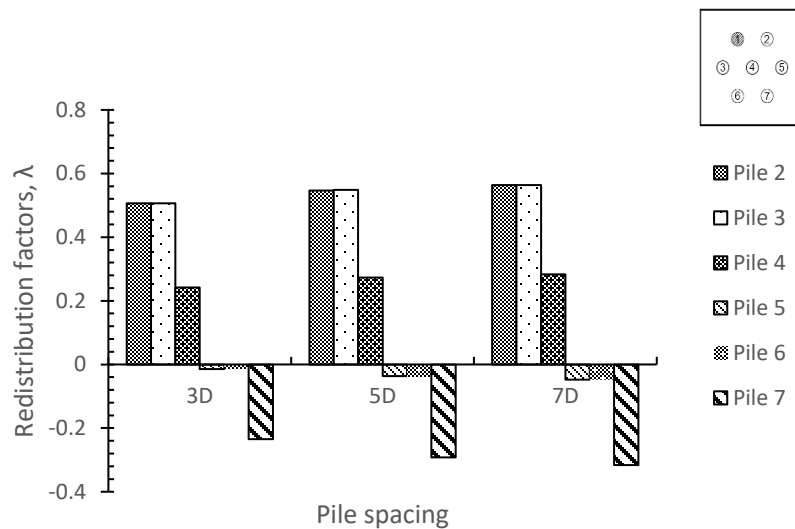


**Figure 3-24: Redistribution factor for 7-pile group foundation when corner pile fails**

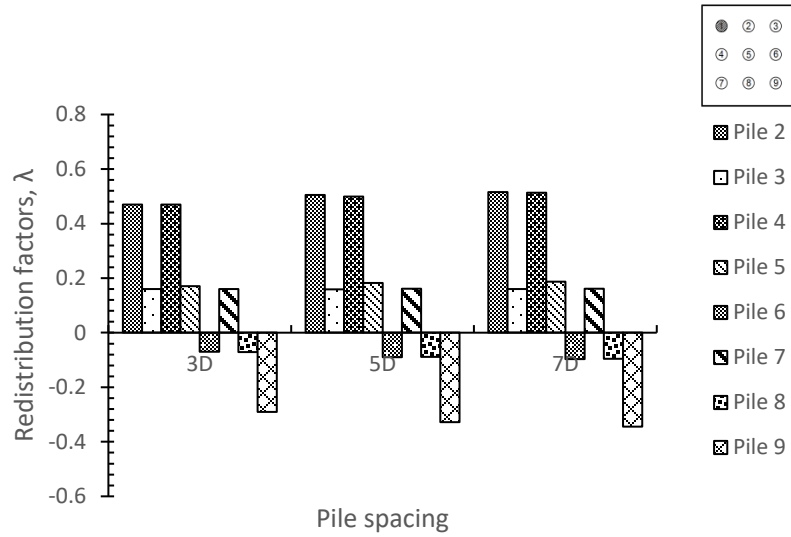


**Figure 3-25: Redistribution factor for 9-pile group foundation when corner pile fails**

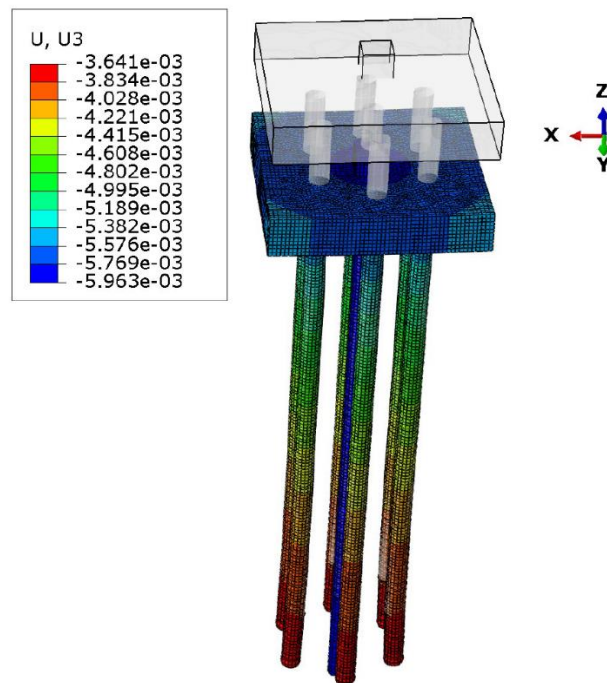


**Figure 3-26: Failure mechanism of the pile group when middle pile fails**

### 3.4.3 Load-rotation behavior of the pile cap

Figure 3-27 presents all the rotational failure mechanisms of the pile cap when one (or more) pile in the group fails. It was found that the rotational behaviors of the pile cap when one pile or more fails follow one of three rotational configurations depending on the location of the failed pile: rotation about x; rotation about y; rotation about x and y, which causes a minor torque that can be neglected according to Kong and Zhang (2004) because it is not likely to occur and the bending moment behavior governs.

The rotation of the pile cap was calculated by calculating the angle between the horizontal plane and the tilted one using simple trigonometric relation, i.e.

$$\theta_i = \tan^{-1}\left(\frac{\delta_2 - \delta_1}{L}\right) \quad (3.9)$$

Where  $\theta_i$  is the angle of rotation of the pile cap,  $\delta_2$  is the maximum displacement at designated plane,  $\delta_1$  is the minimum displacement at designated plane,  $L$  is the horizontal length of the pile cap. Figure 3-28 presents the results of load-rotation behavior of the pile cap for various pile spacing (3D,5D,7D). It is observed that the rotation of the pile cap has increased with the increase of pile spacing. Figure 3-29 presents the failure of corner pile and an edge pile in a 7-pile group foundation. It is worth noting that even though an edge pile failure leads to more critical consequence in terms of its rotation value than the failure of a corner pile, the failure of a corner pile causes rotation in both x-axis and y-axis which results in a more serious consequence that may lead to development of torque and increased bending moment.

The values of rotation pile cap of the least critical scenario for a 5-pile group is compared in Figure 3-30 with the values suggested by Zhang and Ng (2005) for the maximum allowable angular distortions for several building types. It is observed that the presence of a one defective pile causes a 0.0011 rad rotation at the design load, which is much higher than what was suggested by Zhang and Ng (2005) of 0.002 rad at the ultimate loading.

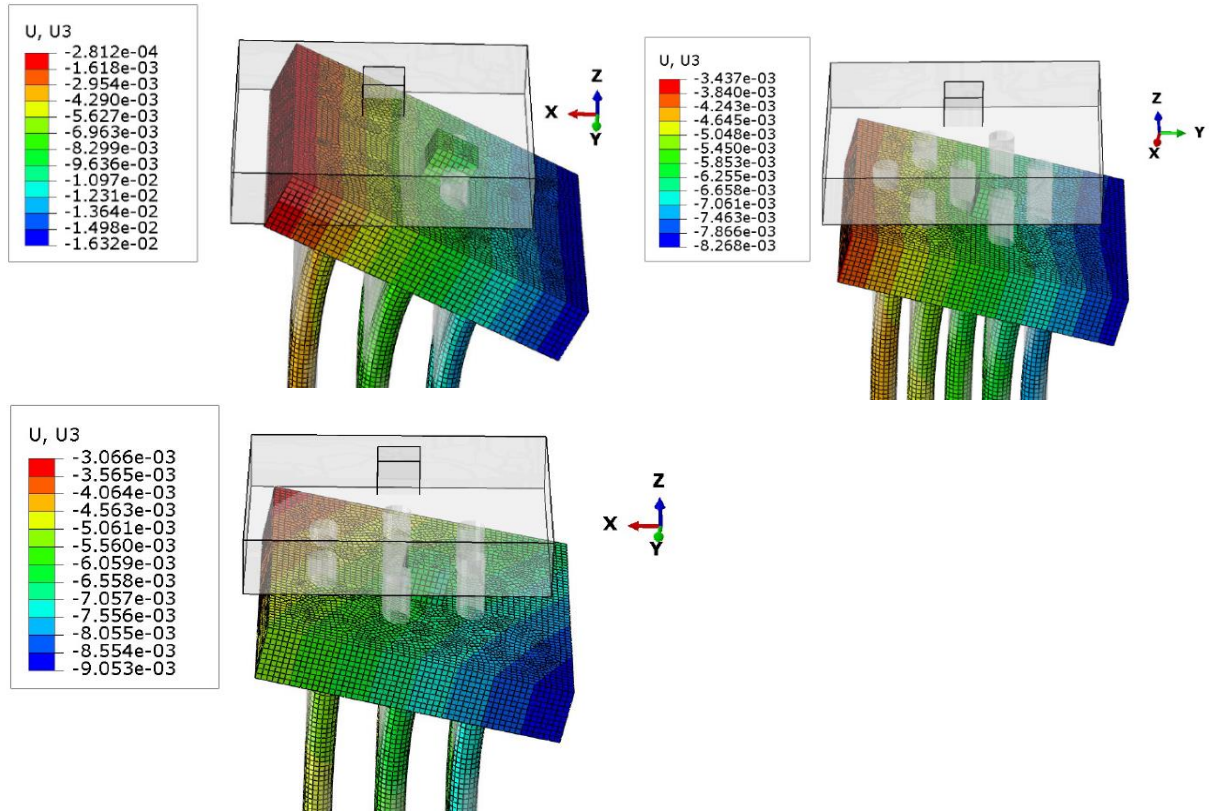


**Figure 3-27: Rotational behavior of 7-pile group pile cap when one or more piles fails in the system**

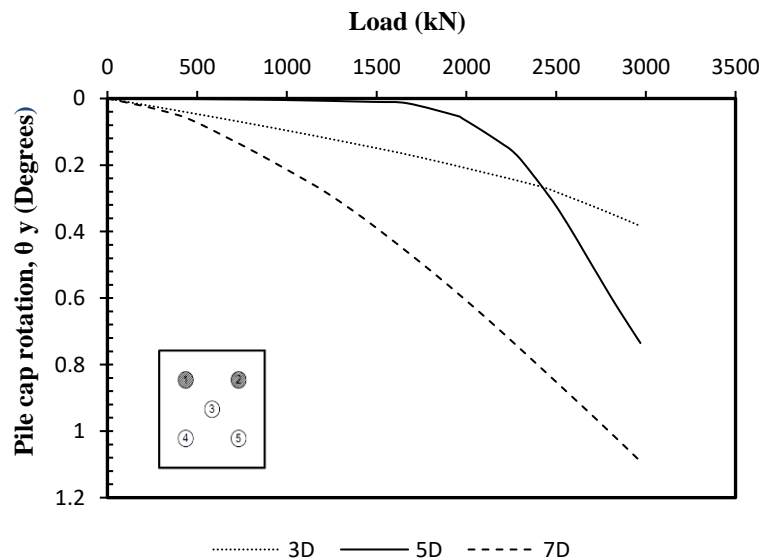


**Figure 3-28: Pile cap load-rotation behavior for different pile spacing when two corner piles fails in the 5-pile group**

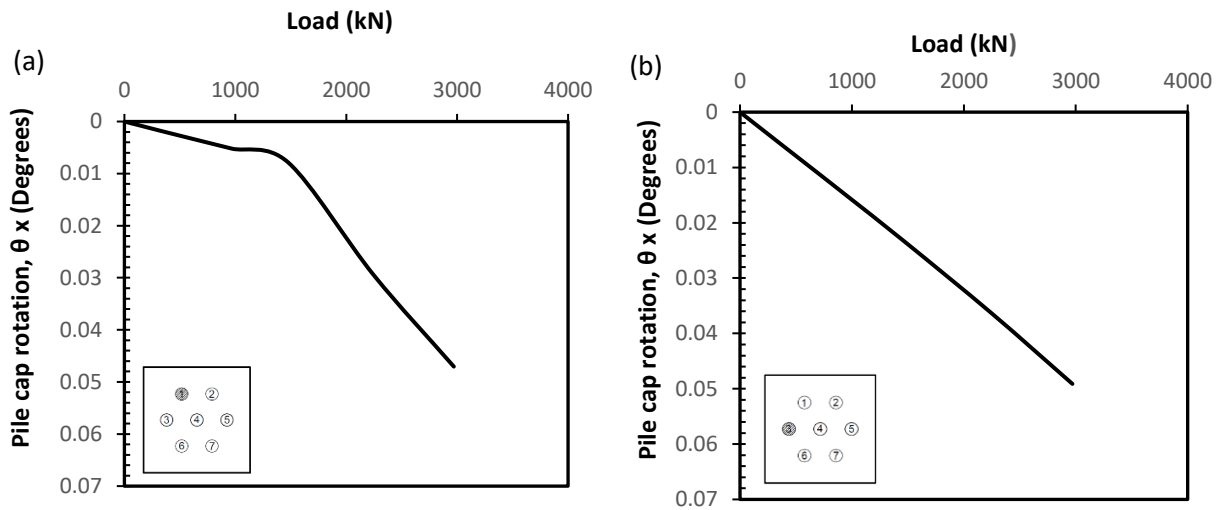


**Figure 3-29: Pile cap load-rotation behavior for a 7-pile group considering two different failure scenarios; a) corner pile b) edge pile**

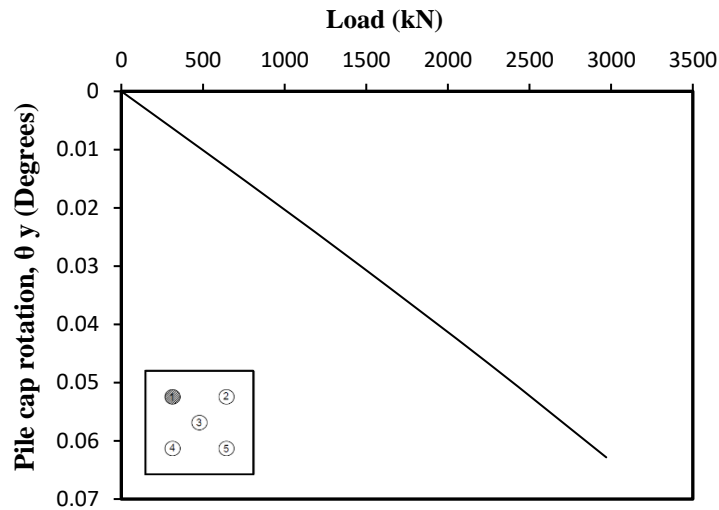


**Figure 3-30: Pile cap load-rotation behavior when one corner piles fails in the 5-pile group**

### 3.4.4 Piles Bending Moment Behavior

The inclination of the pile cap will induce bending moment at the pile heads. The induced bending moment stresses at the pile section is determined by:

$$\sigma = \frac{My}{I} \pm \frac{P}{A} \quad (3.10)$$

Where  $\sigma$  is the normal stress,  $M$  is the moment at the neutral axis,  $y$  is the perpendicular distance to the neutral axis, and  $I$  is the bending inertia of the pile. Figure 3-31 shows the bending moment envelop along the pile shaft for the case of a single corner pile failure and 3D spacing. It is observed that the maximum bending moment occurs at the pile head which was anticipated due to the fixed connection between the piles and the pile cap. The bending moment behavior of the individual piles in the pile group matches the behavior of flexible long piles as shown in Figure 3-31. According to Poulos and Davis (1980) a single pile can be considered a long pile if its relative stiffness,  $K_r < 0.01$ , where:

$$K_r = \frac{E_p I_p}{E_h L^4} \quad (3.11)$$

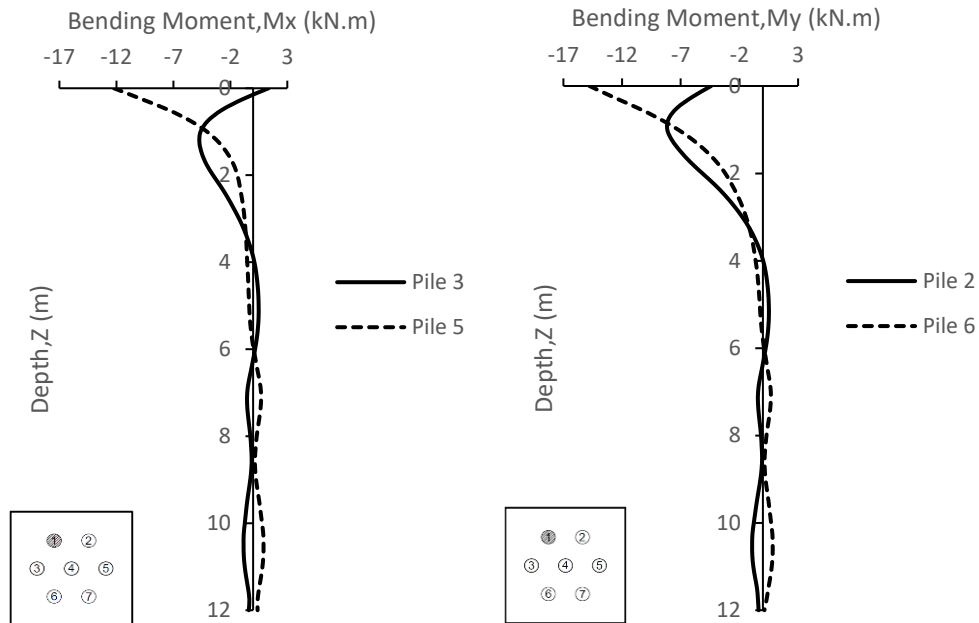
$E_p I_p$  is Flexural rigidity of the pile,  $E_h$  is the weighted average of the elastic modulus of the layered soil, and  $L$  is embedded Length of the pile. The piles considered in the current analyses are thus considered long piles as  $K_r=0.0000231$ .

It is worth noting that in the case of a corner failed pile, the pile cap rotates at the x-y plane and hence induces bending moment  $M_x$  about the x-axis,  $M_y$  about the y-axis, and a minor negligible torque. The notable variation of the moment at the bottom of the pile is a consequence of that minor torque as shown in Figure 3-31. The maximum values of the bending moment  $M_y$  for all piles ranged from -2 to -14.78 kN.m. On the other hand,  $M_x$  values ranged from -12.21 to 1.35 kN.m. Comparing the moment for different piles within the pile group shows that the moment is higher as the pile is farther from the failed pile. As shown in the Figure 3-31, pile 2 experiences the lowest moment whereas pile 6 experiences the highest moment.

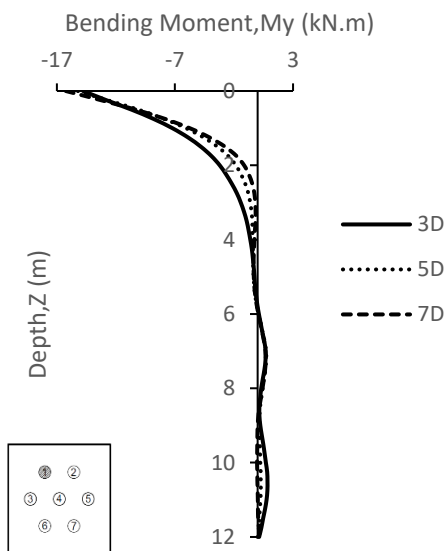
In the case of the failure of an edge pile, the pile cap tends to rotate either about the x-axis or the y-axis depending on the location of the edge pile.

Figure 3-32 illustrates bending moment values along the pile shaft when an edge pile fails with an x-axis pile cap rotation. It is interesting to note that  $M_y$  for all piles along the failed pile axis carried zero moment. In contrast, piles adjacent to the failed pile carried the same magnitude of bending moment but in the opposite direction.

Figure 3-33 shows the maximum  $M_y$  values for different pile spacing when a single corner pile fails. It can be observed that increasing the pile spacing causes a negligible increase in the moment values.



**Figure 3-31: Bending moment envelop of individual piles in a 7-pile group when a corner pile fail**



**Figure 3-32: Effect of center to center pile spacing on the bending behavior of individual piles in a 7-pile group when a corner pile fail**



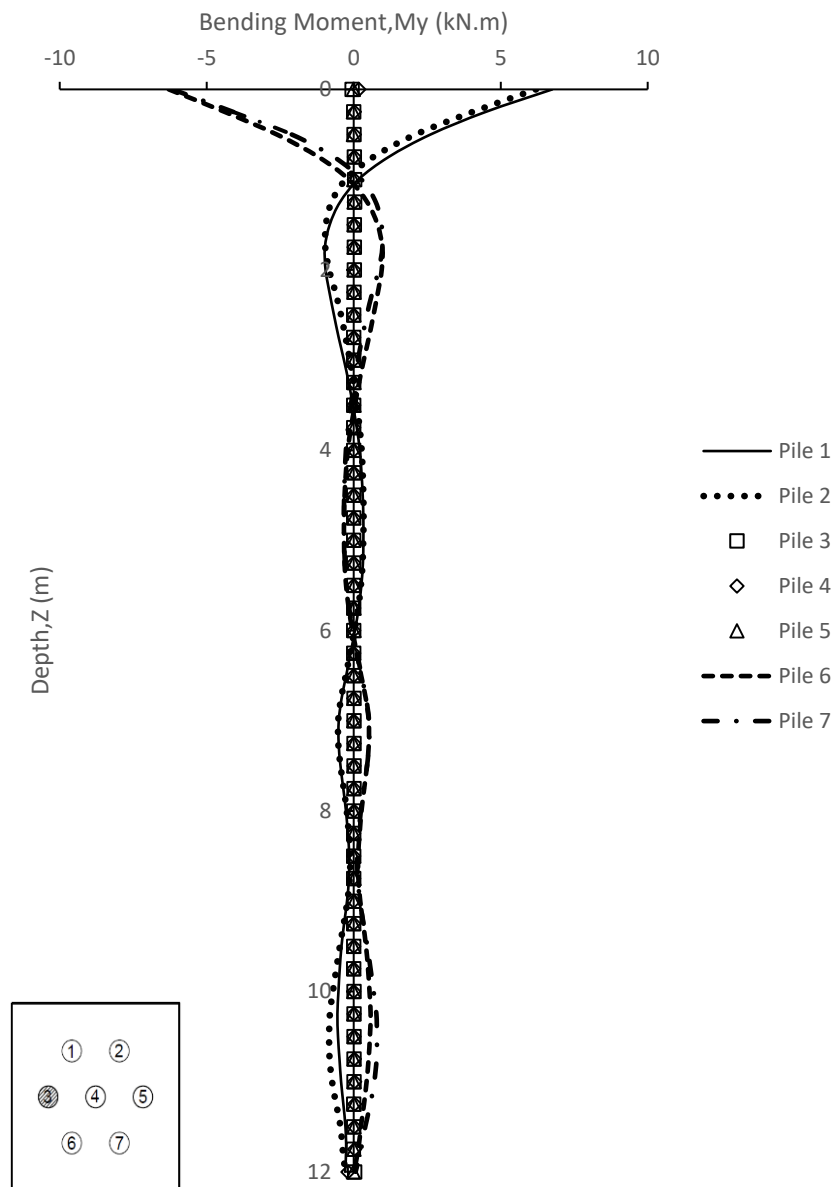


**Figure 3-33: Bending moment behavior of all piles in 7-pile group foundation when an edge pile fails**

### 3.5 Conclusion

Comprehensive parametric investigation was conducted utilizing the FE program ABAQUS to investigate the performance of a geotechnically defected pile group foundations in a medium dense to dense sandy soil in terms of its capacity, load redistribution, pile cap rotation and piles bending moment. Four pile group configurations were considered in the parametric study; 4-piles, 5-piles, 7-piles and 9-piles. The numerical models were validated by comparing the computed results with two different case studies. Based on the results, the main conclusions are as follows:

- As the defected pile location changes or the number of the failed pile increases a significant decrease in the stiffness is noticed.
- It was found that the most critical case for all pile group configurations in terms of their capacity is the failure of the external piles, especially corner piles.
- Total geotechnical failure for the system is noticed when 2 corner piles failed for a 5-pile group foundation and when 3 piles failed (2 corner and 1 edge pile) for a 7-pile group foundation.
- The load redistribution of the system when one pile fails in the group is affected mainly by the existence of eccentricity caused due to the unsymmetrical configuration of the group when one or more pile fails and the disappearance of strut and tie forces in the system.
- As the pile spacing increases, the rotation of the pile cap increases. Nevertheless, increasing the pile spacing has a minimal effect on the bending moment of the individual piles in the group.
- The induced bending moment at the piles increases as the intact pile is farther from the failed pile.

### 3.6 References

- Abdrabbo, F., Abouseeda, H., 2002. Effect of construction procedures on the performance of bored piles. *Geotech. Spec. Publ.* 1438–1454. [https://doi.org/10.1061/40601\(256\)103](https://doi.org/10.1061/40601(256)103)
- Albuquerque, P.J.R., Garcia, J.R., Neto, O.F., Cunha, R.P., Santos Junior, O.F., 2017. Behavioral evaluation of small-diameter defective and intact bored piles subjected to axial compression. *Soils and Rocks* 40, 109–121. <https://doi.org/10.28927/SR.402109>
- Alfarah, B., López-Almansa, F., Oller, S., 2017. New methodology for calculating damage variables evolution in Plastic Damage Model for RC structures. *Eng. Struct.* 132, 70–86. <https://doi.org/10.1016/j.engstruct.2016.11.022>
- Alnuaim, A.M., El Naggar, M.H., El Naggar, H., 2016. Numerical investigation of the performance of micropiled rafts in sand. *Comput. Geotech.* 77, 91–105. <https://doi.org/10.1016/j.compgeo.2016.04.002>
- Balmer, B., Am, C., Ci, C., 2006. Rock mass properties 2 Normal and shear stresses are related to principal stresses by the equations published 1–47.
- Bowles, J.E., 1996. *Foundation Analysis & Design*. The MacGraw-Hill Companies, Inc.
- Buildings Department, 2009. Practice Note for Authorized Persons, Registered Structural Engineers and Registered Structural Engineers. PNAP141.
- Canadian Geotechnical Society, 2006. *Canadian foundation engineering manual*. Richmond, B.C.
- Choi, Y.S., Lee, J., Prezzi, M., Salgado, R., 2017. Response of Pile Groups Driven in Sand Subjected to Combined Loads. *Geotech. Geol. Eng.* 35, 1587–1604. <https://doi.org/10.1007/s10706-017-0194-z>
- Coduto, D.P., 2001. *Foundation Design: Principle and Practices*, Second Edition. Prentice-Hall, Inc, New Jersey.
- Comodromos, E.M., Papadopoulou, M.C., Rentzeperis, I.K., 2009. Pile foundation analysis and design using experimental data and 3-D numerical analysis. *Comput. Geotech.* 36, 819–836. <https://doi.org/10.1016/j.compgeo.2009.01.011>
- CSA A23.3-14/A23.2-14, 2014. *Concrete materials and methods of concrete construction/ Test methods and standard practices for concrete*. Mississauga (Ontario): Canadian Standards Association.
- Cunha, R.P. Da, Cordeiro, A.F., Sales, M.M., 2010. Numerical assessment of an imperfect pile group with a defective pile in both initial and reinforced conditions. *Soils and Rocks* 33(2), 81–93.

- Davisson, M., 1972. High Capacity Piles. Proceedings, Soil Mech. Lect. Ser. Innov. Found. Constr. ASCE 81–112.
- DeBeer, E., 1970. Proefondervindelijke bijdrage tot de studie van het grandsdraagvermogen van zand onder funderingen op staal. English version. *Geotechnique* Vol. 20, 387–411.
- El Sharnouby, M.M., El Naggar, M.H., 2018. Numerical investigation of axial monotonic performance of reinforced helical pulldown micropiles. *Int. J. Geomech.* 18, 1–14. [https://doi.org/10.1061/\(ASCE\)GM.1943-5622.0001161](https://doi.org/10.1061/(ASCE)GM.1943-5622.0001161)
- Elkasabgy, M., El Naggar, M.H., 2019. Lateral Performance and p-y Curves for Large-Capacity Helical Piles Installed in Clayey Glacial Deposit. *J. Geotech. Geoenvironmental Eng.* 145, 04019078. [https://doi.org/10.1061/\(asce\)gt.1943-5606.0002063](https://doi.org/10.1061/(asce)gt.1943-5606.0002063)
- Garcia, J., Albuquerque, P., Neto, O.F., Santos, O., Cunha, R.P., 2017. Numerical evaluation of the influence of defective piles on the behavior of piled raft systems. *ICSMGE 2017 - 19th Int. Conf. Soil Mech. Geotech. Eng. 2017-Sept*, 2747–2750.
- Garnier, J., Gaudin, C., Springman, S.M., Culligan, P., Goodings, D., Konig, D., Kutter, B., Phillips, R., Randolph, M.F., Thorel, L., 2007. Catalogue of Scaling Laws and Similitude Questions in Geotechnical Centrifuge Modeling. *Int. J. Phys. Model. Geotech.* 8(3), 1–23.
- Hobbs, N.B., 1957. Unusual necking of cast in-situ concrete piles. *Proc. 4th International Conf. Soil Mech. Found. Eng.* 3, 40–42.
- Janbu, N., 1963. Soil Compressibility as Determined by Oedometer and Triaxial Tests. *Proc. 3rd Eur. Conf. Soil Mech. Found. Eng.* 1, 19–25.
- K.J.Xu, H.G.POUIOS, 2001. Behaviour of pile group containing defective piles. *14th Int. Conf. Soil Mech. Found. Eng.* 2, 1039–1041.
- K.J.Xu, H.G.Poulos, 2000. Measured and predicted axial response of piles with diameter discontinuities. *Geotech. Eng. J.* 31.
- Kong, L., Zhang, L., 2004. Lateral or torsional failure modes in vertically loaded defective pile groups. *Geotech. Spec. Publ.* 625–636.
- Kulhawy, F.H., 1984. Limiting tip and side resistance: Fact or fallacy. *ASCE Spec. Conf. Anal. Des. Pile Found.* 80–98.
- Kulhawy, F.H., Duncan, J.M., Seed, H.B., 1969. *Finite Element Analyses of Stresses and Movements in Embankments During Construction.* Univ. California, Berkeley.
- Look, B.G., 2007. *Handbook of Geotechnical Investigation and Design Tables.* Taylor & Francis/Balkema, London, UK.
- Lv, Y., Zhang, D., 2018. Geometrical effects on the load transfer mechanism of pile groups: Three-

- dimensional numerical analysis. *Can. Geotech. J.* 55, 749–757. <https://doi.org/10.1139/cgj-2016-0518>
- Mansur, C.I., Hunter, H., 1970. Pile tests - Arkansas river project. *J. Soil Mech. Found. Div.* 96(SM5), 1545–1582.
- Meyerhof, G.G., 1976. Bearing capacity and settlement of pile foundations. *J. Geotech. Eng. Div. ASCE* 102, 195–228.
- Moayed, R.Z., Izadi, E., Mirsepahi, M., 2013. 3D finite elements analysis of vertically loaded composite piled raft. *J. Cent. South Univ.* 20, 1713–1723. <https://doi.org/10.1007/s11771-013-1664-y>
- Petek, K., W.Felice, C., R.D.Holtz, 2002. Capacity Analysis of Drilled Shafts with Defects. *An Int. Perspect. Theory, Des. Constr. Performance.* ASCE 1120–35. [https://doi.org/https://doi.org/10.1061/40601\(256\)80](https://doi.org/https://doi.org/10.1061/40601(256)80)
- Poulos, H.G., 2005. Pile behavior - Consequences of geological and construction imperfections. *J. Geotech. Geoenvironmental Eng.* 131, 538–563. [https://doi.org/10.1061/\(ASCE\)1090-0241\(2005\)131:5\(538\)](https://doi.org/10.1061/(ASCE)1090-0241(2005)131:5(538))
- Poulos, H.G., Davis, E.H., 1980. *Pile foundation analysis and design.* John Wiley & Sons, New York.
- Randolph, M.F., Dolwin, J., Beck, R., 1994. Design of driven piles in sand. *Geotechnique* 44, 427–448. <https://doi.org/10.1680/geot.1994.44.3.427>
- SIMULIA., 2013. ABAQUS/CAE. Dassault Systèmes Simulia Corp.
- SIMULIA, 2013b. 6.13 User Documentation. Abaqus user's guide.
- Tabsh, S.W., O'Neill, N.W., 2001. Structural safety of drilled shaft with minor defect. *Proc. ICCOSSAR'2001 Int. Asso. Struct. Saf. Reliab.*
- Tannant, D.D., Regensburg, B., 2001. *Guidelines for Mine Haul Road Design* 111.
- Terzaghi, K., 1943. *Theoretical Soil Mechanics.* *Theor. Soil Mech.* <https://doi.org/10.1002/9780470172766>
- Terzaghi, K., 1942. Discussion of the Progress Report of the Committee on the Bearing Value of Pile Foundations. *Proceedings, ASCE* Vol. 68, 311–323.
- Vesic, A.S., 1963. Bearing Capacity of Deep Foundations in Sand. *Highw. Res. Rec.* 39, 112–153.
- Yang, Z., Jeremić, B., 2003. Numerical study of group effects for pile groups in sands. *Int. J. Numer. Anal. Methods Geomech.* 27, 1255–1276. <https://doi.org/10.1002/nag.321>

- Zhang, L.M., Wong, E.Y.W., 2007. Centrifuge modeling of large-diameter bored pile groups with defects. *J. Geotech. Geoenvironmental Eng.* 133, 1091–1101. [https://doi.org/10.1061/\(ASCE\)1090-0241\(2007\)133:9\(1091\)](https://doi.org/10.1061/(ASCE)1090-0241(2007)133:9(1091))
- Zhang, Z.M., Yu, J., Zhang, G.X., Zhou, X.M., 2009. Test study on the characteristics of mudcakes and in situ soils around bored piles. *Can. Geotech. J.* 46, 241–255. <https://doi.org/10.1139/T08-119>
- Zhou, W.H., Xu, X., 2015. Shear strength of unsaturated completely decomposed granite soil under different stress state conditions. 15th Asian Reg. Conf. Soil Mech. Geotech. Eng. ARC 2015 New Innov. Sustain. 230–235. <https://doi.org/10.3208/jgssp.HKG-16>

## Chapter 4

# **RELIABILITY ANALYSIS OF PILE GROUP FOUNDATIONS**

---

## 4.1 Introduction

Super- and sub-structures can be designed using two approaches: Limit State Design (LSD) or Working Stress Design (WSD). The former is based on the rational treatment of uncertainties in load, resistance, and the method of analysis, in which the structural elements are designed to achieve predefined target safety and functionality limit states. The latter is based on satisfying stress target limits and overall safety factors against predefined failure modes. The LSD method has been widely adopted by North American structural engineering design codes and practicing engineers since the 1970s due to its proven ability in optimizing and rationalizing the design of structural members (e.g., NBCC, 2015, CSA S16-14, 2014, CSA S6-14, 2014, CSA A23.1-14/A23.2-14, 2014). The LSD approach was first introduced to the geotechnical field in Europe in the 1950s, and was adopted by the Ontario highway bridge design (OHBD) in 1983 (OHBD, 1983) and AASHTO LRFD in 1989 (AASHTO, 1989). The primary states considered for the LSD design philosophy in geotechnical engineering are Ultimate Limit state (ULS) and Serviceability Limit State (SLS). The ULS is related to the ultimate capacity of a geotechnical system designed against prescribed failure modes such as over-turning of a footing, sliding of a foundation, and friction or bearing failure in pile foundation. The Serviceability Limit State (SLS) is associated with the performance of the foundation under working loads which lead to a loss of functionality. Typical SLS for foundations include settlement of footings and lateral displacement of group piles (e.g., Allen, 1975, Griffis, 1993).

Although geotechnical engineering codes in the past two decades were promoting the application of LSD as a rational approach in treating the uncertainties in foundation performance as compared with the conventional WSD, the geotechnical practicing engineering community was slow in adapting the LSD approach. A survey conducted in the United States in 2004 concluded that 90% of respondents used the WSD approach while only 28% used the LSD approach in designing foundations (Paikowsky et al., 2004). The lack of interest from practicing engineers in adopting the LSD approach is primarily due to the following reasons: (i) the high degree of uncertainty in

geotechnical conditions as summarized in Figure 4-1, and (ii) the generally satisfactory past performance of foundations designed using the WSD approach. Considerable research has been devoted in the past decade toward further verifying the superiority of LSD method over the WSD in terms of safety and economy for designing foundations (e.g., Becker 1996a,1996b, Paikowsky et al., 2004, Abdelsalam et al., 2011, AbdelSalam et al., 2012, Oudah et al., 2019). Numerous studies were conducted focusing on employing the LSD approach in calibrating resistance factors for various foundation configurations and in calculating the reliability of various substructure configurations (e.g., Tang et al., 1990, Zhang et al., 2001, Fenton and Griffiths, 2007, Wang, 2009, Kwak et al., 2010, Fenton et al., 2016, Naghibi and Fenton, 2017).

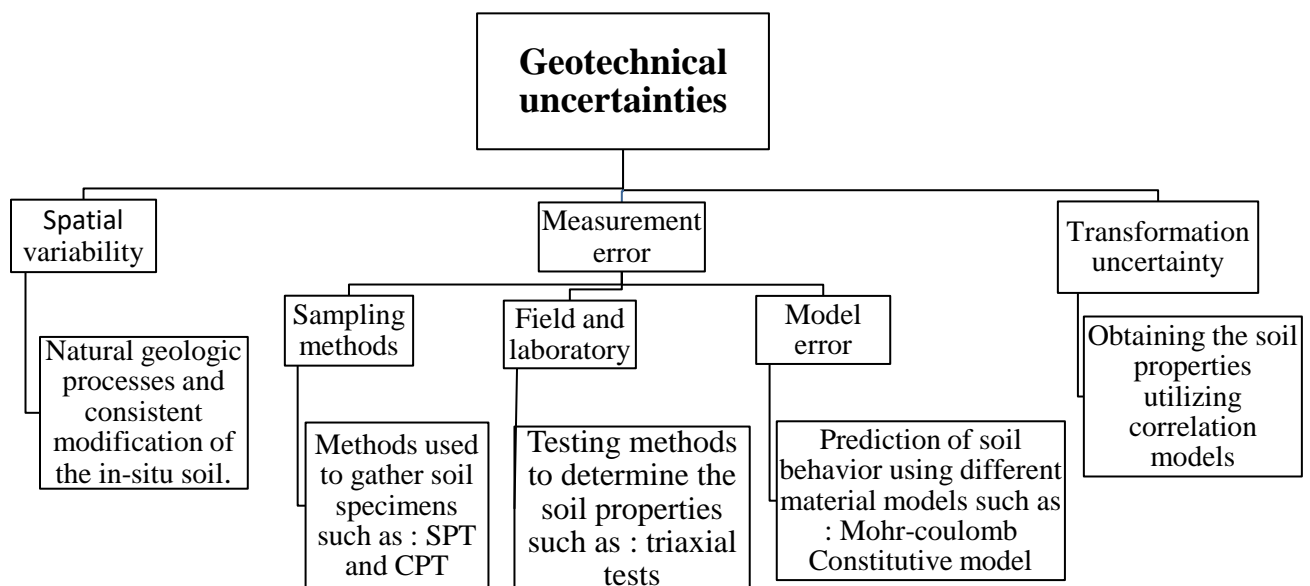


**Figure 4-1: Summary of geotechnical uncertainties based on Phoon and Kulhawy (1999)**

The load and resistance factors in the LSD method are calibrated based on the principles of structural reliability in which the calibration is conducted to achieve predefined target safety limits corresponding to acceptable probability of failure or a reliability index. The historical development of the LSD method for both structural designs and foundation designs were conducted



independently (Becker, 1996a) leading to inconsistency in the target safety limits for individual structures composed of super- and sub-structural components, and in turn, inconsistency in the probability of failure. This discrepancy initiated the need to explore advanced reliability methods such as system reliability to unify the target safety for super- and sub-structures. The recent developments of system reliability-based LSD in unifying the target safety limits are reviewed in the following section.

## 4.2 Recent Development in System-Based Reliability

The literature related to reliability of geotechnical engineering can be divided into two streams; component-based reliability and system-based reliability. The component-based reliability is related to evaluating the reliability of individual sub-structure components not considering the interaction with other sub-structure components nor the effect on the overall sub-structure response (eg., Ching et al., 2009, Zhang et al., 2011, Wang et al., 2011, CSA S16-14, 2014, CSA S6-14, 2014, NBCC, 2015, AASHTO LRFD, 2015). For example, calibrating the resistance factor for individual piles within a group based on the uncertainty in the individual pile response and not considering the uncertainties of the group response. On the other hand, system-based reliability deals with the whole system. Systems in geotechnical engineering usually comprise multiple resistance components, and hence may experience multiple failure modes. For instance, the overall system resistance of a pile foundation is a combination of its frictional and bearing resistances.

Generally, systems in system-based reliability can be categorized into two different groups: parallel systems, and series systems. In parallel systems, the failure of one component in the system will not lead to the failure of the system. While for systems in series, the failure of one component in the system will lead to the failure of the whole system. For instance, for a system consisting of a building and a pile group foundation, the interaction between the pile group foundation and the building can be described as a series system. While the interaction between the building and the pile group foundation can be described as a parallel system. There are two approaches to evaluate the system-based reliability of geotechnical systems: one is related to the interaction between the sub-structural elements, and the other is related to the interaction between sub- and super structural components.

#### 4.2.1 Interaction between the sub-structural elements

Tang & Gilbert (1993) determined the reliability of three different offshore pile systems by comparing the behavior of the pile group with critical piles in design utilizing the second-moment and the first-order methods. They proposed two different factors (complexity factor, CF and redundancy factor, RF) to describe the performance of the pile group system. These factors are based on the initiation of yielding of individual piles in the pile group system. CF is defined as the probability of pile yield over the probability of critical pile yield, and RF is defined as probability of pile yield over the probability of system collapse. They concluded that the probability of system collapse depends mainly on the failure mechanism of the system and load directions, RF ranges from 5 to 42 and CF is equal to unity. The prediction of system loads and probabilities (system and pile yield) at that time were based on simplified numerical models. Thus, further research is required utilizing more sophisticated accurate models.

Other studies ( e.g., McVay et al., 2000 ,Zhang et al., 2005, Kwak et al.,2010, Klammler et al., 2013, Basha and Babu, 2008, Abdelsalam, Sritharan, & Suleiman, 2011, Yang et al., n.d, Fenton, Naghibi, & Griffiths, 2016) conducted reliability analysis and resistance factor calibration for different pile systems. These studies suggested different target reliability indices for single pile and pile group foundations ranging from 2.33 to 3.5 with different probability of failures depending on the target reliability index. Despite the methodical approach of the previous studies, the authors overlooked a vital element of the system-based reliability depicted in the complex system structure interaction which can be represented by the interaction among various system components (building and a pile group system).

#### 4.2.2 Interaction between sub-and super structural elements

Limited studies have examined the system reliability related to the interaction between the superstructure and substructure due to the complex nature of the problem. Zhang et al. (2001) developed a method for calculating the reliability index of axially loaded driven pile group foundation taking into the account the group effect and the interaction between the superstructure and substructure by introducing a system factor. They concluded that the interaction between the

pile groups with superstructure will result in increasing the reliability of the system. For instance, the presence of system effects increased the group reliability index,  $\beta_G$  by 13% for a maximum  $\beta_G = 2.7$  with system effect and 2.3 without the consideration of system effects. However, the method proposed by Zhang et al. (2001) accounts for the system as a whole, where it should account for each individual element in the system (individual piles). In other studies, Paikowsky et al. (2004) and Becker (1996b) accounted for the system effects by suggesting a target reliability index for the substructure higher than the superstructure. Paikowsky et al. (2004) proposed  $\beta_G = 3$  for redundant pile group foundation (5 and more piles) and  $\beta_G = 2.33$  for non-redundant pile group foundation (4 piles and less). On the other hand, Becker (1996b) suggested  $\beta_G = 2-2.5$  for single piles and pile groups. However, the proposed method for calculating the target reliability index considered inconsistent probability of failure for different pile systems (single piles, non-redundant pile group, redundant pile group). Naghibi and Fenton (2017) examined the occurrence of redundancy in individual foundations and system reliability for a redundant pile group foundation. They determined the individual target reliability index of the component of a pile group foundation system by utilizing a predefined target reliability index for system equal to 3. However, this method didn't address the need for unifying the target reliability index for redundant and non-redundant pile group foundation. Oudah et al. (2019) proposed an alternative methodology to calculate the reliability index of individual piles in redundant and non-redundant pile group system based on unifying the target reliability index for the superstructure and substructure. The approach is based on four principles:

1. The probability of failure related to the target reliability index of individual piles in a redundant pile group system cannot exceed a fixed probability of failure equal to  $100 P_{f,system}$  (i.e. 0.135 for system reliability index of 3).
2. Redundant pile group, non-redundant pile groups and single piles have an identical target reliability index. The current LSD philosophy don't account for redundancy in pile groups foundations. It assumes that redundant pile group foundations and non-redundant pile group foundations will have an equivalent target reliability index. While, a redundant pile group foundation should have a higher target reliability index due to the parallel effects.

Therefore, Oudah et al., 2019 suggested an acceptable reliability index for a redundant and non-redundant pile group foundations to achieve a consistent target safety limit for all configurations of pile systems.

3. The interaction between superstructure and substructure can be represented as series system. All the current structural Canadian codes (e.g., NBCC, CSA A23-14 and CSA S16-14) use a target reliability index equal to 3 or higher for different structural applications. Thus, the reliability index of substructure applications should be equal to 3 or higher than the target reliability index used for structural applications as the failure of substructure will lead to the failure of superstructure.
4. The behavior of redundant pile group systems is described as a combination of parallel and series systems. A series system's failure is dependent on the failure of a single pile while the failure of a parallel system requires the failure of the whole pile group system. The probability of failure of a system follows the binomial distribution function. The system can fail if at least  $m$  piles fail out of a  $n$  pile group system. If  $m$  is equal to 1, then this indicates that the system behaves as a series system. On the other hand, if  $m$  is equal to  $n$ , then it indicates that the system behaves as a parallel system. The probability mass function and the system probability of failure,  $P_{f,sys}$  are presented in eq. (4.1) and eq (4.2) respectively, where  $M$  is the number failed piles in the pile group system.

$$P_{f,i(M;n)}(m) = \frac{n!}{m!(n-m)!} P_{f,i}^m (1 - P_{f,i})^{n-m} \quad (4.1)$$

$$P_{f,sys} = P[M \geq m] = \sum_{i=m}^n P_{M;n}(i) \quad (4.2)$$

The target reliability index calculations of the individual piles in a redundant pile group foundation depend mainly on the number of failed piles a system can accommodate prior to failure,  $M$ , with the assumption that the failure of individual piles will not affect the resistance of the pile cap and there will not be any residual forces in the failed piles. The simplified formula of  $M$  is described in Eq. (4.3)

$$M = n - \left(\frac{n}{\gamma}\right) \quad (4.3)$$

Where  $n$  is the number of piles and  $\gamma$  is the system-based equivalent pile safety factor. The relationship between the  $\gamma$  and  $n$  and the individual piles reliability index is directly proportional. As the  $n$  and  $\gamma$  factors increase, the individual piles reliability index value will increase. The equation proposed by Paikowsky (2004) and refined by Oudah et al. (2019) is as follows:

$$\gamma = \frac{\lambda_L}{\phi_s} \quad (4.4)$$

Where  $\lambda_L$  is the equivalent load factor, and  $\phi_s$  is the resistance factor,  $\phi_s$ .

The unified system-based approach proposed by Oudah et al. (2019) represents a major advancement in the current research effort dedicated towards rationalizing the design of sub- and super-structure to yield consistent target safety limits. The work by Oudah et al. (2019) utilized a simplified method to determine the system-based equivalent pile safety factor,  $\gamma$ , which is a key parameter used in the calibration of the resistance factor of individual piles within a group system. A scientific-based approach is utilized in this research to calculate  $\gamma$ .

### 4.3 Objectives

The objectives of this chapter are to calibrate the resistance factors for redundant group piles based on a refined analysis of the system-based equivalent pile safety factor,  $\gamma$  and to determine/ propose a new approach to determine the number of piles the pile group system can accommodate prior to failure,  $M$ . A Finite element parametric study analysis was conducted to determine the most suitable  $\gamma$  factor for different pile group configurations. These values were used to calibrate the resistance factors of the pile group foundations using the system-based reliability analysis suggested by (Oudah et al., 2019).

## 4.4 Methodology for Calibrating the Resistance Factors Based on System-Based Reliability

The Resistance factor calibration framework of this research is summarized in Table 4-1.

**Table 4-1: Resistance factor calibration process**

Step 1	Gather the required statistical data for different design methods
Step 2	Calculate $\gamma$ factor utilizing a comprehensive FE parametric analysis
Step 3	Calculate M factor which depends mainly on the number of piles and $\gamma$ factor
Step 4	Calculate the probability of failure of individual piles and the system using the method proposed by (Oudah et al., 2019) from Eq.4.1 and 4.2
Step 5	Calculate the individual pile target reliability index using a system reliability index = 3
Step 6	Choose an adequate resistance factor calibration method
Step 7	Calibrate the resistance factor for different design methods

### 4.4.1 Calculations of $\gamma$ factor

The method proposed by Oudah et al. (2019) describes the behavior of a redundant pile group foundation as a combination of series and parallel systems taking into consideration the system effects (interaction between superstructure and substructure). However, the estimation of the factor  $\gamma$  is not only dependent on the two variables ( $\lambda_L, \phi_s$ ), it also depends on the failure of the individual piles in a pile group system. The  $\gamma$  factor depends primarily on the ability of the pile cap to redistribute the forces upon failure of individual piles within a pile group foundation. Pile caps can be defined as a structural element that attains the function of transferring the load from the superstructure to the substructure. CSA A23-14 code has addressed two main design approaches for designing reinforced concrete pile caps: sectional method and strut and tie method. The selection of the method is mainly dependent on the span to depth ratio  $L/D$ . For slender pile caps ( $L/D > 1$ ),

the flexural behavior governs, and the sectional method can be used. For deep pile caps ( $L/D < 1$ ), the arching action is the main resisting mechanism, and the strut and tie method must be used (Meléndez et al., 2019). The proposed method by the code utilizes a hypothetical truss that consist of compression struts, tension ties and nodal zones. Figure 4-2 shows the typical 3D strut and tie model for a pile cap. The load is transferred from the column to the piles using diagonal struts and horizontal ties between the piles. However, strut and tie methodology doesn't account for the global stability of the system. The presence of a failing pile in a pile group foundation will lead mostly to a lateral deflection and rotation of the pile cap towards the failing pile with induced bending moment at the adjacent piles (Poulos, 1997) which affects the stability of the pile cap and hence cause a significant impact on the distribution of the forces as shown Figure 4-3. This behavior is expected due to the elimination of the diagonal strut that links the axial load from the column to the failing pile. To yield accurate results and eliminate the complexity associated with the sophisticated structural behavior of the pile cap, next section will focus on examining the impact of failing one pile in a pile group foundation with different failure scenarios on the redistribution of the forces upon failure of individual piles within a pile group foundation utilizing a FE parametric analysis.

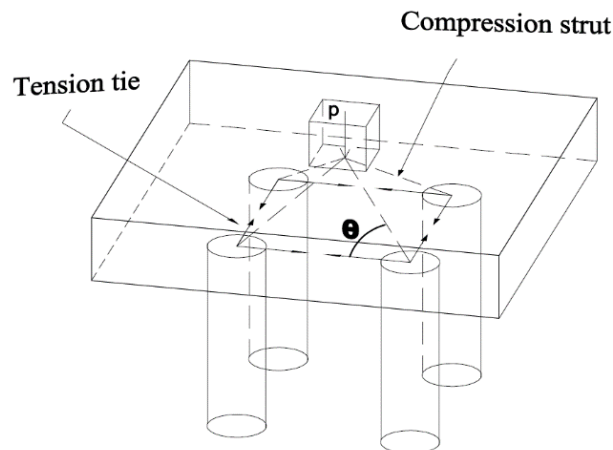


**Figure 4-2: Typical 3D strut and tie model for four-pile cap**

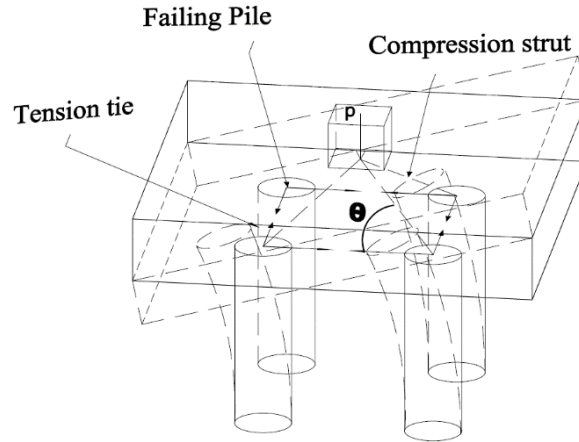


**Figure 4-3: Illustration of failure mechanism of pile group under axial loading when one pile fails**

Utilizing the parameters related to individual pile failure in calculating the system-based equivalent pile safety factor would yield to a more refined estimation. This is for the sole purpose of following a deterministic approach instead of the iterative approach used in eq (4.5).

The suggested approach to calculate  $\gamma$  marks it as a function of the following variables: original design pile safety factor, ability of the pile cap to redistribute the load off the failed pile, and the pile group configuration. The influence of the pile group configuration includes: pile spacing, number of piles, and the location of the failed pile with respect to the adjacent intact piles, can be quantified using redistribution factors,  $\lambda$  (i.e., ratio of the axial load redistributed from the failed pile to the adjacent piles). The new proposed equation for the system-based equivalent pile safety factor is shown below:

$$\gamma = \frac{Q_{u,i}/(n-1)}{P_{ex,i} + \lambda P_{fail}} \quad (4.5)$$

Where  $Q_{u,i}$  is the total ultimate applied load,  $n$  is the number of piles,  $P_{ex,i}$  is the axial load existing on Pile  $i$ ,  $\lambda$  is a redistribution factor, and  $P_{fail}$  is the axial load existed on the failed pile. There are numerous methods in the literature to predict the ultimate axial capacity of piles ( $Q_{u,i}$ ) from a load-displacement curve. In this study, the interpretation of the ultimate axial capacity of pile group is



be based on the Davisson's failure criteria as suggested by Kwak et al. (2010), Paikowsky et al. (2004) and AbdelSlam, et.al (2012).

The parameters in Eq (4.5) will be evaluated through a Finite element (FE) parametric study investigation that is explained in section 4.5.

#### 4.4.2 Individual piles reliability index

The safety factor of the system is usually determined using the reliability index. For a normally or log-normally distributed load and resistance it can be defined mathematically as the number of standard deviations, from the mean value, until the safety margin becomes zero and it is mainly dependent on the probably of failure of the system, i.e:

$$\beta = -\Phi^{-1}P_f \quad (4.6)$$

Where  $\beta$  is the reliability index,  $P_f$  is the probability of failure, and  $\Phi^{-1}$  is the inverse of the cumulative distribution function for a normal distribution function which was calculated using a built-in MATLAB code.

The calculations of individual piles target reliability index,  $\beta_i$  in this paper was determined to achieve a system target reliability index equal to 3 taking into consideration the parallel and series effects of the system. This was done for the purpose of unification of target reliability index between the substructure and the superstructure.

#### 4.4.3 Resistance factor calibration method

The ultimate limit state occurs when the applied load  $\geq$  the resistance proposed by AASHTO LRFD (2015) for deep foundations as follows:

$$\Phi R_n \geq \eta \sum \gamma_i Q_i \quad (4.7)$$

Where  $\Phi$  is the resistance factor,  $R_n$  is the Ultimate resistance,  $\eta$  is the modifier to account for ductility, operational performance and redundancy,  $\gamma_i$  is the load factor, and  $Q_i$  is the load effect.

There are several methods in the literature to calibrate the resistance factor. The most widespread methods in the field of geotechnical engineering are the Monte Carlo simulation (MCS), the first order second moment methods (FOSM), and the First/second-order reliability methods (FORM/SORM). However, FOSM is the simplest and the most used method amongst the three methods available (Allen, 2005). This is because using FOSM, large data can be used to calculate the probability of failure and overcome the calculation of a distribution function (Paikowsky et al., 2004). According to Shreider (1966), MCS is the simplest method for reliability analysis. However, it is time consuming due to the intensive iterative process required to yield to accurate results. Moreover, Kwak et al. (2010) conducted a comparison between FOSM and MCS methods and found that there is no significant difference between the two methods in the case of a non-linear limit-state function. Another comparison was made by Paikowsky (2003) between FORM and FOSM. The results indicate that FOSM have more rational values than FORM. The author also concluded that FOSM methods provide slightly lower values for the resistance factor by almost 10%, which indicates that FOSM has a higher margin of safety than the FORM method. Mbarka et al. (2010) have also conducted a comparison between different reliability analysis methods. The results demonstrate that FOSM provides a reasonable approximation for the cumulative distribution function of the safety factor and the reliability index, especially if it was modeled using a sophisticated finite element model.

Applying FOSM, Paikowsky et al. (2004) reached a closed form solution considering both dead load and live load and assuming lognormal distribution for the resistance as shown below:

$$\Phi_s = \frac{\lambda_R \left( \frac{\gamma_D Q_D}{Q_L} + \gamma_L \right) \sqrt{\frac{1 + COV_{Q_D}^2 + COV_{Q_L}^2}{1 + COV_R^2}}}{\left( \frac{\lambda_{Q_D} Q_D}{Q_L} + \lambda_{Q_L} \right) e^{\beta_i \sqrt{\ln \left[ (1 + COV_R^2)(1 + COV_{Q_D}^2 + COV_{Q_L}^2) \right]}}} \quad (4.8)$$

Where  $COV_R$ ,  $COV_{Q_L}$  and  $COV_{Q_D}$  are the coefficient of variation of the resistance, live load and dead load respectively.  $\lambda_R$ ,  $\lambda_{Q_L}$  and  $\lambda_{Q_D}$  are the mean resistance bias factors (the average capacity over the predicted capacity) for the resistance, live load and dead load respectively.  $\beta_i$  is the

individual piles target reliability index.  $\gamma_D, \gamma_L$  are the dead load and live load factors respectively.  $Q_D/Q_L$  is dead load over live load ratio.

## 4.5 Parametric Study to Calculate $\gamma$

Figure 4-4 demonstrates the typical foundation considered in the parametric study, which consists of the column, pile cap, and individual piles. Figure 4-5 shows the soil type and dimensions used for all models. As mentioned previously, the system-based equivalent pile safety factor,  $\gamma$ , is mainly influenced by the distribution of the forces upon failure of individual piles in a pile group system. To ensure comparable results between different pile group configurations, the pile cap design is adjusted between models to satisfy minimum code requirements. For the purpose of this study, two types of analysis are performed: Ultimate and Serviceability Limit States. The former analysis involves inducing failure in the target pile by reducing its capacity to zero. The latter involves softening the soil around the target pile which mimics increased settlement in the target pile. Three pile group configurations are analyzed: five pile, seven pile and nine pile group as shown in Figure 4-6. For each configuration, the loaded column area, pile spacing, and pile diameter are varied. The different parameter values analyzed are summarized in Figure 4-7 . A total of 110 models are included in the parametric study.

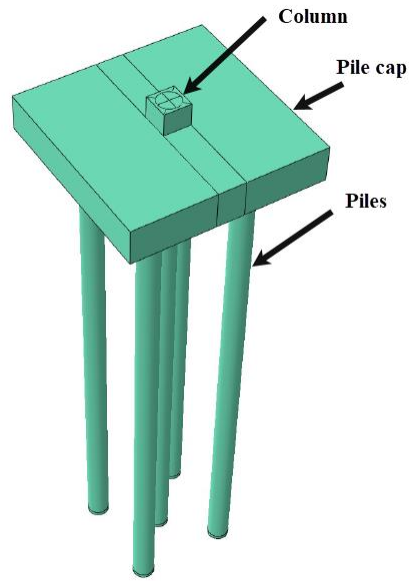


Figure 4-4: Typical foundation considered in the FE parametric study

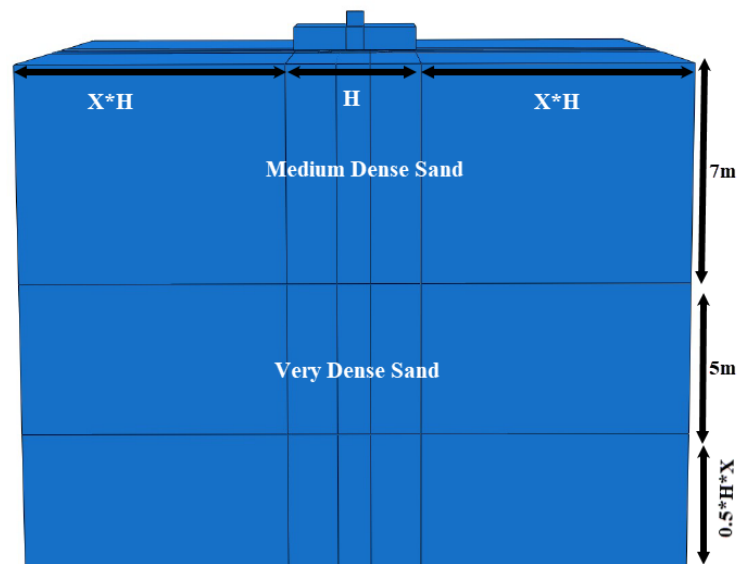
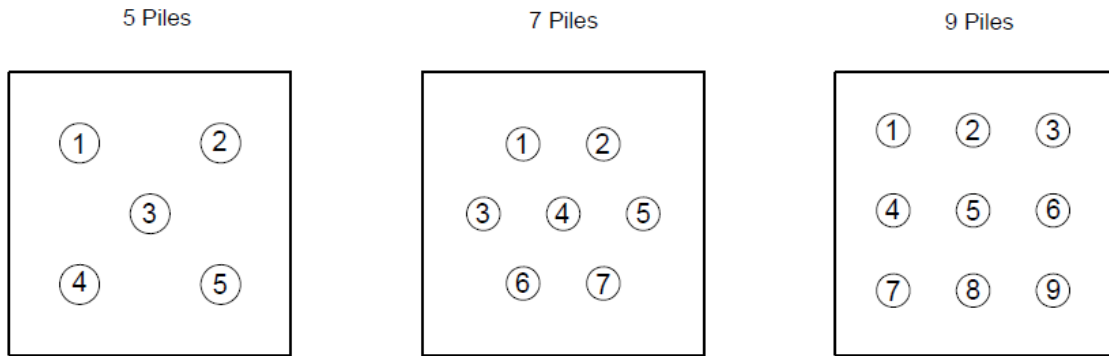
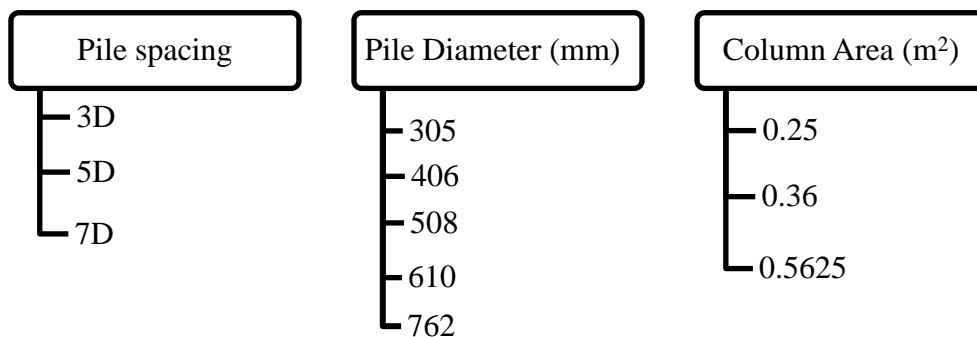


Figure 4-5: Soil type and dimensions considered in the FE parametric study



**Figure 4-6: Pile group configurations considered in the FE parametric study**



**Figure 4-7: Different parameter considered in the FE parametric study**

## 4.6 Model Development

### 4.6.1 Finite element geometry and boundary conditions

Pile group problems are a three-dimensional in nature. Thus, the soil and the pile group were simulated in three-dimensional (3D) space utilizing the finite element program ABAQUS. The column, pile cap, soil, and closed ended steel pipe piles were modelled using 8 node, first order, reduced integration solid element (C3D8R). The connection between the pile cap and the steel pipe piles were assumed to be rigid. The concrete column is modeled as a rigid element since the response of the column does not impact the results. The column area is only used to transfer the load from the superstructure to the substructure. The soil at the base of the model is restrained in

all directions, while the sides are allowed to move in the vertical direction only. The pile-soil interface was simulated using surface to surface contact method based on a penalty contact constraint, with a tangential behavior defined by coulomb's frictional model. No slippage will occur at the pile soil-interface, unless the contact shear stresses have exceeded the critical shear stresses. The critical shear stress is a function of the coefficient of friction ( $\tan\Phi$ ). The friction coefficient was assigned A value of 0.57,0.7 for all models. While, the normal behavior which is also uses the penalty method is defined as "hard" contact with separation allowed.

#### 4.6.2 Constitutive material model and model parameters

The behavior of the concrete pile cap and the closed ended steel pipe piles were simulated using linear elastic model. The mechanical properties of concrete used in the model (elastic modulus,  $E_s$  and Poisson's ratio) were conducted in accordance to CSA-A23.3-14 where  $E_s$  is equal to  $4500\sqrt{f_c'}$ . Table 4-2 shows the material properties for the concrete pile cap and the steel piles. Two layers of medium dense to dense sand were simulated using linear elastic perfectly plastic material model with the Moher-coulomb failure criteria. The elastic behavior is defined by Young's modulus ( $E_s$ ), Poisson's ratio ( $\nu_s$ ). While, the plastic behavior of the model is controlled by the cohesion ( $c$ ), internal friction angle ( $\Phi$ ) and dilation angle ( $\Psi$ ). Table 4-4 summarizes the Soil Material properties used in the model.

**Table 4-2: Material properties for the steel pile considered in the FE model**

Parameter	Pile cap	Piles
Young's modulus E (Mpa)	24647.5	200000000
Poisson's ratio $\nu_p$	0.15	0.28
unit weight (kN/m <sup>3</sup> )	25	78.5

**Table 4-3: Soil parameters considered in the FE model**

Soil Type	Young's modulus $E_s$ (Mpa)	Poisson's ratio $\nu_s$	Friction angle $\phi$ (degrees)	Dilation angle $\Psi$ (degrees)	Dry unit weight $\gamma_s$ (kN/m <sup>3</sup> )	Cohesion $c$ (Kpa)
Medium dense sand	40	0.3	30	0	18	1
dense sand	60	0.3	35	5	18	4

### 4.6.3 Analysis Result

Tables 4-4 to Table 4-6 present  $\gamma$  factor for different combinations of the column area, pile diameter, and pile spacing. Out of the three parameters,  $\gamma$  is only affected by varying the pile spacing. This is because  $\gamma$  is mainly dependent on the angle of the strut and tie, which changes based on the pile spacing. As the pile spacing increases, the strut and tie angles decrease as presented in Figure 4-3, and hence decrease the diagonal compression force which eventually leads to reducing  $\gamma$ . However, varying the column area and pile diameter does not have any effect on the strut and tie angles. Figure 4-8 presents the effect of the pile spacing on the  $\gamma$  factor for different pile configurations and failure scenarios. The results show that the pile spacing is inversely proportional to the  $\gamma$  factor. As the pile spacing increases  $\gamma$  decreases linearly. This was expected as the behavior of closely spaced pile groups is similar to the behavior of a large single pile, where there will not be any relative movement between the piles and the soil between the piles. It is also worth noting that the failure of pile 1 (corner pile) has the highest effect on  $\gamma$ , while the failure of pile 3 (middle pile) has the lowest effect. This is due to the stiffness of the pile cap since code-compliant pile caps are relatively rigid to avoid punching. For rigid pile caps no local deformation will occur at the middle piles, thus the load will be redistributed to the outer piles. Corner piles will carry the highest axial load, while middle piles will carry lowest axial load. The second reason is related to the failure mechanism of the pile cap. The rotation of the pile cap towards the failing pile when one pile fails in the system will lead to a significant change to the distribution of the forces. The highest axial load will transfer to the adjacent piles when the failing pile is surrounded with a smaller number of piles due to the increase of settlement.

**Table 4-4: Parametric study results of 5 piles in a pile group foundation for different design variables and failure scenarios**

Case A (Pile 1) <sup>a</sup>		Case B (Pile 3) <sup>a</sup>		Case C (Pile 4) <sup>a</sup>	
Effect of the Column Area					
Column Area (m <sup>2</sup> )	$\gamma$	Column Area (m <sup>2</sup> )	$\gamma$	Column Area (m <sup>2</sup> )	$\gamma$
0.25	1.7414	0.25	1.7317	0.25	3.0927
0.36	1.7403	0.36	1.7743	0.36	3.0926
0.5625	1.7273	0.5625	1.7944	0.5625	3.0780
Effect of Pile diameter					
Diameter (m)	$\gamma$	Diameter (m)	$\gamma$	Diameter (m)	$\gamma$
0.305	1.7036	0.305	1.7943	0.305	2.9479
0.406	1.7403	0.406	1.7743	0.406	3.0926
0.508	1.5169	0.508	1.5995	0.508	2.7450
Effect of Pile Spacing					
Spacing	$\gamma$	Spacing	$\gamma$	Spacing	$\gamma$
3D	1.7403	3D	1.7743	3D	3.0926
5D	1.3204	5D	1.3816	5D	2.5663
7D	0.9852	7D	1.0198	7D	1.9965

<sup>a</sup> refer to Figure 4-6 for pile group configuration



**Table 4-5 : Parametric study results of 7 piles in a pile group foundation for different design variables and failure scenarios**

Case A (Pile 1) <sup>a</sup>		Case B (Pile2) <sup>a</sup>		Case C (Pile 5) <sup>a</sup>	
Effect of the Column Area					
Column Area (m <sup>2</sup> )	$\gamma$	Column Area (m <sup>2</sup> )	$\gamma$	Column Area (m <sup>2</sup> )	$\gamma$
0.25	1.9459	0.25	2.1381	0.25	2.9398
0.36	1.9454	0.36	2.1478	0.36	2.9613
0.5625	1.9445	0.5625	2.1503	0.5625	3.2071
Effect of Pile diameter					
Diameter (m)	$\gamma$	Diameter (m)	$\gamma$	Diameter (m)	$\gamma$
0.305	1.9454	0.305	2.1478	0.305	2.9613
0.406	1.9796	0.406	2.2392	0.406	3.1908
0.508	1.7592	0.508	1.9762	0.508	2.8828
Effect of Pile Spacing					
Spacing	$\gamma$	Spacing	$\gamma$	Spacing	$\gamma$
3D	1.9454	3D	2.1478	3D	2.9613
5D	1.6824	5D	1.9624	5D	2.8816
7D	1.3757	7D	1.6022	7D	2.3631

<sup>a</sup> refer to Figure 4-6 for pile group configuration

**Table 4-6: Parametric study results of 9 piles in a pile group foundation for different design variables and failure scenarios**

Case A (Pile 1) <sup>a</sup>		Case B (Pile2) <sup>a</sup>		Case C (Pile 5) <sup>a</sup>	
Effect of the Column Area					
Column Area (m <sup>2</sup> )	$\gamma$	Column Area (m <sup>2</sup> )	$\gamma$	Column Area (m <sup>2</sup> )	$\gamma$
0.25	1.9459	0.25	2.1381	0.25	2.9398
0.36	1.9454	0.36	2.1478	0.36	2.9613
0.5625	1.9445	0.5625	2.1503	0.5625	3.2071
Effect of Pile diameter					
Diameter (m)	$\gamma$	Diameter (m)	$\gamma$	Diameter (m)	$\gamma$
0.305	1.9454	0.305	2.1478	0.305	2.9613
0.406	1.9796	0.406	2.2392	0.406	3.1908
0.508	1.7592	0.508	1.9762	0.508	2.8828
Effect of Pile Spacing					
Spacing	$\gamma$	Spacing	$\gamma$	Spacing	$\gamma$
3D	1.9454	3D	2.1478	3D	2.9613
5D	1.6824	5D	1.9624	5D	2.8816
7D	1.3757	7D	1.6022	7D	2.3631

<sup>a</sup> refer to Figure 4-6 for pile group configuration

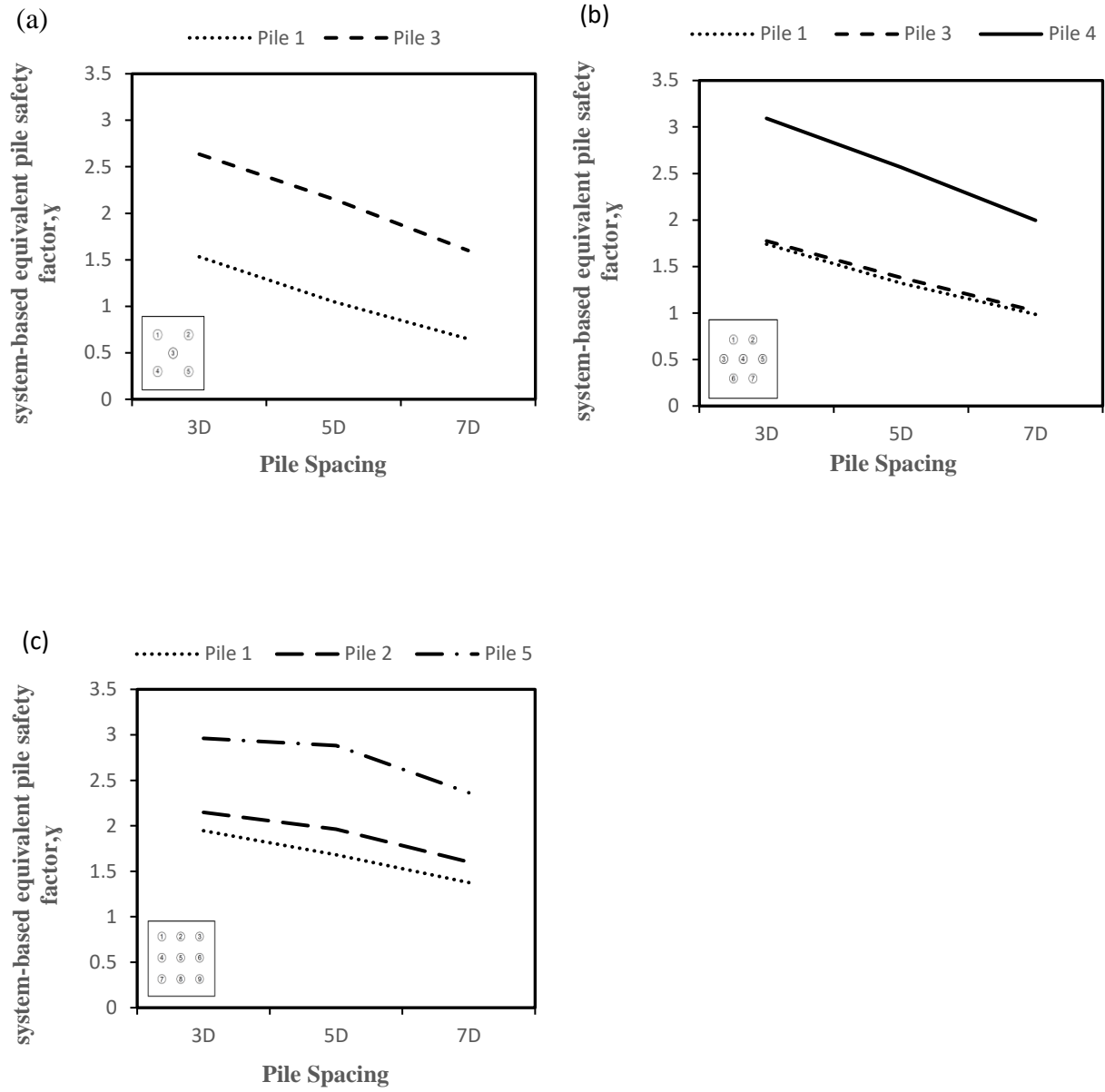


**Figure 4-8: Effect of pile spacing on  $\gamma$  factor for different pile configurations and failure scenarios a) 5 piles; b) 7 piles; c) 9 piles**

## 4.7 M value based on the failure of one pile or more

Oudah et al. (2019) proposed a method to determine the number of piles the system can accommodate prior to failure. In this method, M was based on the number of piles in the group, and the system equivalent safety factor,  $\gamma$ , of the individual piles in a redundant pile group system. This approach considered the failure of only one pile in calculating the factor of safety,  $\gamma$ , and overlooked a more critical scenario which is the failure of more piles. The failure of more piles in the group may have a more significant effect on the factor of the safety of the system than the failure of one pile due to the complex behavior of the pile group system. This section will present a more refined approach to determine the M value based on the failure of one or more piles in the group. The proposed approach utilizes an equivalent factor of safety, FS, (i.e., global factor of safety for the system) based on a simplified relation proposed by Barker et al., (1991) for the purpose of setting a failure criterion for the system. This will be achieved by comparing the nominal capacity of the intact pile group system as presented in Eq (4.9) with the failed pile group capacity taking into the consideration different failure scenarios, utilizing the FE parametric analysis done in chapter 3.

$$\text{nominal capacity} = \frac{\text{Capacity of intact pile group}}{FS} \quad (4.9)$$

Where:

$$FS = \frac{\gamma_D \left( \frac{DL}{LL} \right) + \gamma_L}{\phi \left( \frac{DL}{LL} + 1 \right)} \quad (4.10)$$

Where FS, is an equivalent safety factor,  $\gamma_D$  is the dead load factor,  $\gamma_L$  is the live load factor, DL/LL is the dead load over live load ratio, and  $\phi$  is the resistance factor of the system which was determined from Eq (4.8) based on a reliability index index,  $\beta_s = 3$ .

Figure 4-9 illustrates the suggested framework to calibrate resistance factor for pile group foundations based on M value.

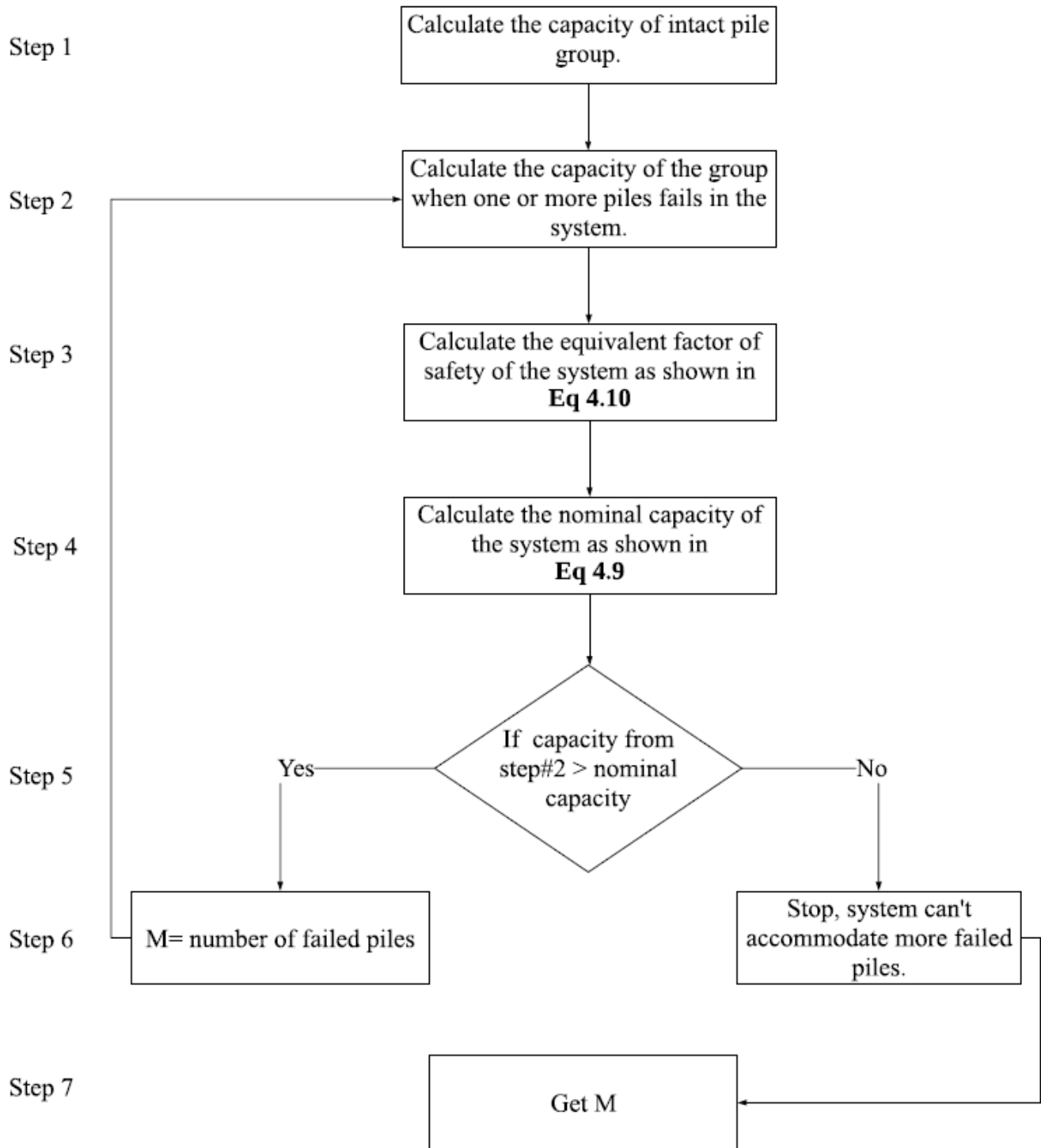


**Figure 4-9: Flow chart presenting the framework of calibrating resistance factor for pile group foundations based on M value**

## 4.8 Resistance factor calibration of redundant group piles

### 4.8.1 Survey of statistical data

To calibrate the resistance factor for an axially loaded driven piles the estimation of the COV (Coefficient of variation), and bias ratio parameters are essential for an accurate resistance factor calibration process. The COV can be defined as the ratio between the standard deviation and the mean of sample population. Additionally, the bias factor can be defined as the ratio between the measured capacity and the predicted capacity. The measured capacity of the pile is usually interpreted from a static load test (SLT), whereas the predicted capacity of the pile is determined using empirical and semi-empirical formulas. There are several methods proposed in the literature to determine the measured and predicted axial capacity of pile foundations. Nevertheless, in this research the predicted and measured capacities of the piles was included as a design parameter using statistical analysis. All the statistical information (ie., COV and bias ratio) required for this research was obtained from AbdelSlam, et.al (2012) which is based an electronic data base known as PILOT (i.e., pile load tests in Iowa). Iowa DOT have conducted a large electronic data base for the purpose of calibrating resistance factor for different types of pile foundations, it contains more than 270 pile tests.

The statistics of bias and COV for a sandy soil are shown in Table 4-7. The COV and mean bias ratios have been obtained for the most used design methods in North America for driven piles in sand (Nordlund, Bluebook,  $\beta$ -Method, SPT Meyerhof). The selected COV and mean bias ratio are 0.92 and 0.53 for (Nordlund method), 1.18 and 0.36 for Bluebook method which is a combination of  $\alpha$ -Tomlinson (Tomlinson, 1980) and the SPT-Meyerhof, 0.88 and 0.47 for ( $\beta$ -Method), and 1.74 and 0.66 for (SPT- Meyerhof method), respectively. Additionally, the COV and the bias factor for dead and live loads were chosen as the values used for calibrating the resistance factor in the NBCC code. The COV and bias ratio for the dead load were 0.1 and 1.05, respectively, while he COV and bias ratio for the live load were 0.17 and 0.9, respectively.

**Table 4-7: Summary of database used in the resistance factor calibration (AbdelSlam, et.al 2012)**

Category	Pile resistance calculation method	Soil type	Design Method	No. of pile tests	Mean Bias	COV
Driven Piles	Static Methods	Sand	Nordlund	34	0.92	0.53
			Bluebook	34	1.18	0.36
			$\beta$ -Method	34	0.88	0.47
			SPT- Meyerhof	34	1.74	0.66

#### 4.8.2 Calculations of the number of piles the system can accommodate, M

The value of M was calculated based on two different methods as discussed in the preceding sections, In the first method M value was determined based on a system equivalent pile safety factor,  $\gamma$  as discussed in section 4.4.1. In the second method M value was determined by comparing the critical cases of the defected pile groups obtained from the numerical analysis (chapter 3) with the intact pile group foundation as discussed in section 4.7. Table 4-8 presents a comparison between the two methods. It is interesting to note that M values was found to be identical for the two methods at a 3D pile spacing. However, as the pile spacing increases M value decreases linearly for the first method and remains constant in the second one until 5D spacing and then it decreases. This variation of M between the two methods is attributed due to fact that both methods have a different theoretical bases, where in the first method the value of M is dependent on the factor of safety of one pile in the group which gives an approximate conservative solution. However, in the second method M value is based on a more rational deterministic method, where the capacity of the failed pile group system (i.e., failure of one pile or more) is compared to the intact pile group system.

Table 4-9 presents the calculated M values (Method 2) used for calibrating the final resistance factors for different design methods, spacing, and pile group configurations (5 piles, 7 piles and 9 piles).

**Table 4-8: Comparison in M values using two different methods**

M-values	5 Piles			7 Piles			9 piles		
	3D	5D	7D	3D	5D	7D	3D	5D	7D
<b>Method 1</b>	2	1	0	3	2	0	4	3	2
<b>Method 2</b>	2	2	1	3	2	2	4	4	3

**Table 4-9: M-values (Method 2) for different pile group configurations, different design methods and pile spacing**

M-values	5 Piles			7 Piles			9 Piles		
	3D	5D	7D	3D	5D	7D	3D	5D	7D
Spacing									
Nordlund Method	2	2	1	3	2	2	4	4	3
Bluebook Method	1	1	1	2	2	1	3	2	2
$\beta$ Method	2	1	1	3	2	2	4	3	3
SPT Method	2	1	1	3	2	2	4	3	3

### 4.8.3 Calculation of individual pile reliability index

The calculations of reliability indices of individual piles in a redundant pile group for a driven pile is shown in this section. The system target reliability index for all pile groups is equal to 3. The individual pile reliability index calculations were based on a binomial system response for a redundant pile group foundation using Eq (4.1) and Eq (4.2). The  $\gamma$  factor was calculated based on Eq (4.5) and FE parametric analysis. The analysis results of the FE parametric study showed that the pile spacing affects the  $\gamma$  factor the most with the failure of the corner pile. Table 4-10 shows the calculated reliability indices for individual piles for different pile configurations and spacing. It can be noted that the calculated reliability index of individual piles in the group for a  $\beta_G = 3$  is inversely proportional to the number of piles and spacing. Which was anticipated, because as the number of piles increases the impact of pile defect decreases due the existence of pile redundancy in the system.



**Table 4-10: The calculated individual piles reliability index for different pile group configurations**

Reliability Index			
Number of piles	5 piles	7 piles	9 piles
3D	1.62	1.39	1.23
5D	2.27	1.81	1.55
7D	2.27	2.4	1.93

#### 4.8.4 Results and discussion

The individual pile resistance factor was calibrated for 3 different redundant pile group configurations (5 piles, 7 piles and 9 piles) with a system target reliability index equal to 3, utilizing the statistical data shown in Table 4-7. Figure 4-10 to Figure 4-12 demonstrate the calibrated resistance factors for different design methods for driven piles in medium dense to dense sand. Also, different DL/LL ratios were used to cover a broader range of structural applications; 1, 2,3 and 4. The results showed that the proposed resistance factor values vary from 0.31 to 0.61, 0.52 to 0.86, 0.34 to 0.63, and 0.45 to 0.96 for different design methods: Nordlund, Bluebook,  $\beta$ -Method, and SPT Meyerhof respectively. It is worth noting that the highest values are for the SPT-97 design method. This can be explained by the fact that the SPT-97 has the highest mean bias ratio. The methodology used in this research to calculate the resistance factor is based on a code-compliant pile group foundation. Accordingly, these values can be used by geotechnical engineers for designing pile group foundations in sand.

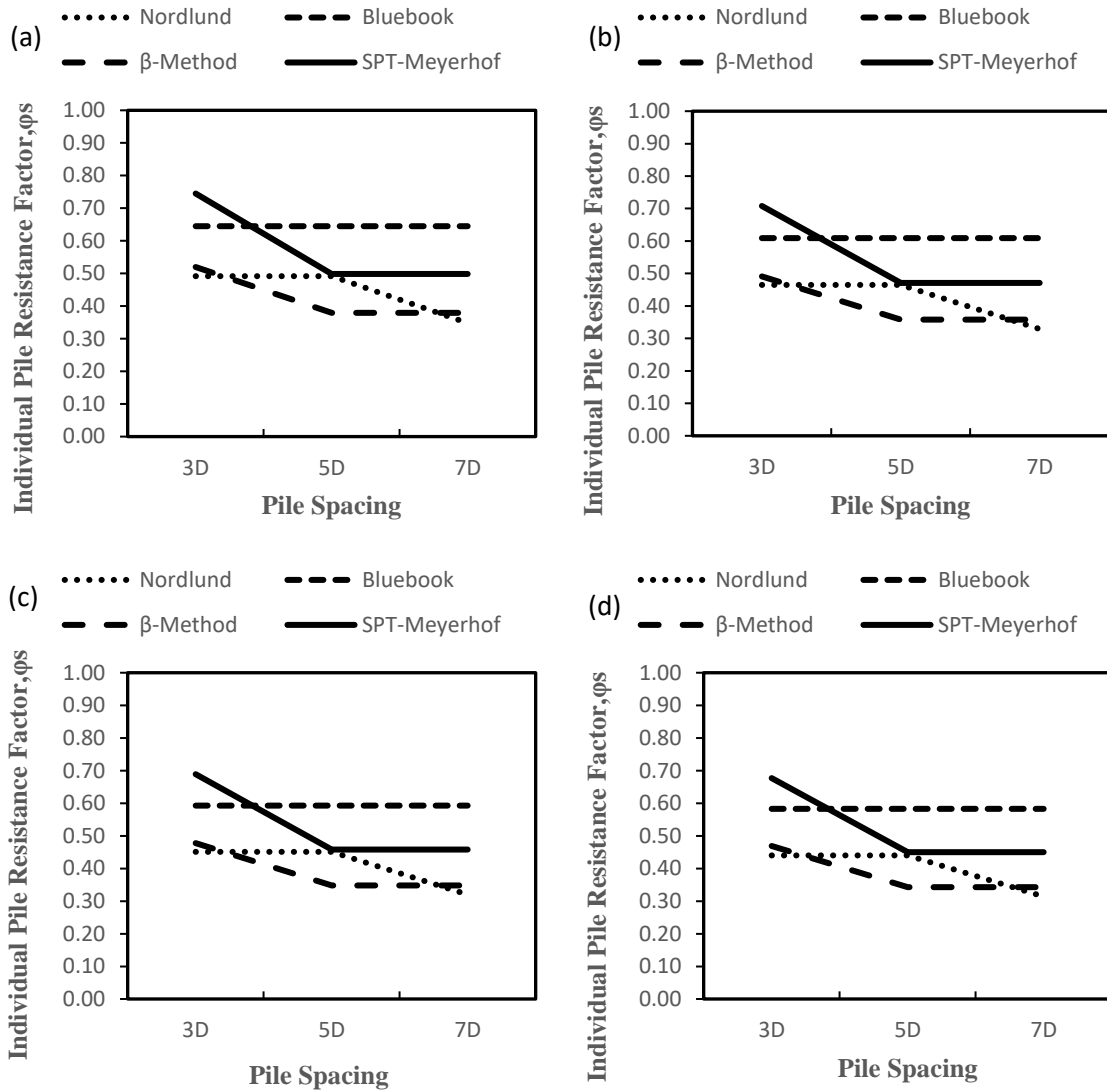


**Figure 4-10: Calibrated resistance factor for 5 piles in a pile group foundation for different DL/LL a) 1; b) 2; c) 3; d) 4**

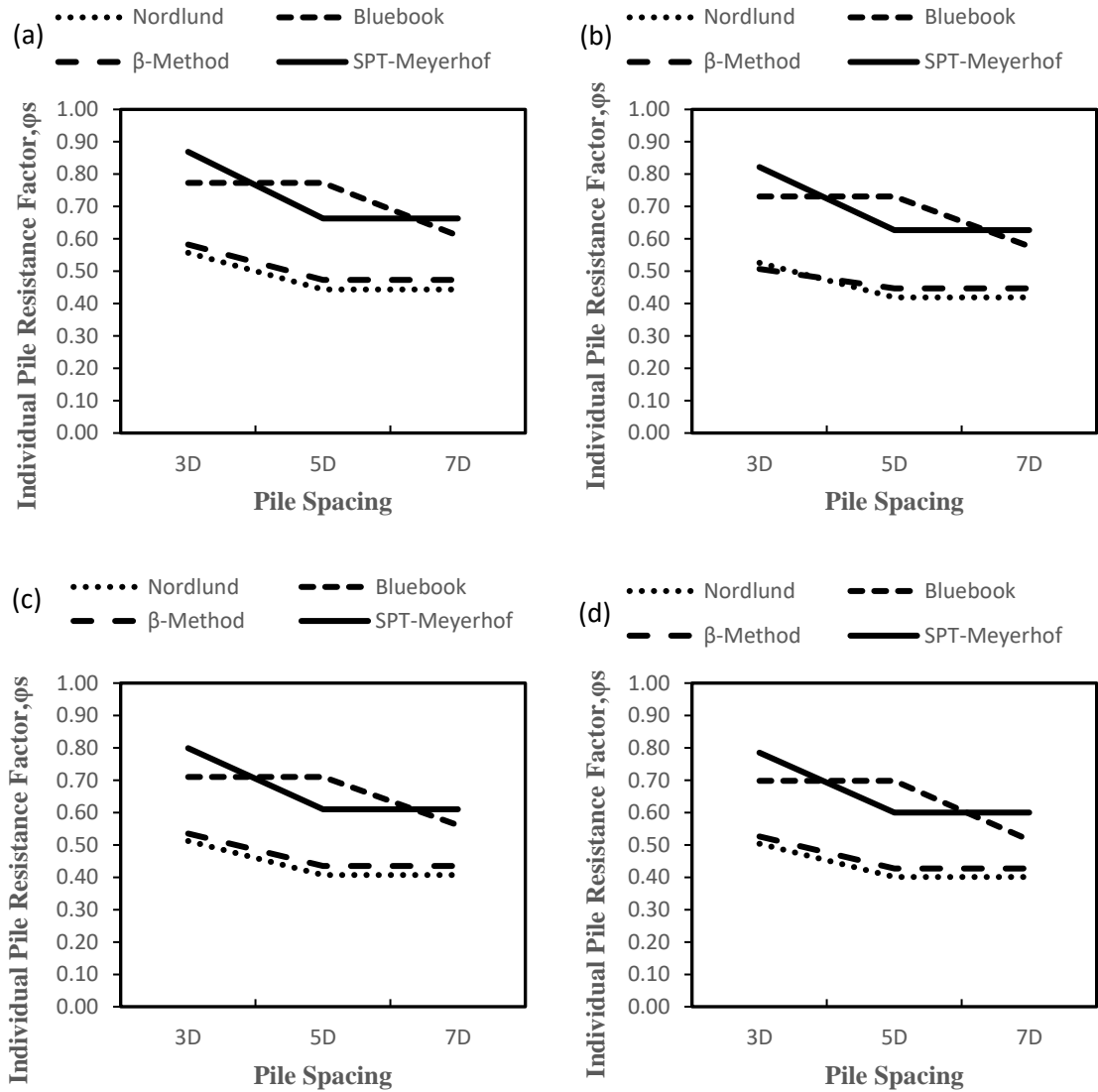


**Figure 4-11: Calibrated resistance factor for 7 piles in a pile group foundation for different DL/LL a) 1; b) 2; c) 3; d) 4**

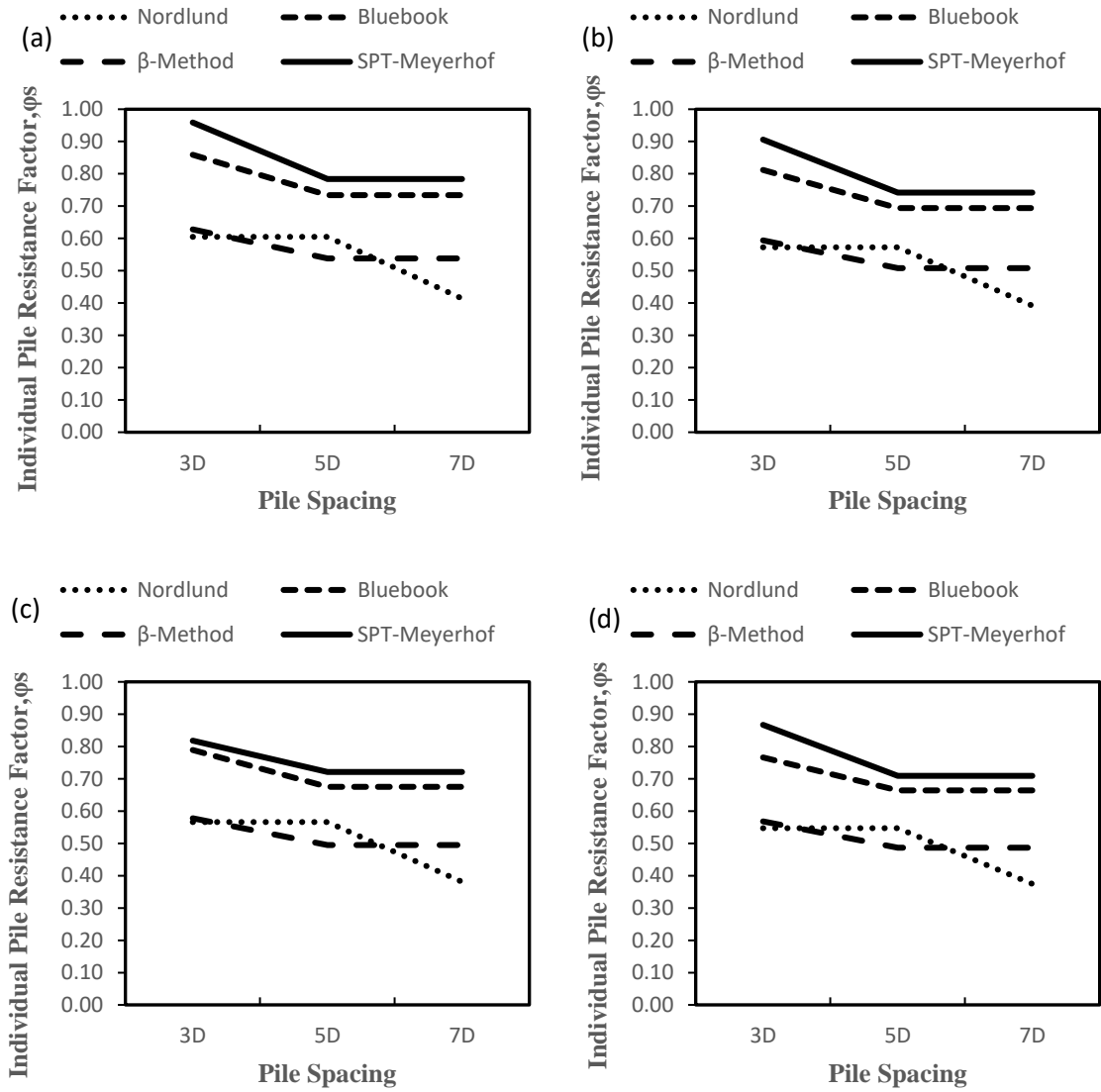


**Figure 4-12: Calibrated resistance factor for 9 piles in a pile group foundation for different DL/LL a) 1; b) 2; c) 3; d) 4**

## 4.9 Conclusion

This chapter presents calibrated resistance factors for different pile group configurations (5 piles, 7 piles and 9 piles), pile spacing (3D,5D and 7D) , design methods, and DL/LL ratios in a medium dense to dense sandy soil using the unified system-based reliability analysis proposed by (Oudah et al., 2019). This work is to promote and encourage the use of the LSD approach in practical design versus the more common WSD. A more refined approach to calculate the system-based equivalent pile safety factor  $\gamma$ , and the number of piles the system can accommodate,  $M$  was presented utilizing a finite element parametric investigation where the effects of column area, pile diameter and pile spacing were considered. Based on the results of the numerical model, the following can be concluded:

- $\gamma$  factor is mainly dependent on the ability of the pile cap to redistribute the forces upon failure of individual piles within a pile group foundation.
- The stiffness and the failure mechanism of the pile cap are the main factors that affect the redistribution of the forces in a pile group foundation.
- Varying the column area and pile diameter have no effect on the  $\gamma$  factor, and this is because the column area and the pile diameter are not function of the strut and tie angle.
- Pile spacing affects  $\gamma$  the most. As the pile spacing increases  $\gamma$  factor decreases linearly. This is due to the decrease of the strut and tie angle and consequently decrease of the compression force in the diagonal strut.
- The maximum and minimum number of failed piles the system can accommodate before failure for different design methods and spacing,  $M= 2,1$  for 5-pile group,  $M= 3,1$  for 7-pile group, and  $M= 4,2$  for 9-pile group.
- The resistance factor calculations for the SPT-97 design method gave the highest resistance factor due to the high mean bias ratio. While, Nordlund method gave the lowest resistance factor values due to the low bias ratio.
- The proposed resistance factor values varied from 0.31 to 0.61, 0.52 to 0.86, 0.34 to 0.63, and 0.45 to 0.96 for different design methods: Nordlund, Bluebook,  $\beta$ -Method, and SPT Meyerhof, respectively.

## 4.10 References

- AASHTO, 1989. Guide Specifications for Strength Evaluation of Existing Steel and Concrete Bridges, American A. ed. Washington, DC.
- AASHTO LRFD, 2015. Bridge design specifications. Washington, D.C.: American Association of State Highway and Transportation Officials.
- AbdelSalam, S.S., Ng, K.W., Sritharan, S., Suleiman, M.T., Roling, M., 2012. Development of LRFD Procedures for Bridge Pile Foundations in Iowa — Volume III: Recommended Resistance Factors with Consideration of Construction Control and Setup, Iowa Department of Transportation. <https://doi.org/10.13140/RG.2.1.2434.6080>
- Abdelsalam, S.S., Sritharan, S., Suleiman, M.T., 2011. LRFD resistance factors for design of driven H-piles in layered soils. *J. Bridg. Eng.* [https://doi.org/10.1061/\(ASCE\)BE.1943-5592.0000253](https://doi.org/10.1061/(ASCE)BE.1943-5592.0000253)
- Allen, D.E., 1975. Limit States Design - a Probabilistic Study. *Can. J. Civ. Eng.* 2, 36–49. <https://doi.org/10.1139/l75-004>
- Allen, T.M., 2005. Development of the WSDOT pile driving formula and its calibration of load and resistance factor design (LRFD), Rep. No. WA-RD 610.1. Washington State Department of Transportation, Seattle, WA.
- Barker, R.M., Duncan, J.M., Rojiani, K.B., Ooi, P., Tan, C.K., Kim, S.G., 1991. Manuals for the Design of Bridge Foundations., NCHRP Report 343. TRB, National Research Council, Washington, DC.
- Basha, B.M., Babu, G.L.S., 2008. Target reliability based design optimization of anchored cantilever sheet pile walls. *Can. Geotech. J.* 45, 535–548. <https://doi.org/10.1139/T08-004>
- Becker, D.E., 1996a. Eighteenth Canadian geotechnical colloquium: Limit states design for foundations. Part I. An overview of the foundation design process. *Can. Geotech. J.* <https://doi.org/10.1139/t96-124>
- Becker, D.E., 1996b. Eighteenth Canadian geotechnical colloquium: Limit states design for foundations. Part II. Development for the national building code of Canada. *Can. Geotech. J.* <https://doi.org/10.1139/t96-125>
- Ching, J., Phoon, K.K., Hu, Y.G., 2009. Efficient evaluation of reliability for slopes with circular slip surfaces using importance sampling. *J. Geotech. Geoenvironmental Eng.* 135, 768–777. [https://doi.org/10.1061/\(ASCE\)GT.1943-5606.0000035](https://doi.org/10.1061/(ASCE)GT.1943-5606.0000035)
- CSA A23.3-14/A23.2-14, 2014. Concrete materials and methods of concrete construction/ Test methods and standard practices for concrete. Mississauga (Ontario): Canadian Standards Association.

- CSA S16-14, 2014. Design of steel structures. Mississauga (Ontario): Canadian Standards Association.
- CSA S6-14, 2014. Design of highway bridges. Mississauga (Ontario): Canadian Standards Association.
- Fenton, G.A., Griffiths, D. V., 2007. Reliability-based deep foundation design. *Geotech. Spec. Publ.* 1. [https://doi.org/10.1061/40914\(233\)1](https://doi.org/10.1061/40914(233)1)
- Fenton, G.A., Naghibi, F., Griffiths, D. V., 2016. On a unified theory for reliability-based geotechnical design. *Comput. Geotech.* 78, 110–122. <https://doi.org/10.1016/j.compgeo.-2016.04.013>
- Griffis, L.G., 1993. Serviceability limit states under wind load. *Eng. J.* 30, 1–16.
- Kwak, K., Kim, K.J., Huh, J., Lee, J.H., Park, J.H., 2010. Reliability-based calibration of resistance factors for static bearing capacity of driven steel pipe piles. *Can. Geotech. J.* 47, 528–538. <https://doi.org/10.1139/T09-119>
- Mbarka, S., Baroth, J., Ltifi, M., Hassis, H., Darve, F., 2010. Reliability analyses of slope stability. *Eur. J. Environ. Civ. Eng.* <https://doi.org/10.1080/19648189.2010.9693293>
- McVay, M.C., Birgisson, B., Zhang, L., Perez, A., Putcha, S., 2000. Load and Resistance Factor Design (LRFD) for Driven Piles Using Dynamic Methods - A Florida Perspective. *Geotech. Test. J.* 23, 55–66.
- Meléndez, C., Sagaseta, J., Sosa, P.F.M., Rubio, L.P., 2019. Refined Three-Dimensional Strut-and-Tie Model for Analysis and Design of Four-Pile Caps. *ACI Struct. J.* 116, 15–30. <https://doi.org/10.14359/51714485>
- Naghibi, F., Fenton, G.A., 2017. Target geotechnical reliability for redundant foundation systems. *Can. Geotech. J.* 54, 945–952. <https://doi.org/10.1139/cgj-2016-0478>
- NBCC, 2015. National building code of Canada. Ottawa (Ontario): National Research Council.
- OHBD, 1983. Ontario highway bridge design code, 2nd ed. Mi. ed. Downsview, Ont.
- Oudah, F., El Naggar, M.H., Norlander, G., 2019. Unified system reliability approach for single and group pile foundations – Theory and resistance factor calibration. *Comput. Geotech.* 108, 173–182. <https://doi.org/10.1016/j.compgeo.2018.12.003>
- Paikowsky, S.G., 2003. Practical Lessons Learned from Applying the Reliability Methods to LRFD for the Analysis of Deep Foundations. [https://doi.org/10.1142/9789812704252\\_0009](https://doi.org/10.1142/9789812704252_0009)
- Paikowsky, S.G., Bjorn, B., MaVay, M., Nguyen, T., Kuo, C., Baecher, G., Ayyub, B.M., Stenerseen, K., O'Malley, K., Chernauskas, L., O'Neill, M., 2004. Transportation Research Board (TRB), Washington D.C., USA, NCHRP REPORT 507.

- Poulos, H.G., 1997. Behavior of pile groups with defective piles. 14th Int. Conf. Soil Mech. Found. Eng. 871–876.
- Shreider, Y.A., 1966. The Monte Carlo Method, 1st ed. Pergamon.
- Tang, W.H., Gilbert, R.B., 1993. Case study of offshore pile system reliability. the 25th Annual OTC, Houston, Texas, U.S.A, 677–686.
- Tomlinson, M.J., 1980. Foundation design and construction, 6th ed. Longman Scientific and Technical, Essex, UK.
- Tang, W.H., Woodford, D.L., Pelletier, J.H., 1990. Performance reliability of offshore piles. Proc. Annu. Offshore Technol. Conf. , 299–308.
- Wang, Y., 2009. Reliability-Based economic design optimization of Spread Foundations. J. Geotech. Geoenvironmental Eng. 135, 954–959. [https://doi.org/10.1061/\(ASCE\)GT.1943-5606.0000013](https://doi.org/10.1061/(ASCE)GT.1943-5606.0000013)
- Wang, Y., Cao, Z., Au, S.K., 2011. Practical reliability analysis of slope stability by advanced Monte Carlo simulations in a spreadsheet. Can. Geotech. J. 48, 162–172. <https://doi.org/10.1139/T10-044>
- Yang, Z.X., Guo, W.B., Jardine, R.J., Chow, F., n.d. Can. Geotech. J. 1–46.
- Zhang, J., Zhang, L.M., Tang, W.H., 2011. New methods for system reliability analysis of soil slopes. Can. Geotech. J. 48, 1138–1148. <https://doi.org/10.1139/t11-009>
- Zhang, L., Li, D.Q., Tang, W.H., 2005. Reliability of bored pile foundations considering bias in failure criteria. Can. Geotech. J. 42, 1086–1093. <https://doi.org/10.1139/t05-044>
- Zhang, L., Tang, W.H., Ng, C.W.W., 2001. Reliability of axially loaded driven pile groups. J. Geotech. Geoenvironmental Eng. 127, 1051–1060. [https://doi.org/10.1061/\(ASCE\)1090-0241\(2001\)127:12\(1051\)](https://doi.org/10.1061/(ASCE)1090-0241(2001)127:12(1051))



## Chapter 5

# **SUMMARY, CONCLUSION AND RECOMMENDATIONS**

---

### 5.1 Summary

This thesis presents a comprehensive numerical parametric investigation of different geotechnically defected pile group configurations (4 piles, 5 piles, 7 piles, 9 piles) in a medium dense to dense sand using the program ABAQUS/Standard. The thesis examined the axially loaded defected pile group system in terms of its capacity, load redistribution, rotation of the pile cap, and bending moment at the piles. The thesis then introduced a new method in system-based reliability analysis of pile group foundations, to calibrate the resistance factor for pile groups and determine the number of piles the system can accommodate before failure.

### 5.2 Conclusions

Based on the Numerical investigation of defected pile group foundations, the main conclusions are listed below:

1. The load-settlement behavior of the defected and intact pile group foundations are similar. However, a significant decrease in the stiffness of defected group is noticed, as the defected pile location changes or the number of the failed pile increases.
2. The load redistribution of the system upon failure of one pile in the group is affected mostly by the eccentricity caused by the unsymmetrical configuration of the group due to pile failure and the disappearance of strut and tie forces in the system.
3. The rotation of the pile cap increases as the pile spacing increases which shows a minimal effect on the bending moment at the individual piles in the group.
4. The induced bending moment at the piles decreases as the intact pile is farther from the failed pile.
5. The most critical sequence for all pile group configurations in terms of their capacity is the failure of the external piles, especially corner piles.

Based on reliability analysis of pile group foundations, the following main conclusions are drawn:

1. The  $\gamma$  factor is not affected by varying the column area and pile diameter because the column area and the pile diameter do not affect the strut and tie angle.
2. Changing the pile spacing is the most critical parameter that affects  $\gamma$ . The pile spacing and  $\gamma$  factor have an inverse correlation. This is because of the decrease of the strut and tie angle and consequently decrease of the compression force in the diagonal strut.
3. The resistance factor obtained for the SPT-97 design method is the highest due to the high mean bias ratio. On the other hand, Nordlund method produced the lowest resistance factor as a result of the low bias ratio
4. The main factors that affect the redistribution of the forces in a pile group foundation is the stiffness and the failure mechanism of the pile cap.
5. The maximum and the minimum number of failed piles the system can accommodate before failure for different design methods and spacing,  $M= 2,1$  for 5-pile group,  $M= 3,1$  for 7-pile group, and  $M= 4,2$  for 9-pile group respectively.
6.  $\gamma$  factor is relying on the ability of the pile cap to redistribute the forces upon failure of individual piles within a pile group foundation.
7. It was found that the proposed resistance factor values varied from 0.31 to 0.61, 0.52 to 0.86, 0.34 to 0.63, and 0.45 to 0.96 for different design methods: Nordlund, Bluebook,  $\beta$ -Method, and SPT Meyerhof, respectively.

### 5.3 Future work and recommendations

The current research outlines the overall performance of an axially loaded defected pile group foundation and proposing resistance factors for pile group foundations in sandy soil, which can be extended to explore any of the following directions:

1. Using the same methodology of the current research, the pile group foundations can be investigated to calibrate the resistance factor using a different type of soils (clay and silt), pile configurations, and installation methods (bored, cast-in-place)

2. Study the effect of defected pile group under lateral loads or under dynamic loads to propose different ranges of resistance factors under different type of loading for pile group foundations.

## Curriculum Vitae

**Name:** Abdalla Elhadi Adlan Alhashmi

**Post-secondary Education and Degrees:** United Arab Emirates University  
Al-Ain, United Arab Emirates  
2011-2016 BSc

**Honours and Awards:** John Booker Award  
2019

**Related Work Experience:** Structural Engineer  
Circle Engineering Consultant Company, Dubai  
2017-2018  
Teaching Assistant  
The University of Western Ontario  
2018-2019